The regulation of leaf thickness in rice

(*Oryza sativa* L.)

A thesis submitted by

Supatthra Narawatthana

For the degree of Doctor of Philosophy

Department of Animal and Plant Sciences

The University of Sheffield

July 2013

Abstract

The regulation of leaf thickness in rice (*Oryza sativa* L.)

S. Narawatthana

One of the most important targets to improve crop yield is leaf photosynthetic capacity. Leaf thickness is one parameter closely associated with photosynthetic function and is strongly influenced by the level of irradiance. Generally, high light grown leaves are thicker, have higher light-saturated rates of photosynthesis, higher amounts of Rubisco and a higher chlorophyll a:b ratio than shade grown leaves. However, the developmental stage at which leaf thickness is set and how it is set are unclear. In this thesis I investigate the outcome on leaf thickness of changing irradiance level at specific points in the development of leaf 5 of rice plants via a series of transfer experiments from high light (HL) to low light (LL) at specific stages of leaf development. The results from these experiments show that the P2- to P4-stage of rice leaf development represents a developmental window during which final thickness can be altered via light regime. Analysis of photosynthetic capacity and gas exchange of the leaves from the transfer experiments indicated some correlation of leaf thickness with biochemical/physiological adaptation to the prevailing irradiance level. Interestingly, whilst HL induced the development of thicker rice leaves with a visibly larger mesophyll cell size, transferral of the leaves to LL conditions at any developmental stage led to a LL-acclimated photosynthetic response. To identify lead genes potentially involved in the growth response of young leaves to the prevailing light environment, I performed a microarray analysis of leaf primordia at P3-stage undergoing a leaf-thickness response to altered irradiance level. A number of lead genes were identified and a selection process based on independent expression analyses was performed to narrow the number of candidates for future functional analysis. An initial analysis of some of these genes is reported.

Acknowledgements

I was fortunate to have Prof. Andrew Fleming as my supervisor. His innovative attitude toward science and endless encouragement has been essential to finish the work. I am most grateful for your consistent support. I am grateful for other guidance available from Prof. Paul Quick who also gave me the opportunity to do my PhD. The financial support from Thailand Agricultural Research Development Agency (ARDA) is gratefully acknowledged.

I was lucky to be a member of a very innovative research group, Dr. Asuka Kuwabara, Dr. Anna Kasprzewska, Dr. Jen Sloan and Marion Bouch generously gave their valuable time guidance and encouragement. My warmest thanks are to you. Special thanks to Majorie Lundgren for the helpful guidance on using the LI-COR and physiological works. Thanks to the lab manager, Bob Keen, for all the kind supports.

I would also like to acknowledge Ramil Mauleon (IRRI) who did the microarray analysis. Many thanks to Dr. Stephen Rolfe and Julia Van Campen for their helps on the microarray result.

The D59 member, Dr. Hoe Han Goh, Dr. Xiao Jia Yin, Dr. Phakpoom Phraprasert, Dr. Adam Hayes, Dr. Chloé Steel, Dr.Simon Wallace, Dr.Caspar Chater, Rachel George, Thomas Harcourt, Nazmin Yaapar and many others, deserves special thanks for making the day at the lab more enjoyable and memorable. In particular, I want to thank Nisa Patikarnmonton, Oratai Weeranantanapan, Dr.Natwadee Poomipark, Dr.Khanita Kamwilaisak, Dr.Patompon Wongtrakoongate, Dr.Rossukon Keawkaw, Dr.Chatchawal Phansopha, Dr.Sawaporn Siriphanthana, Chomchon Fusinpaiboon, Sujunya Boonpradit, and many other Thai friends for all kinds of support during these years. My life in Sheffield was made truly memorable. I would also like to thank Pattamapon Prachomrat, for always being there for me.

I would like to thank my family for the endless love and unconditional supports. My parents, Pathawee and Arjin, my sisters, Ann, Koi, my niece Rida, and also my brother in-law have formed an excellent safety net which I could always rely on. My loving thanks are to you all.

Abbreviations

A	Net carbon dioxide assimilation
ANOVA	Analysis of variance
Chl a:b	Chlorophyll *a* / chlorophyll *b* ratio
C_i	Substomatal carbon dioxide concentration
CO_2	Carbon dioxide
DAS	Days after sowing
DIG	Digoxigenin
dNTPs	Deoxynucleotide triphosphates
EDTA	Ethylenediaminetetraacetic acid
FDR	False discovery rate
g	Gram
g_m	Mesophyll conductance
g_s	Stomatal conductance
HCl	Hydrochloric acid
HL	High light condition (700 µmol m^{-2} s^{-1})
HL-leaves	Leaves grown under HL
hr(s)	Hour(s)
IRRI	International Rice Research Institute
J_{max}	Maximum rate of electron transport
LB	Luria-Bertani medium
LHC	Light harvesting complex

LL	Low light condition (200 µmol m^{-2} s^{-1})
LL-leaves	Leaves grown under LL
P1	P1-stage leaf
P2	P2-stage leaf
P3	P3-stage leaf
P4	P4-stage leaf
P5	P5-stage leaf
PAR	Photosynthetically active irradiance
PBS	Phosphate buffer saline
$\boldsymbol{P_{max}}$	Light saturated-rate of photosynthesis
PPFD	Photosynthetic photon flux density
PSI	Photosystem I
PSII	Photosystem II
P-stage	Leaf plastochron age
$\mathbf{R_d}$	Dark respiration rate
RQ	Relative quantitation
RT	Room temperature
Rubisco	Ribulose-1,5-bisphosphate carboxylase oxygenase
RuBP	Ribulose-1,5-bisphosphate
s	Second
$\boldsymbol{S_c}$	Chloroplast surface area
$\boldsymbol{S_{mes}}$	Mesophyll surface area

SAM	Shoot apical meristem
SDS-PAGE	Sodium dodecyl sulphate- Polyacrylamide gel electrophoresis
SSC	Saline-sodiumcitrate buffer
TAE	Tris acetic acid EDTA buffer
Tris	Tris(hydroxymethyl) aminomethane
v/ v	Volume/ volume
$V_{c_{max}}$	Maximum rate of carboxylation of Rubisco
w/v	Weight/ volume

Contents

Figure contents

Table contents

Chapter 1 |Introduction

1.1 Introduction

Asian rice (*Oryza sativa* L.) is one of the most important crops in the world. There are 2 major subspecies of *Oryza sativa* L.; *indica,* which is known as long grain rice, and *japonica,* which is commonly known as short grain rice. Both paddy and upland cultivars of these subspecies have been produced mainly in Asia and paddy rice is harvested from approximately 164 million ha of land worldwide (FAOSTAT, 2011). However, world population is expected to increase by 2.3 billion people between 2009 to 2050, leading to increasing food demand with consequences for agricultural land expansion and water use efficiency (FAO, 2009). To meet burgeoning food demand for an increasing world population, a more productive and sustainable means of rice production is urgently required.

The specific parameter which determines yield potential in crops is the radiation use efficiency or RUE (the amount of biomass produced per unit of radiation energy intercepted). In a comparison to other C3 crops, rice has a relatively low RUE (Mitchell et al., 1998) and this is the major limitation in yield potential. An increase in leaf level photosynthetic capacity has been suggested as a way of increasing RUE in rice (Hubbart et al., 2007; Sheehy et al., 2008). Therefore, there is renewed interest in improving the value of P_{max} (the maximum photosynthetic rate per unit leaf area) which is important in determining leaf photosynthesis.

Leaf thickness is an important morphological characteristic that associates with maximum photosynthetic rate (P_{max}) and yield potential. For example, the International Rice Research Institute (IRRI) has incorporated leaf thickness into the profile of New Plant Types (NPT) or ideotype (Cassman, 1994; Peng, 2008). By influencing cell number and the number of chloroplasts per unit area, and the determination of total chlorophyll, protein and RubisCO content, leaf thickness has a strong impact on the amount of light absorbed, CO_2 assimilation rate and nitrogen (N) content of the leaf and correlates with the maximum photosynthetic rate (P_{max}) (Syvertsen et al., 1995; Smith et al., 1997; Garnier et al., 1999; Oguchi et al., 2003). Leaf anatomy is also closely associated with photosynthetic function and is strongly influenced by the level of light irradiance, a vital source for plant growth. High light grown leaves are

thicker and have higher light-saturated rates of photosynthesis, higher amounts of RubisCO and protein components of electron transport and ATP synthesis, a higher chlorophyll a/ b ratio and greater nitrogen content than shade grown leaves (Murchie and Horton, 1997; Weston et al., 2000; Terashima et al., 2001).

A previous study of rice leaves (Murchie et al., 2005) suggested that the character of high-light leaves is regulated by endogenous and environmental factors which are set within the leaf sheath, i.e., early in the developmental process. In particular, signalling mechanisms involved in the control of leaf thickness act before leaf emergence from the sheath. However, the developmental stage at which these morphological changes occur is unclear and indeed the genetic mechanism that controls the thickness of leaves is unknown. A main overall aim of the research described in this thesis was to increase our understanding of the control of rice leaf thickness. In the following sections, I provide an overview of leaf development and our state of knowledge of the control of leaf thickness.

1.2 Leaf anatomy and morphology

The leaf is a plant organ specialised for photosynthesis and is involved in other crucial processes such as transpiration. Leaves are typically bilaterally symmetrical and flattened but there is diversity in leaf form, shape and size among plant species. Typically, a structurally complete leaf of an angiosperm consists of a blade (lamina) and petiole (which connects the blade to the stem) and stipules that are found at the base of the petiole in many dicotyledons. Grass leaves have a different architecture to those of dicots as they are divided into two primary sections: the leaf blade or lamina and the leaf sheath. The leaf sheath is the proximal region and surrounds the shoot apex and runs parallel to the culm (stem). There is a boundary consisting of ligule and auricle between the leaf blade and the sheath (Figure 1.1).

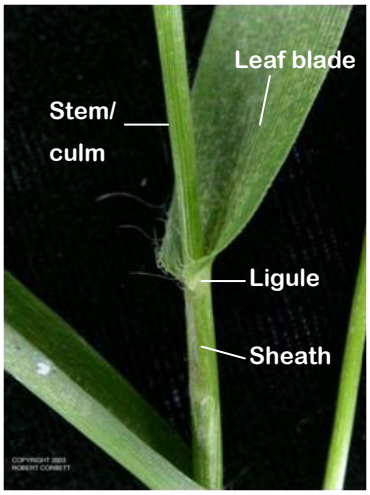

Figure 1.1 Example of grass leaf morphology. Leaf morphology of *Dichanthelium dichotomum*. Adapted from Corbett (2011) orbett, 2011)

The tissues that form the leaf are divided into three types; an epidermis covering the upper and lower surfaces of the leaf, the parenchyma tissue between the upper and lower epidermis (which is commonly called mesophyll) and the vascular tissue or veins. The epidermis mostly consists of a single-cell layer of thick walled epidermal cells covered with a cuticle that prevents dehydration. There are many stomata perforating predominantly the abaxial side of the leaf, which serve in the exchange of gases, including CO_2. Each stoma is surrounded by a pair of guard cells which regulate the rate of transpiration by opening and closing the central pore of stoma. The mesophyll is composed of chlorenchyma cells and is the primary location of photosynthesis. In most dicot leaves, the mesophyll is differentiated into palisade parenchyma and spongy parenchyma, which are not found in the monocots. The palisade parenchyma cells are columnar in shape, contain large numbers of chloroplasts and are generally packed closely together. The spongy mesophyll cells are usually ball-shaped with large intercellular spaces, which allow for the interchange of gases, and usually contain fewer chloroplasts than the palisade cells. Water and nutrients move into these tissues via the xylem tissue in the veins, and the sugar products of photosynthesis are translocated to other parts of the plant via the phloem tissue. Xylem and phloem are arranged in vascular bundles, surrounded by tissue called the bundle sheath.

1.2.1 Rice leaf anatomy

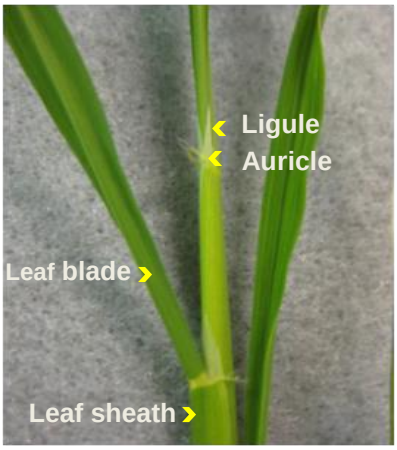

Figure 1.2 Rice leaf morphology showing the 3 main parts; leaf blade, leaf sheath and the boundary between leaf blade and sheath composed of ligule and auricle.

According to the classic description of the development of rice (Itoh et al., 2005), the adult rice leaf is strap-like and divided into three distinct regions along the proximal-distal axis and is also polarized along the adaxial-abaxial axis. The leaf sheath forms the proximal region and surrounds the shoot apex. The young rice leaves are enclosed in the sheaths of the older leaves, protecting them from physiological and physical damage. The major site of photosynthesis is blade or lamina in the distal part of the leaf. Between the blade and the sheath is the boundary that consists of the three distinct parts. Firstly, the lamina joint or collar is a whitish region located in the base of the blade. The collar is responsible for bending the leaf blade toward the abaxial side. Secondly, the ligule, which is usually differentiated into two segments in mature leaves, is membranous. The other part, positioned at the leaf margins, are the auricles which are a pair of small appendages containing long hairs, as shown in Figure 1.2. Over the epidermis layer of the entire rice leaf surface, except for the adaxial surface of the sheath, there are numerous papilla and trichomes.

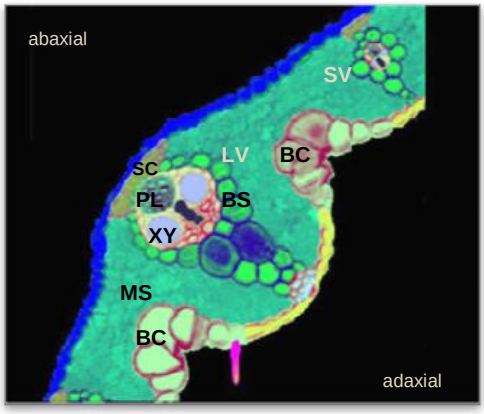

Figure 1.3 Cross section of mature rice leaf**.** LV, large vascular bundle; SV, small vascular bundle; SC, sclerenchymatous cell; MS, Mesophyll layer; PL,phloem; XY, xylem; BS, bundle sheath cell; BC, bulliform cell. Adapted from Mercade et al. (2009). (Mercade et al., 2009))

The internal anatomy of rice leaves (Figure 1.3) consists of 3 tissue systems; the dermal tissue system, the vascular tissue system and the ground tissue system. In the adaxial side of leaf blade epidermis there are bulliform cells, a group of cells in the dermal tissue system arranged in vertical rows between the vascular bundles. The rice mesophyll tissue, which is mostly made up of folded parenchyma cells, is composed of lobed chlorenchyma cells that are approximately twice as long as they are wide with the long axis oriented perpendicular to the vascular tissue (Sage and Sage, 2009). The chlorenchyma cells are densely packed with chloroplasts, the organalle responsible for photosynthesis. The vascular bundles of rice leaf are enclosed in the bundle sheath and are divided into three types according to their size: the midrib, the major veins and the minor veins. The midrib is located at the centre of the rice leaf with the minor and major veins running pararell to it, between the midrib and the leaf margin. The sequence and repeating pattern of major and minor veins are symmetrical. Generally, there are two minor veins close to the midrib then the first major vein next to them, after which there is a repeating pattern of four or five minor veins between each major vein until the final major vein adjacent to the leaf marjin (Smillie et al., 2012). The adaxial and abaxial suface of the vascular bundles is the location of xylem and phloem respectively. In addition, there are schlerenchymatous fibers both on adaxial

and abaxial sides of vascular bundles of the leaf blade but only on the abaxial side of leaf sheath.

1.3 Leaf development

The main event during embryo formation of a flowering plant is the development of a root and shoot axis. The embryo is divided into two opposite ends to become the root and shoot system (Dashek and Harrison, 2006). The root and shoot system produces several kinds of plant organs with a diversity of functions from special regions of dividing cells, called meristems. These meristems consist of the cells which undergo repeated cycles of growth and division to generate new cells. Cell divisions followed by enlargement and differentiation of the derivative cells at the shoot apical meristem (SAM) and root apical meristem give rise to the shoot and root system respectively.

The SAM, once formed in the embryo or in an axillary position, initiates organ primordia throughout its life with regular spacing (phyllotaxy) and a regular timing (plastochron). Leaves are produced repeatedly from cells within the organogenic region on the flanks of the SAM in a pattern characteristic for the species (Walbot, 1985; Sussex, 1989; Smith and Hake, 1992; Sylvester et al., 1996; Sinha, 1999; Ezhova, 2007). The tissue layers at the SAM can be divided into the tunica and the corpus and in monocots, there are one or two tunica layers at the SAM (Esau, 1977). Research in maize has shown that the L1 layer gives rise to the protoderm that will form the epidermis through controlled anticlinal divisions. The mesophyll, bundle sheath, and vascular tissue originate from anticlinal and periclinal divisions in the L2 layer (Satina et al., 1940; Poethig, 1984; Turnbull, 2005).

Numerous investigations indicate that the SAM itself, the size of shoot apex and the pre-existing primordia can influence the placement of initiating primordia. Moreover, biophysical constraints may also pose a role in primordium placement (Snow and Snow, 1932; Sussex, 1955; Snow and Snow, 1959; Fleming et al., 1997). Despite the diversity in the morphological characteristic (such as form and size), leaves share common developmental pathways and the initial stages of leaf development show common patterns of

genetic regulation, including the effect of auxin (Turnbull, 2005; Ezhova, 2007).

1.3.1 Leaf developmental landmarks

According to Sylvester (1996), developmental landmarks can be used to divide the process of leaf development into 3 stages. During the organogenesis stage (the first stage) the initial leaf cells on the flanks of SAM are set aside as founder cells of the initiating leaf followed by a change in polarity and rates of cell division, and the emergence of a protuberance or leaf primordium, which essentially translates the inside-outside symmetry of the SAM into the adaxial-abaxial symmetry of leaf (Turnbull, 2005). In the second stage, referred to as primary morphogenesis, ground-plan patterning and the development of internal leaf architecture (histogenesis) are established. The third stage of leaf development is differentiation of the leaf by coordinated processes of cell division, expansion and differentiation. The latter stage is referred to as the secondary morphogenesis stage at which the fundamental leaf architecture originated at the early stage of leaf development can be modified during leaf expansion. It has been shown that the histogenesis stage overlaps the morpogenetic phases in time (Sylvester et al., 1996; Turnbull, 2005).

Leaf developmental stages can be defined by plastochron number in order of increasing age. Thus, Plastochron1 (P1) represents the youngest leaf primordium just after the protrusion flanking the SAM. As this leaf grows, another leaf is eventually formed on the SAM, at which point the first leaf is said to enter the P2 stage of development. When the meristem forms a third leaf, the oldest leaf is defined as entering the P3 stage of development (Sharman 1942). The plastochron staging of leaves allows a developmental staging independent of absolute age of a leaf, facilitating comparison of leaves in different experiments and under different conditions.

1.3.2 Cell division and leaf development

Cell division in plants is comparable to that described in other eukaryotes and Figure 1.4 shows the current model for activation of the plant cell cycle via the E2F-Rb pathway. A serial process of protein phosphorylation

and dephosphorylation of the cell cycle engine gives rise to a coordinated progression of a cell through each phase of the cell cycle. For example, the E2F transcriptional factor and the retinoblastoma repressor act in the E2F-Rb pathway (Shen, 2002) as a key mechanism controlling the decision of continuing or stopping cell division. The pathway controls the transition of the cell cycle from G1 to S phase, when DNA synthesis occurs, by indirect activation or repression of genes involved in DNA synthesis and further elements of the cell cycle. E2F encodes a transcription factor whose activity is repressed by Rb, leading to the repression in expression of genes required for progress to S phase. Once Rb is phosphorylated by plant cyclin-dependent kinase (CDKs), it is unable to repress E2F, thus leading to the de-repression of gene expression, affecting progression to S phase and cell proliferation. It is known environmental triggers must somehow feed into the control of these central cell cycle pathways, but the mechanism underpinning the environmental control of cell division remains unclear.

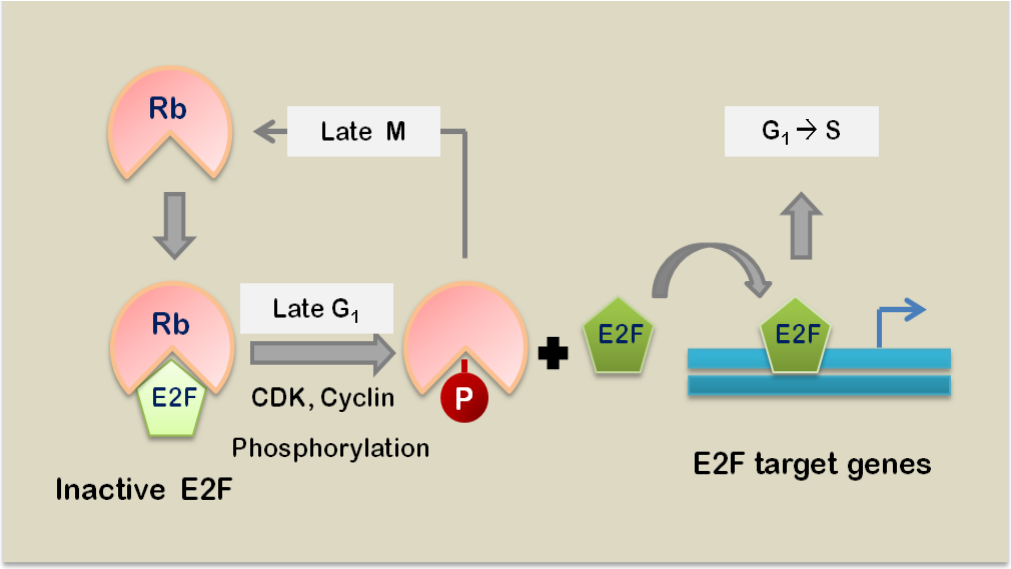

Figure 1.4 Model for activation of the plant E2F–Rb pathway at the G1-to-S-phase transition. In growth-arrested cells and during early G1 phase, hypophosphorylated Rb binds E2F and consequently inhibits the E2F transcriptional activity. During late G1 and early S phase, Rb is hyperphosphorylated, first by CDK–cyclin-D (CycD) and then by CDK–cyclin-A (CycA) kinases, resulting in the dissociation of Rb from the Rb–E2F complex. The released E2Fcomplex actively promotes transcription of E2F-target genes involved in cell-cycle regulation, DNA synthesis and replication, and chromatin assembly.

Precise spatial, temporal, and developmental regulation of cell division activity in meristems is required for continuing organogenesis and plastic growth in response to a changing environment (Doerner, 1994), such as temperature and irradiance. This means that it is vital to have complex regulatory pathways and signaling systems that communicate environmental constraints to control the time and extent of cell division.

1.3.3 Molecular regulation of leaf development

Over the last decade extensive investigations have provided an increasing understanding of the genetic regulation of leaf development, although most of this has involved the study of dicot leaves rather than grasses. Genes play a major role in the determination of events at the molecular level throughout all phases of leaf development including initiation and the development of organ identity, architecture and growth. Some of these genes and the processes they control are briefly described here.

The formation of leaf primordia, in most angiosperms, arises from the cells of all layers of the SAM (Ezhova, 2007). The hormone auxin plays a role in selecting the group of cells which form the leaf promordium and provides for the formation of new local regions of auxin accumulation which determine the positioning of new primordia. The gradient of auxin is controlled by the expression of genes which encode proteins controlling auxin transport. For instance, the PIN1 gene encodes for a transmembrane transporter protein which exerts the main control of auxin efflux and the demarcation of leaf primodia in *Arabidopsis thaliana* (Friml, 2003; Friml et al., 2003; Reinhardt et al., 2003). Mutation of PIN1 in Arabidopsis mutants affects the distribution of auxin resulting in defective cotyledon development and blocked leaf initiation (Ezhova, 2007).

In addition to the demarcation of future lateral organs, local auxin concentration also activates the function the protein expansin which has an important role in increasing of plant cell wall extensibility. Thus, primordium-like bulges, which later developed leaf-like structures, were formed when beads loaded with purified expansin were placed on tomato apical meristem.

Thus expansin can induce tissue expansion and leaf initiation (Fleming et al., 1997).

The class 1 KNOtted1-like homebOX (KNOX) family of homeodomain genes encode homeodomain-containing proteins. SHOOTMERISTEMLESS (STM) of Arabidopsis and LeT6 of tomato are examples of these proteins which are typically expressed in the SAM but whose expression is down-regulated at the site of primordium initiaton (Lincoln et al., 1994; Long et al., 1996; Smith et al., 1996; Turnbull, 2005). Mutations of the Class I KNOX gene STM1 lead to the loss of shoot meristems in Arabidopsis (Barton and Poethig, 1993). In leaves, the downregulation of KNOX genes is regulated by MYB family transcriptional regulators such as PHANTASTICA (PHAN) in Antirrhinum (Waites et al., 1998) and ROUGH SHEATH2 (RS2) in maize (Tsiantis et al., 1999). Moreover, the leaves of PHAN gene mutants of Antirrhinum show that this gene plays a key function in the control of leaf polarity and the specification of the adaxial domain (Waites and Hudson, 1995). In addition, the determination of the abaxial domain and asymmetric development and expansion of Arabidopsis leaves requires function of the YABBY and KANADI gene families (Eshed et al., 2004).

Leaf expansion requires the coordination of overall tissue expansion with cell division. In Arabidopsis, the zone of cell division, which is distributed throughout the leaf at the beginning of organ development, tends to be restricted to the more basal portions of the blade as the blade enlarges (Kang and Dengler, 2002). The expression of the CINCINNATA (CIN) gene of Antirrhinum is hypothesized to be correlated with this orderly basipetal suppression of cell proliferation by sensitizing tissues to the cell cycle arrest front (Nath et al., 2003). While CIN correlates with cell cycle arrest stage during blade expansion, JAGGED (JAG) has been shown to have an antagonistic effect by suppression of cell cycle arrest (Ohno et al., 2004). Moreover, the auxin regulated gene ARGOS is also required for maintaining cell proliferation by connecting auxin induction signals to the regulators of the cell cycle, ANTIGUMENTA (ANT1) and CYCD3 (Hu et al., 2003).

The organisation of internal leaf tissue anatomy requires a complex genetic regulation to co-ordinate cell division and other developmental

processes. A study in tobacco (McHale and Koning, 2004) revealed a role for NTPHAN (Nicotiana tabacum ortholog of PHANTASTICA) as a key molecular component in the translation of the adaxial-abaxial domain identity into tissue specific cell proliferation patterns. The expression of NTPHAN was found initially throughout the leaf primordia, but the expression became restricted to the middle mesophyll layer in the expanding leaf. It is suggested that NTPHAN down-regulates the class I KNOX gene, NTH 20, in adaxial mesophyll, thus mediating the determinate state of anticlinal cell divisions (McHale and Koning, 2004).

1.3.4 Rice leaf development

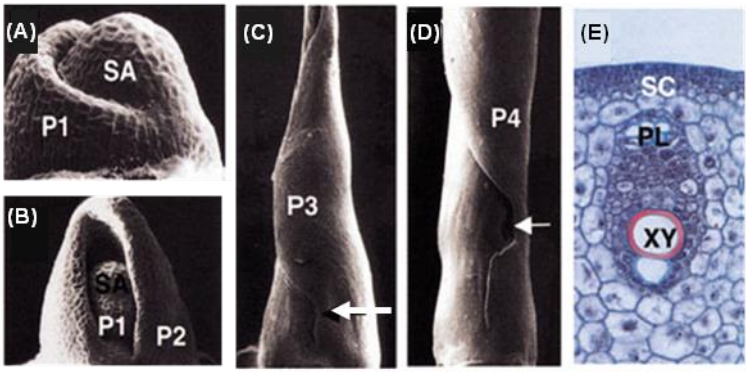

Figure 1.5 Leaf developments in rice. (A) SEM image of SAM and late P1 primordium. (B) SEM image of early P1 and P2 primordium. (C) SEM image of the P3. The arrow indicates the blade–sheath boundary. (D) SEM image of the P4.Elongation of the sheath (below the arrow) does not yet start. (E) Cross-section of large vascular bundle of P4 leaf sheath. SC, sclerenchymatous cell; PL, phloem; XY, xylem; SA, shoot apical meristem. Adapted from Itoh et al.(2005).

In rice (Oryza sativa L.), the leaf primordium is first recognized as a small bulge on the flank of the SAM. The primordium then grows towards the shoot apex and the opposite side of the SAM. After that, the primordium forms into a crescent-shaped (P1-stage), as shown in Figure 1.5A, and becomes hood-shaped (P2-stage) as a result of rapid cell division and elongation in the apical and marginal regions, as showed in Figure 1.5B. The initiation of the procambial strand at the leaf center is established at this stage. When the two margins of the leaf primordium overlap and enclose the SAM, the shape of the leaf primordium changes into cone-like (P3-stage), as shown in Figure 1.5C,

and the blade–sheath boundary is visible. Ligule primordium protrusion, which originates from periclinal divisions of epidermal cells, appears at the blade–sheath boundary of the adaxial surface along with the establishment of the other internal tissues (Itoh et al., 2005). At this stage the vascular bundles cover the total width of the leaf and the vascular tissues of xylem and phloem are established at the mid-vein. Furthermore, the initiation of epidermal specific cells, such as the stomata and bulliform cells occurs.

After the stage of ligule primordium differentiation, elongation of the leaf blade proceeds rapidly during P4 stage (Figure 1.5 D), while elongation of leaf sheath is suppressed until leaf blade elongation is complete (Itoh et al., 2005). At this stage the epidermis specific cells and the vascular bundle of P4 leaf sheath are visible (Figure 1.5 E). The different stages of rice leaf development, as defined by plastochron number and molecular markers, can be summarised as follows.

Stage: I1

Leaf organogenesis is initiated by partitioning of the meristem into a region of founder cells that are destined to become a future leaf (Sylvester et al., 1996). The founder cells are distributed around the circumference of the SAM and at this stage a rice PNH/ZLL homologue (OsPNH1), a gene preferentially expressed in the developing vascular bundle, starts to be expressed in the central region of the founder cells (Nishimura et al., 2002). It has been suggested that OsPNH1 may be a key factor in regulating developmental signaling of the central domain in leaf founder cells, and has been considered to be the initial important event for the development of organized phyllotaxy. For example, defect in the localized expression of OsPNH1 leads to random phyllotaxy (Nishimura et al., 2002).

Research (Miyoshi et al., 2004) has revealed a function for the PLASTOCHRON1 (PLN1) gene which encodes a cytochrome P450 protein, CYP78A11, as a timekeeper of rice leaf initiation. It has been suggested that CYP78A11 might be involved in biosynthesis of fatty acids which may act as signaling molecules required for leaf development. The PLN1 gene plays a role

in developing leaf primordia and affects the timing of successive leaf initiation, as well as the termination of vegetative growth in rice (Miyoshi et al., 2004).

Study of the SHOOT ORGANIZATION (SHO) gene revealed an important role of this gene in maintaining the proper organization of the SAM (Itoh et al., 2000). SHO mutants showed an increased rate of leaf production with random phyllotaxy. In addition, mutants of three SHO loci exhibited an abnormal meristem, altered phyllotaxy, short plastochron and threadlike leaves. It has been suggested that SHO genes may have functions relating to two regulatory processes: the maintenance of proper SAM organization and the regulation of leaf morphology (Itoh et al., 2000).

Stage: P1

At this stage the leaf primordium of rice initiates in a crescent-shape on the flanks of the SAM and the rate of division in P1 cells is higher than that in the SAM (Itoh et al., 2000b). Molecular markers can be used to identify the P1 stage. For instance, the expression of rice SCARECROW gene, OsSCR, starts at this stage in the epidermal layer. It has been proposed that OsSCR is involved in asymmetric division of cortex/ endodermis progenitor cells, and during stomata and ligule formation, by establishing the polarization of cytoplasm (Kamiya et al., 2003). Furthermore, the regulator of midrib formation and carpel specification in rice, the DROOPING LEAF (DL) gene, is also first expressed in the central region of the P1 leaf primordium. It has been proposed that DL gene regulates midrib formation by inducing cell proliferation in the central region of the leaf (Yamaguchi et al., 2004).

Stage: P2

At this stage the rice leaf primordium is hood-shaped on the flanks of SAM, but no molecular markers specific for this stage of leaf development have yet been reported. However, OsSCR, DL, and OsPNH1 continue to be expressed in the P2 primordium (Nishimura et al., 2002; Kamiya et al., 2003; Yamaguchi et al., 2004).

Stage: P3

At this stage the margins of the primordium overlap and completely enclose the SAM, leading to a long-conical shape, and the blade-sheath boundary forms. The ligule primordium is first observed at the P3 primordium. Moreover, the epidermal cells at the leaf tip can be distinguished from the internal cells at this stage (Itoh et al., 2005). The OsSCR gene is expressed in the P3 primordium (Kamiya et al., 2003).

Stage: P4

The leaf blade elongates rapidly in the P4 primordium. The expression of the OsSCR, DL, and OsPNH1 molecular marker genes are down-regulated at this stage (Nishimura et al., 2002; Kamiya et al., 2003; Yamaguchi et al., 2004).

Stage: P5

At this stage the leaf sheath starts to elongate before the leaf emerges from the sheath of P6 leaf (Itoh et al., 2005).

Stage: P6

The P6 represents the mature form of the rice leaf. The leaf blade bends at the lamina joint.

1.4 Photosynthesis

The main concept of photosynthesis is the capture of energy contained in photons by a pigment, e.g., chlorophyll in the leaf, and conversion of this energy into the chemical energy of organic molecules. Thus, this process exploits solar energy for the production of carbohydrates from carbon dioxide (CO_2) and water (H_2O). The basic equation of photosynthesis is

$$nCO_2 + 2nH_2O \xrightarrow{\text{Light}} (CH_2O)n + nO_2 + nH_2O$$

;where n is the number of CO_2 molecules combining with water (H_2O) to form the carbohydrates $(CH_2O)n$, and releasing n molecules of oxygen (O_2) to the environment.

Photosynthesis is a complicated process consisting of three key processes; light reactions, which is the process of conversion of the light energy into chemical energy; the diffusion of CO_2 from the atmosphere through stomata into leaves and to plastids; and the dark reactions, in which chemical energy is used to synthesise carbohydrate from CO_2. These photosynthetic reactions in green plants take place in chloroplasts.

1.4.1 Light reactions

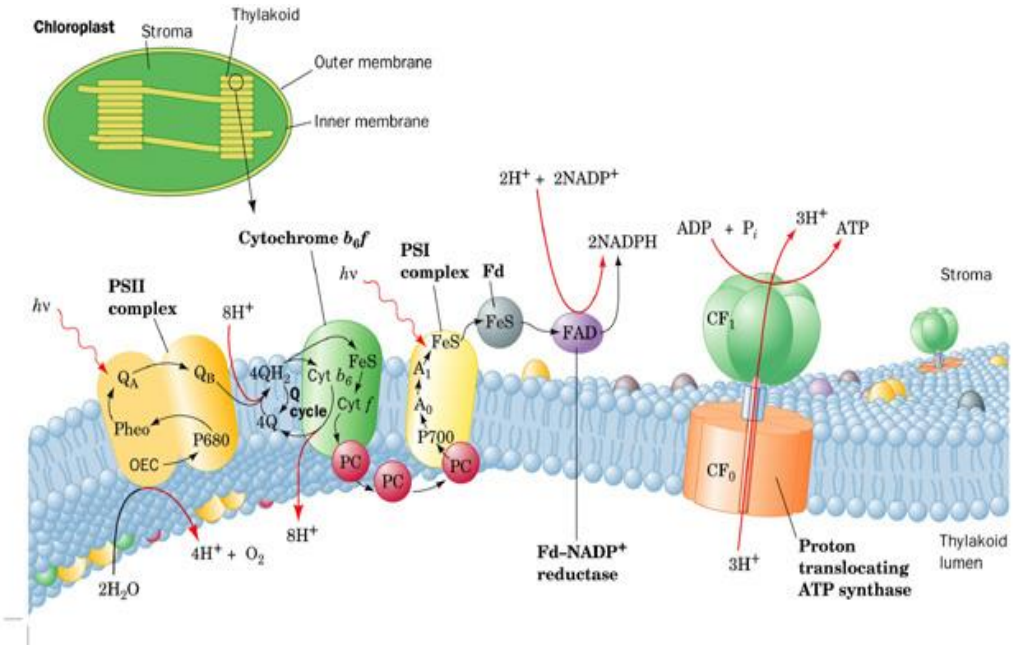

Figure 1.6 A diagram showing an overview of light reaction process in photosynthesis. The light reaction occurs in the thylakoid membrane of chloroplast. Light energy obsorbed by the plant pigments is used to produce ATP and NADPH; the high-chemical energy and high reducing power molecules, respectively. The ATP and NADPH are required for the Calvin cycle which incorporates CO_2 into organic molecules. Taken from Voet and Voet (2004).

The light reactions take place on thylakoid membranes inside a chloroplast (Figure 1.6). The first step of photosynthesis is the absorption of light energy by pigments in the chloroplast. Incident light energy occurs in

discrete units, photons. The energy of a photon (E) depends on wavelength of the light (λ) as given by

$$\boldsymbol{E = hc/\lambda}$$

; where h is Planck's constant (6.62 x 10^{-34} J s) and c is the speed of light (2.998 x 10^{8} m/s). This inverse relationship implies that a photon of light with a shorter wavelength (e.g "blue" light has a higher energy than a photon of "red" light). Although blue and red light are different in total energy, they can both be used in photosynthesis. However, only radiation with wavelengths between 400-700 nm is photosynthetically active radiation (PAR).

Chlorophyll is the major photosynthetic pigment in plants and can be categorised into five different types; chlorophyll a, b, c, d. Chlorophyll a is commonly found in all aerobic organisms, but the content of the other chlorophylls varies with the environment and the type of organism (Hart, 1988). In plants, a number of chlorophylls and carotenoids are located within chloroplast to form photosystems. In the light reactions of photosynthesis, a pigment molecule absorbs light energy and then transfers the energy to other pigments until it reaches a reaction centre, a complex of several proteins, chlorophylls and other co-factors assembled together to execute a redox potential sufficient to oxidise water, which is the primary energy conversion reaction of photosynthesis. In plants, there are two different photosystems, each with a different reaction centre. Photosystem I (PS I) has optimal light absorption at 700 nm (reaction centre P700) whereas photosystem II (PS II) has optimal light absorption at a wavelength of 680 (P680 reaction centre). Both PS I and PS II are cooperatively involved in the light reactions of photosynthesis which is initiated when the light energy transferred to the P680 of PS II causes removal of an electron from the reaction centre. The P680 then requires an electron which is taken from a water molecule, so that O_2 is released. The electron from P680 is boosted to a higher energy level, passed to the primary acceptor, Pheophytin (Pheo), before it reduces plastoquinone (PQ) to plastoquinol (PQH_2), which is formed on the stromal side of the thylakoid membrane. PHQ_2 is a lipophilic molecule diffusing in the membrane to a transmembrane protein, cytochrome b6 complex (Cyt b_6) and entering the Q cycle (Figure 1.6). This cycle produces reduced plastocyanin (PC) inducing

proton (H^+) gradients across the thylakoid membrane and the release of H^+ chloroplast stroma into lumen side of thylakoid membrane generating proton motive force which is required for ATP (adenosine triphosphate) production. Then, the energised electron from PC passes through the series of redox reactions to reach P700 of PS I, as illustrated in Figure 1.6. In PS I, the electron is either transferred to Ferodoxin before reaching the final electron acceptor, $NADP^+$ which is then reduced to NADPH (reduced nicotinamide adenine dinucleotide phosphate) or transferred to Cytochrome b in the thylakoid lumen contributing to the proton extrusion and production of ATP accordingly. Two NADPH and four ATP molecules are required in the Calvin cycle (dark reactions) to reduce one molecule of CO_2 in the dark reactions (Salisbury and Ross, 1992, Lawler, 1993).

1.4.2 Calvin cycle

Calvin cycle (or the dark reactions) of photosynthesis lead to CO_2 being fixed and converted into carbohydrate using a series of chemical reactions known as the Calvin cycle (Bassham et al., 1950). The Calvin cycle occurs in the stroma of chloroplast and consists of three main phases: carboxylation, reduction and regeneration. In the Calvin cycle, $C0_2$ is captured by ribulose-1,5-bisphosphate carboxylase/oxygenase (RubisCO) which incorporates the CO_2 into a ribulose-1,5-bisphosphate (RuBP) molecule. This leads to the formation of a 3-C compound product, phosphoglycerate (PGA). This pathway is called the C_3 photosynthetic carbon reduction cycle or C_3 photosynthesis, and the plants that use this pathway to fix CO_2 are called C_3 plants. However, there are some plants called C_4 plants which have developed a preliminary step to the Calvin cycle using phosphoenalpyruvate (PEP) instead of RuBP at the beginning of CO_2 fixation, producing a 4-C compound product, oxaloacetic acid (OAA).

In C_3 plants, PGA is then progressed through the next steps of carboxylation and reduction using ATP and NADPH produced in the light reactions. In the reduction phase, PGA is reduced to phosphoglyceraldehyde-3-phosphate (G3P), which can either be used to produce more complex sugars, such as sucrose, or utilised in the regeneration phase where it requires ATP to

regenerate RuBP for another cycle of the dark reaction (Taiz and Zeiger, 2010).

1.4.3 Carbon dioxide supply for photosynthesis

CO_2 is the major substrate for photosynthesis and is supplied from the atmosphere into plant leaves via stomata. For photosynthesis, CO_2 diffuses through the interior of the leaf to reach the chloroplast, where it is incorporated into carbohydrates, and water vapour diffuses out through the stomata. Stomata are microscopic pores in the outer epidermal surfaces of leaves which occur in variable numbers (0-3 x 10^8 m^{-2}) on upper (abaxial) or lower (adaxial) surfaces or both surfaces. The total stomatal pore area is about 1% of leaf surface area. Stomatal conductance (g_s) is a measure of gas exchange (CO_2 and water) controlled via regulation of stomatal pore width. Thus, plants control the efflux of water during transpiration and CO_2 influx during photosynthesis via closing or opening of the pores.

Stomata are involved in two conflicting demands of photosynthesis: permitting CO_2 uptake for photosynthesis while restricting water loss via transpiration. Stomatal conductance is known to be correlated with leaf photosynthesis (Wong et al., 1979) and plants grown under a variety of ambient CO_2 concentrations, leaf water potentials and irradiances show large difference in stomatal conductance and, thus, photosynthetic rate. In rice (*Oryza sativa*, L.), leaf photosynthetic rate is highly correlated with stomatal conductance and well-watered conditions (Kusumi et al., 2012).

Net leaf photosynthesis (A) can be calculated by a biochemical model of photosynthesis based on RubisCO kinetics and the regeneration of RuBP which depends on the supply of ATP and NADPH produced by the light reactions (Farquhar et al., 1980; Caemmerer and Farquhar, 1981). In the model, net photosynthesis (A_n) is calculated by the equation

$$A_n = \min(w_c, w_j) - R_d$$

;where R_d is dark respiration rate, w_c is the RubisCO-limited rate of photosynthesis

$$w_c = \frac{V_{max}(c_i - \Gamma_*)}{c_i - K_c(1 + \frac{O_i}{K_0})}$$

,and w_j is the light-limited rate allowed by RuBP regeneration

$$w_j = \frac{J(c_i - \Gamma_*)}{4(c_i + 2\Gamma_*))}$$

;where c_i is the partial pressure (Pa) of CO_2 or the intercellar CO_2 , Γ_* is CO_2 compensation point, O_i is the partial pressure of oxygen or also known as the ambient air pressure, K_c and K_o are Michaelis-Menten's constants of carboxylation and oxygenation of RubisCO, respectively. V_{max} is the maximum rate of carboxylation (μmol CO_2 m^{-2} s^{-1}) which is proportional to the amount RubisCO proteins. J is the electron transport rate (μmol m^{-2} s^{-1}) which depends on the amount of PAR absorbed by chlorophylls in leaf or ϕ (μmol photon m^{-2} s^{-1}) as the equation

$$0.7\,J^2 - (J_{max} + 0.385\,\emptyset)\,J + 0.385 J_{max}\,\phi = 0$$

The initial slope of the light responsed curve of non-stressed plants (Figure 1.7), based on light or apparent quantum yield (ϕ), describes the efficiency with which light is converted into fixed carbon. According to the light response curve, at low light intensities photosynthetic rate increases linearly with irradiance, with the light-driven electron transport limiting photosynthesis. At high light intensities, photosynthesis becomes light saturated and is limited by carboxylation rate that depends on CO_2 diffusion and amount of activated RubisCO (Lambers et al., 1998). In rice, it has been shown that, under high light condition and ambient CO_2, it is RubisCO rather than the amount of the electron transport machineries which limits photosynthetic rate (Hidema et al., 1991).

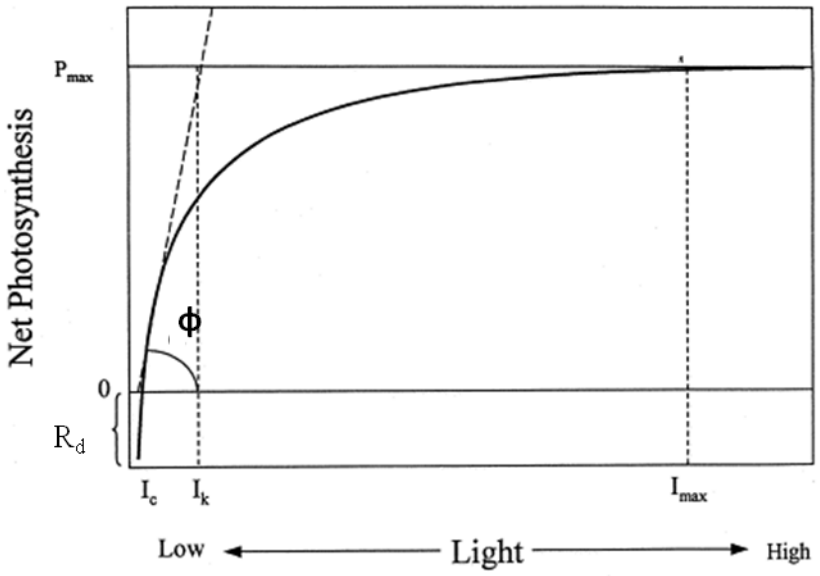

Figure 1.7 Theorethical response curve of photosynthesis to irradiance illustrating maximum photosynthesis (P_{max}), maximum photosynthetic irradiance (I_{max} the minimum irradiance that support P_{max}), compensation irradiance (I_c) and saturating irradiance (I_k). The initial slope of the curve gives the quantum yield (ϕ). R_d is dark respiration rate. At low irradiance, photosynthetic rate is light-limited; at higher irradiance the photosynthetic rate is carboxylation limited. Adapted from Touchette and Burkholder (2000).

1.5 Leaf thickness: current state of knowledge

Leaf thickness is a morphological characteristic correlated to species strategy of resource utilization (Vile et al., 2005). It plays an important role in the amount of light absorbed, CO_2 assimilation rate and nitrogen (N) content of the leaf (Syvertsen et al., 1995; Garnier et al., 1999). In addition, leaf thickness is a morphological trait influenced by the endogenous and environmental factors such as light irradiance (Murchie and Horton, 1997; Terashima et al., 2001; Hanba et al., 2002; Hanba et al., 2004) and CO_2 concentration. For instance, it has been found that leaves of crop species exhibit greater increase in leaf thickness than wild species when grown under elevated CO_2 conditions (Pritchard et al., 1999). Light is a vital resource for plant growth, thus in response to changes in light availability plants develop sun and shade leaves. Sun leaves have a higher light-saturated rate of photosynthesis (P_{max}) on a leaf area basis, greater leaf thickness and greater

nitrogen content than shade leaves (Björkman 1981; Walters and Horton 1995; Murchie and Horton 1997; Walters 2005).

One mechanism by which sun leaves or high-light grown leaves achieve a high P_{max} is by producing thicker leaves. In dicots, variation in thickness is largely due to the formation of taller palisade cells and/ or increase in proportion of palisade versus spongy mesophyll (Lambers et al., 1998). Yano and Terashima (2001) found an increase in the number of cell layers in the palisade tissue of sun leaves. Thick leaves are advantageous to achieve a high P_{max} due to having an extensive mesophyll surface area (S_{mes}). Figure 1.6 illustrates the plausible strategies for increasing S_{mes} which is strongly related to P_{max} (Terashima et al., 2011).

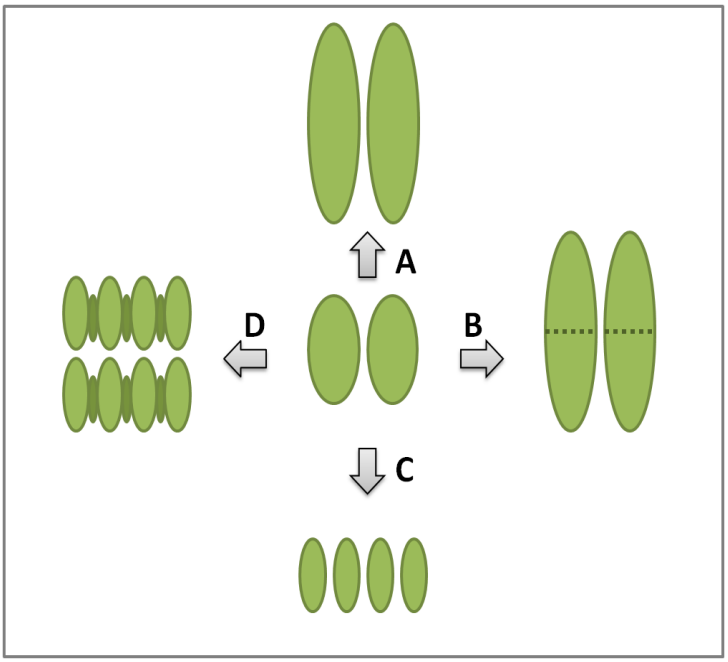

Figure 1.8 Various strategies which plants use for increasing leaf mesophyll surface areas. **A**, cell elongation. **B**, cell elongation accompanied by cell division. **C**, decrease in cell size. **D**, Armed cells of grass species having lobes. In grass leaves, armed cells have large cell surface areas. The leaves with larger cells would expand faster and be thicker to have enough area to accommodate chloroplasts. Adapted from Terashima et al. (2011).

In rice, high light-grown leaves were generally thicker and had a larger cell size, with no difference in cell number either measured at the position of bulliform cells or between bulliform cells and vascular bundle, as shown in

figure 1.7 (Murchie et al., 2005). There are fewer chloroplasts per unit leaf area in low-light grown leaves compared with high light-grown leaves, mainly due to a decrease in thickness of the mesophyll. Shade leaves maximize light capture through enhanced efficiency of photon capture, with more chlorophyll associated with the light harvesting complex (LHC) and a lower chlorophyll a:b ratio. Sun leaves have larger amounts of Calvin-cycle enzymes per unit leaf area due to more cell layers, a larger number of chloroplast per cell, and a higher amount of stroma where these enzymes are located. Moreover, sun leaves also have more stroma-exposed thylakoid membranes, which contain b_6f cytochromes and ATPase. All these components determine photosynthetic capacity at leaf level (Lambers et al., 1998). However, the mechanism that regulates leaf thickness development in sun leaves remains to be ascertained.

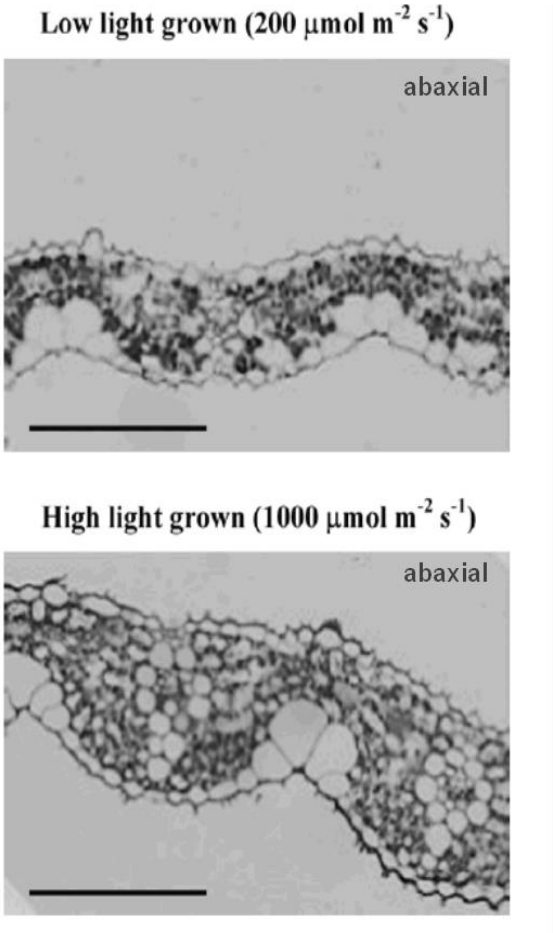

Figure 1.9 Cross-sections of rice leaves grown under low light and high light showing the differences in leaf thickness. Bar = 0.1 mm. Taken from Murchie et al. (2005).

Previous analysis has revealed that the expression of genes involved in light-harvesting was down-regulated in rice leaves, at post-leaf extension stage, transferred from high to low light, with no change in expression of RubisCO genes. However, the expression of genes involved in photo-protection was upregulated (Murchie et al., 2005). Data from this research suggest that leaf thickness, which correlates with higher RubisCO protein level, is determined and set before emergence from the leaf sheath. However, the leaf blade of grasses such as rice develops within the leaf sheath and is not directly exposed to the external conditions such as light. Therefore the development of the leaf in response to light intensity seems to rely on other exposed parts (mature leaves) generating signals which are then sent to the young developing leaves. The presence of a signal from mature leaves to developing leaves has been reported in dicotyledonous plants such as Arabidopsis and tobacco (Lake et al., 2001; Thomas et al., 2004). Systemic signal triggering photo-acclimation in rice was implied in the study of Hubbart et al. (2012). However, the nature of the signal (both in dicots and monocots) and the target these signals in the developing younger leaves remain unknown. Thus, many questions remain with respect to the control of leaf thickness.

1.6 Aims

1. To identify the developmental stage at which control of leaf thickness occurs in response to altered light regime.

2. To study rice leaf morphology changes in response to altered light regime.

3. To investigate the correlation between rice leaf anatomy and leaf performance after acclimation to different light regimes.

4. To study the acclimation of photosynthesis to irradiance level in relation to rice leaf development.

5. To identify the genes potentially involved in the control of leaf thickness in response to altered light regime.

1.7 Objectives

1. To perform a histological analysis of developmental stages of rice leaves under different light regimes to identify when and where changes in cell division and growth, which lead to altered leaf thickness, occur.

2. To use information from (1) to study rice leaf photosynthesis in response to the different light regimes.

3. To use information from (1) to perform a targeted microarray analysis to compare gene expression profiles over time which underpin change in leaf thickness.

1.9 Hypotheses

1. Leaf thickness is set within the leaf sheath during a specific stage of rice leaf development.

2. Changes in leaf thickness affect leaf performances.

3. Change in gene expression underpins the control of leaf thickness.

Chapter 2 | MATERIALS AND METHODS

2.1 Materials

2.1.1 General chemicals

General laboratory chemicals of analytical grade, molecular grade or equivalent were generally ordered from Sigma-Aldrich (USA), Fluka (UK), BDH (UK) Fisher Sciencetific (UK), or Melford (UK). Enzymes and reagents were supplied by Roche (USA), Bioline (UK), Promega (USA), or Invitrogen (USA). Custom oligonucleotides were synthesised by Sigma Lifescience (UK). Plasmid miniprep kits and DNA agarose gel extraction kits were from Qiagen (Germany). Water used for preparing buffers, rice hydroponic growth media and solutions was either reverse osmosis (RO) or deionised ultra-high-purity (UHP*)* water from ELGA ion exchange system (ELGA*,* UK). Molecular work involving DNA of RNA was performed using nuclease-free water from Ambion (Invitrogen, USA).

2.1.2 Plant materials and growth conditions

Seeds of the indica rice cultivar *Oryza sativa* L. cv. IR64 were supplied by Dr. Erik Murchie (University of Nottingham). The seeds were washed three times in UHP water and germinated in 5.5 cm diameter petri-dishes lined with water-soaked papers and sealed with parafilm (Parafilm M, Alcan packaging, UK) for 5 days in a growth chamber controlled at an air temperature 28± 0.2^{o}C with a 12/ 12 hour day/ night cycle and 50±5% relative humidity (RH). A combination of metal halide and tungsten halogen bulbs were used as a light source providing an irradiance of 700 µmol m^2 s^{-1} and 200 µmol m^2 s^{-1} in a high light (HL) chamber and low light (LL) chamber respectively. The 5 days after sowing (DAS) seedlings were then transferred to grow hydroponically in growth medium containing 1.4 mM NH_4NO_3, 0.6 mM $NaH_2PO_4{\cdot}2H_2O$, 0.5 mM K_2SO_4, 0.8 mM $MgSO_4$, 0.009 mM $MnCl_2{\cdot}4H_2O$, 0.001 mM $(NH_4)_6Mo_7O_{24}{\cdot}4H2O$, 0.037 mM H_3BO_3, 0.003 mM $CuSO_4{\cdot}5H_2O$, 0.00075 $ZnSO_4{\cdot}7H_2O$, 0.2 mM $CaCl_2{\cdot}2H_2O$, 0.07 mM Fe-EDTA, pH was adjusted to 5.5 (Murchie et al., 2005). Growth conditions were controlled at 28^{o}C, 50-60% RH, and a 12h/ 12h day/ night cycle. Irradiance for high light (HL) and low light (LL) growth is 700 µmol m^{-2} s^{-1} and 200 µmol m^{-2} s^{-1} respectively. In the

hydroponic system, rice seedlings were individually put in an open bottom 1.5 ml microcentrifuge tube held in a polystyrene rack floating on the hydroponic solution. The surface of the hydroponic floating system was covered by black plastic to prevent the growth of algae as in Figure 2.1 (adapted from Dr. Erik Murchie's lab).

Figure 2.1 The rice seedlings growing in the hydroponic system that is established by using an open bottom 1.5 ml microcentrifuge tube and floating polystyrene rack.

For propagation of the rice seeds, seedlings were heat treated at 40^{o}C for 72 hours and then germinated in the petri-dishes were transferred onto 900 ml square pots containing 350 g of Levington M3 compost and 10 g of Osmocote (Scotts Co. Ltd., UK) and grown at 27 ± 0.2 ^{o}C under a 12-hour photoperiod with irradiance of 1,000 µmol m^{-2} s^{-1} and 50±5% RH. The rice plants were grown in a flooded system in which water was automatically maintained at the level of soil surface. The panicles were bagged. The rice plants were grown for approximately 3 months before harvesting the seeds.

2.2 Methods in leaf morphological study

2.2.1 Analysis of leaf plastochron index

The descriptions of leaf morphology at different plastochron stage during rice leaf development (Itoh et al., 2005) were used as a reference in identification of leaf developmental stages. The cotyledon was counted as the first leaf. The 3rd leaf (Lf3) of rice plants was used as a proxy to establish a plastochron index relating to the developmental stage of the 5th leaf (Lf5). Lf3 was considered to have emerged when its tip appeared above the preceding leaf 2 sheath and then measured its length over time. A number of rice plants with differences in length of Lf3 growing either under high light (HL) or low light (LL) condition were dissected under a stereo-microscope (Leica MZ12, Leica, Germany) to remove all successive leaves and explore the developmental stage of Lf5 inside. Five developmental stages designated as P1, P2, P3, P4 and P5 stage were identified in relation with Lf3 emergence length. The data were collected and used as a reference for other experiments.

2.2.2 Measurement of leaf growth

Leaf blade lengths were measured from leaf tip to collar, the boundary between leaf blade and sheath. Maximum width of leaf blades was measured and averaged from two different positions at the middle, widest part of the leaf. Leaf areas were determined by scanning of leaf blade and the scanned images of leaf blade were processed and analysed using ImageJ (Schneider et al., 2012).

Leaf absolute extension rate at time j (AERj) over two time points was calculated by using the following equation (Hunt, 1982);

$$AER_j = (l_j - l_{j-1}) / (t_j - t_{j-1}),$$

where l is leaf length, t is time, and l_j and l_{j-1} are measurements at times t_j and t_{j-1} is the previous time point.

2.2.3 Measurement of leaf thickness

For leaf thickness measurement, the middle part of fully expanded Lf5 samples were cut then fixed in Carnoy's fixative solution containing absolute ethanol and acetic acid (4:1 (v/v)). The fixation step was done by vacuum infiltration for 30 minutes and the leaf samples were left for further fixation and decolourisation at room temperature (RT) overnight. The fixative solution was then replaced by absolute ethanol for 2 times, 30 minutes. The samples were then dehydrated with absolute ethanol overnight. The ethanol was removed before the pre-infiltration step using a mixture of Technovit 7100 Liquid 1 (Hareus Kulzer, Germany) and absolute ethanol (1:1) that was performed by vacuum infiltration for 30 minutes, and then the samples were kept in the solution overnight before continuing with the infiltration step. In the infiltration step, the leaf samples were infiltrated with fresh 100% Technovit 1 solution composing of 100 ml Technovit 7100 Liquid 1 and 1 g Hardener 1 (Technovit 7100 kit, Hareus Kulzer, Germany) by vacuum infiltration for 30 minutes and kept in the solution for 2 days before embedding. For embedding, the samples were pre-stained with 0.01% neutral red dye in Technovit 1 solution for 30 minutes before embedding in the polymerised resin made by mixing of Technovit solution 1 and Hardener 2 (Technovit 7100 kit, Hareus Kulzer, Germany) in a 15:1 ratio. The lids of 1.5 ml microcentrifuge tube were used as the mould for embedding. The samples were embedded in the resin which was solidified in 2 hours then covered with aluminum foil before further incubation at 37^{o}C for 1 hour to allow further solidification of the surface part of the resin. The embedded samples were then removed out of the moulds before mounting on Histobloc mounting blocks using Technovit 3040 kit (Hareus Kulzer, Germany). After mounting, the embedded leaf samples were sectioned at 2 μm using a microtome (Leica RM2145, Leica, Germany) with a Technovit® Histoblade (Hareus Kulzer, Germany) and attached onto a glass cover slip before staining with 10% toluidine blue in 100 mM phosphate buffer pH 7.0 and mounted onto a glass slide with DPX mounting medium (Fisher, UK). The stained leaf sections were observed using a light microscope (Olympus BX51, Olympus, Japan) connected to a camera (Olympus DP71, Olympus, Japan) at the 20x magnification. Images of the leaf sections were taken for leaf thickness measurement using ImageJ (Schneider et al., 2012).

Two separate measurements of leaf thickness at minor veins and at bulliform cells were taken.

2.2.4 Stomatal density

Leaf segments were taken from the middle part of leaf blades before fixing in the Carnoy's fixative solution for overnight. Before observation, the samples were hydrated with 50% (v/v) ethanol before bleaching in 50% (v/v) economic bleach (Ottimo Supplies, UK) and left until the samples become transparent (about 3 days) at RT. The leaf samples were the treated with 20 µl of chloral hydrate/ glycerol solution, containing 10 g chloral hydrate, 1 g glycerol and 2.5 ml water, before observation using differential interference contrast microscopy (Olympus BX51, Olympus, Japan). For stomatal counting of both adaxial and adaxial surface, at least 3 fields of view captured in regions across the leaf width and were used in epidermal cell file width and measurement using ImageJ (Schneider et al., 2012). The images were also used in the analysis of guard cell and supporting cell complex size. For stomatal density, all stomata in each field of view bounded by two minor veins were counted. For stomatal size, at least 10 stomata/field of view were counted, with data captured from stomata in each row of cells containing stomata.

2.3 Methods in physiological study

2.3.1 RubisCO protein analysis

Seventeen leaf discs (4.5 mm^2/disc) taken from mature Lf5, were ground to a powder in liquid nitrogen by using a pre-cooled micro-pestle and extracted with 50 mM Tris-HCl (pH7.0), 10 mM MgCl2, 1 mM EDTA, 5 mM dithiothreitol, 5% (w/v) insoluble polyvinylpolypyrrolidone and 10% (v/v) glycerol. The crude extracts were centrifuged at 15,000xg for 15 minutes, the supernatants collected, and then protein concentration was estimated by the Bradford protein assay method (Bradford, 1976) using a UV/ Vis spectrophotometer Lambda 40 (Perkin-Elmer, USA). For estimation of RubisCO content on a leaf area basis, the proteins extracted from the leaf samples were separated by SDS-PAGE on a 12.5% (w/v) separating gel (from acrylamide/ bis-acrylamide 30% solution, Sigma, USA) with 4% (w/v) stacking gel in 1x

SDS-PAGE running buffer (24.8 mM Tris, 0.192 mM glycine, 0.1% (w/v) SDS) using a standard Laemmli procedures (Laemmli, 1970) for 1 hour at 150 volts constant, then stained with Brilliant Blue G colloidal concentrate (Sigma, USA) for 30 minutes before de-staining with a de-staining solution (30% (v/v) methanol, 10% (v/v) ethanol and distilled water) for 2 hours. A linear-response between band density and amount of protein loaded onto the gel was calibrated. The protein band intensity of the RubisCO large sub-unit was quantified in scanned gels (Canoscan 3000, Canon) using ImageJ (Schneider et al., 2012). At least 6 leaves were analysed per treatment.

2.3.2 Chlorophyll analysis

Leaf discs (5 discs/ leaf) were taken using a leaf borer and extracted 3 times with a total volume 1 ml of 80% Ethanol at 70°C for 20 minutes. The crude extracts were centrifuged at 7000xg for 5mins and then the supernatant were collected. The supernatants from the three extractions (total volume 1 ml) were pooled and incubated in darkness for 1 hour before measurement using a UV/ Vis spectrophotometer Lambda 40 (Perkin-Elmer, USA). The absorbance of chlorophyll a and b were measured at 665 nm and 649 nm, respectively. Leaf pigments were quantified using the following equations (Lichtenhaler and Wellburn, 1983).

$$\boldsymbol{c_a} = 13.95\ A_{665} - 6.88\ A_{649}$$

$$\boldsymbol{c_b} = 24.96\ A_{649} - 7.32\ A_{665}$$

$$\boldsymbol{Chlorophyll\ a{:}\,b} = \frac{C_a}{C_b}$$

; Where chlorophyll *a* is $\boldsymbol{c_a}$, chlorophyll *b* is $\boldsymbol{c_b}$.

2.3.3 Photosynthetic light response measurement

Photosynthetic light response measurements were taken from the widest part of the fully expanded 5th leaf (Lf5) using a Li-Cor 6400 portable photosynthesis system (Licor Biosciences, USA). The mean value of the leaf width measured from 2 different positions was noted and used for calculation of the leaf area contained in the leaf chamber IRGA. The leaves were dark

adapted in a dark growth chamber for 1 hour before measurement that the plants were covered using a black plastic bag if plants tranfering was needed. Then, the photosynthetic CO_2 assimilations were measured at 28°C block temperature, 400 µmol mol^{-1} CO_2 was supplied with 400 µmol mol^{-1} s^{-1} flow rate. The chamber fan was set at "Fast". The range of photosynthetic photon flux density (PPFD) value used in this experiment is listed in Table 4.1. Blue light was provided at 10 % of total photosynthetically active radiation (PAR). The leaves were exposed to each PPFD and left for data stabilization for at least 1 minute and maximum of 3 minutes. Prior to data recording, the IRGA was set for automatica equilibration (match) of reference and analysis gasses.

2.3.4 CO_2 response measurement, The A/C_i curve

The net CO_2 assimilation response to the variation of CO_2 concentration in rice leaf was studied using the widest part of the fully expanded Lf5. The mean value of the leaf width measured from 2 different positions was noted and used for calculation of the leaf area contained in the IRGA chamber. The leaves from all sample groups were acclimated in the high light chamber for 1 hour before measurement. Photosynthetic CO_2 assimilation was measured at 28°C block temperature, 1000 µmol m^{-2} PAR, with 400 µmol s^{-1} flow rate using a Li-Cor 6400 portable photosynthesis system (Licor Biosciences, USA).To prevent stomatal closure, blue light at 10 % of total PAR was provided. The chamber fan was set at "Fast". The range of atmospheric CO_2 used in this experiment is listed in Table 4.2. The leaves were exposed to each CO_2 concentration and left for data stabilization for at least 1 minutes and maximum of 3 minutes. Prior to data recording, the IRGA was set for automatically equilibration (match) of reference and analysis gasses.

The net CO_2 assimilation were recorded and put into the PS-FIT A/C_i fitting curve model created in Microsoft excel file by C.J. Bernacchi, modified from Bernt Fischer's original design. Photosynthetic parameters were calculated by the curve fitting model. The concentration of CO_2 within the leaf (C_i) is calculated as follows:

$$C_i = \frac{\left(g_{tc} - \frac{E}{2}\right) C_s - A}{g_{tc} + \frac{E}{2}}$$

;where g_{tc} is the total conductance to CO_2, E is transpiration rate, C_s is the atmospheric concentration of CO_2 and *A* is net photosynthesis (Caemmerer and Farquhar, 1981).

2.3.5 Analysis of carbon isotope discrimination

Leaf discs (4.5 mm^2/disc) were taken from mature Lf5, 15 discs/ sample, and dried at 70°C oven for 24 hrs, ground into smaller pieces before weighing, then loaded into an ANCA GSL 20-20 mass spectrometer (Sercon PDZ Europa, UK) for $^{13}C/^{12}C$ ratio analysis. Briefly, the samples are loaded into tin capsules and placed for burning in a furnace at 1000°C whilst in an atmosphere of oxygen. The tins were ignited and burned exothermally which caused temperature raising and oxidization of the samples. Complete combustion was confirmed by passing the combustion products through a bed chromium oxide at 1000°C by using a helium gas. A 15 cm layer of copper oxide followed by a layer of silver wool completed the combustion and removed any sulphur. Then, the products were passed through a second furnace containing 600°C copper where absorption of excess oxygen and reduction of nitrogen oxides to elemental nitrogen were occurred. A trap containing anhydrous magnesium perchlorate was then used to remove water before the gas stream was passed into a gas chromatograph (GC) and then passed into a mass spectrometer where the $^{12}CO_2$ and $^{13}CO_2$ are ionized and separated by mass using a magnetic field. The isotope species were detected separately and from the ratio the level of ^{13}C can be calculated. Calibration using known the PDB standards allows total carbon and ^{13}C content to be obtained from each sample. At least 6 leaves were analysed/treatment. The ratio of unknown to standard isotope distribution is $\delta^{13}C$, which can be calculated from the following equation (Lawlor, 1993).

$$\delta 13C\ (‰) = \frac{\left({}^{13C}/_{12C}\right)\text{unknown substance} - \left({}^{13C}/_{12C}\right)\text{standard}}{\left({}^{13C}/_{12C}\right)\text{standard)}} \text{ x } 1000$$

2.4 Methods in gene expression analysis

2.4.1 RNA extraction

Total RNA was extracted using the guanidine thiocyanate method using TRIzol® reagent (Invitrogen, USA). Rice leaf primordia at P3 stage of leaf 5 (60 leaf primordia/ sample group) were dissected and stored at -80ºC before grinding in liquid nitrogen using a pre-cooled micro-pestle. The ground leaf primordia were then homogenized by grinding in 500 µl TRIzol® reagents before incubation for 2 minutes at 37ºC and then 5 minutes at room temperature. Chloroform (100 µl) was added and mixed with the homogenised tissues before further incubation at room temperature for 5 minutes. The homogenised tissues were centrifuged at 12,000xg at 4ºC for 10 minutes. The colourless upper aqueous phase was collected and then mixed with 300 µl of isopropyl alcohol before incubation at -20ºC overnight. Centrifugation at 12,000xg was then performed to collect the precipitated RNA before a washing step using 80% ethanol. The RNA pellets were air dried and dissolved in 20 µl of nuclease-free water. RNA concentrations were measured at 260 nm by using a NanoDrop machine (NanoDrop8000, Thermo Scienetific, USA) and standardised using agarose gel electrophoresis with 1.5% (w/v) agarose gel in 1x TAE (40 mM Tris, 20 mM acetic acid, 1 mM EDTA), run in 1x TAE buffer at 50 volts for 2 hours.

2.4.2 Microarray analysis

Rice plants were grown under high light condition (HL) until Leaf 5 (Lf5) developed to P3 stage and then were collected for micro-dissection and RNA extraction as 0 hr-HL sample. A number of rice plants were transferred from HL to low light (LL) and then RNA was extracted from the P3-stage Lf5 after 6 or 24 hours of transfer (Figure 5.1). There were 5 different sample groups used in this study, i.e., 0 hour HL, 6 hours HL, 6 hours LL, 24 hours HL and 24 hours LL. The microarray analysis of 3 replicates per sample group was performed using Affymetrix 57K Rice gene chip (Affymetrix, USA) containing 57381 probesets by NASC's Affymetrix service (NASC, University of Nottingham).

Microarray data analysis was done using MicroArray Analysis Of VAriance (MAANOVA) statistical analysis package which is a part of the Bioconductor project (http://www.bioconductor.org/packages/release/bioc/html/maanova.html) run in the R programming (available at http://www.r-project.org/). The Robust Multichip Average (RMA) algorithm (Bolstad et al., 2003) was used for background adjustment, normalisation and probe-level summarisation of the microarray samples by using the R package. Differentially expressed genes (DEGs) were identified using T-test and the fold changes between the log2 mean values for each comparison were calculated. John Storey's false discovery adjustment (jsFDR) method (Storey, 2002) was performed. The adjusted p-value threshold was 0.05. Annotations of the probesets were done using Rice.na33.annot.csv file and NetAffx-Rice (NetAffx™ Analysis center, http://www.affymetrix.com/ analysis/index.affx).

2.4.3 cDNA synthesis (Reverse transcription)

2 µg of total RNA as measured by using a NanoDrop machine (NanoDrop8000, Thermo Scienetific, USA) and standardised by using gel electrophoresis was cleaned using a DNA-free™ kit (Ambion, Invitrogen, USA) containing 1.5 µL 10x DNase buffer and 1 µL rDNase in a 15 µL reaction mixture with 1 hour incubation at 42°C in a heat block (Grant, UK). The enzyme was inactivated with 1 µL inactivation buffer and incubation for 30 min at 37°C. 1 µg of total RNA (DNA-free) was then used as a template for first-strand cDNA synthesis by mixing with 1 µg of oligo-d(T)18 primer (Promega, USA) in a total volume of 20 µl, heated at 70ºC for 5 minutes and then incubated at 4ºC for 2 minutes before reverse transcription, in a total volume of 50 µl in the reaction mixture containing 5 µl of MMLV-RT buffer solution, 500 µM dNTPs, 200 units MMLV-Reverse transcriptase RNase H minus (Promega, USA) at 42ºC for 1 hour.

2.4.4 Quantitative polymerase chain reation (qPCR)

The cDNAs used in this study were from the 6 hrs HL and 6hrs LL sample groups (Figure 5.1). Real-time quantitative PCR (qPCR) were performed in 96 well plates sealed with optical adhesive covers (ABI PRISM®, Applied Biosystems, USA) using the qPCR reaction mixture in total volume of 20 µl contained 2 µl of cDNA (obtained from 1 µg RNA), 10 µl of 2x

SYBR®Green PCR Mastermix (Applied Biosystems, USA), 1 µl of 10 µM forward primer and 1 µl of 10 µM reverse primer (primer sequences for all the genes of interest are listed in Table 2.1). Primers were designed using Primer 3 (available at http://frodo.wi.mit.edu/).

The elongation factor gene, eEF1A was used as an endogenous control in this study. Standard curve method was used for pre-screening the Ct values of the primers by using 4 different concentrations of cDNA obtained by 2 fold-serial dilutions. The qPCR experiments were performed in triplicate for each gene of interest and run for 40 cycles as in Figure 2.2 using an ABI StepOnePlus™ Real-Time PCR system (Applied Biosystems, USA) and then analysed by StepOne Software (version 2.2, Applied Biosystems, USA).

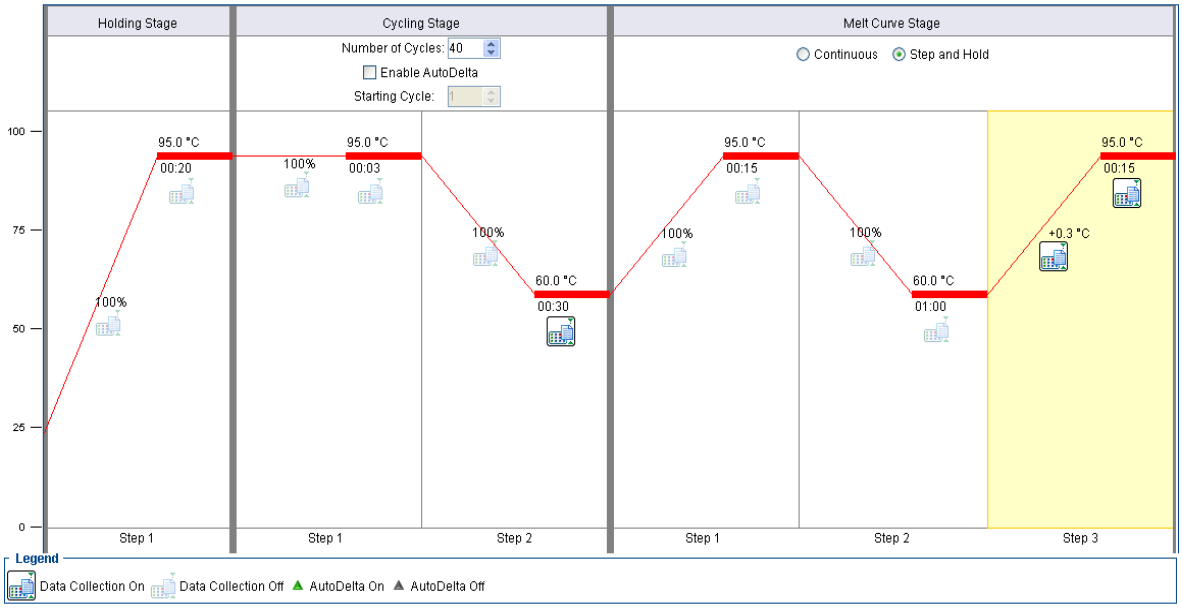

Figure 2.2 The qPCR conditions set in the ABI StepOnePlus™ Real-Time PCR system (Applied Biosystems, USA).

Table 2.1 Sequences of primers used in q-PCR.

Gene	Primer Name	Sequence (5'→3')	Tm (^{o}C)	Amplicon size (bp)
Os03g0178000 Elongationfactor, eEFIa	**eEFIa_F**	GTCATTGGCCACGTCGACTC	68.1	118
	eEFIa_R	TGTTCATCTCAGCGGCTTCC	67.7	
Os05g0433000 Serine/threonine-protein kinase SAPK4	**SAPK4_F**	TGGAGTATGCATCTGGTGGA	64.2	181
	SAPK4_R	GGTGCAATATATGCCGGAGT	63.5	
Os.16037.1.S1_at	**16037_F**	TCAGATGGAGTTCCCCCATT	65.5	151
	16037_R	TTTGATACAATCCAGCTACAG CA	63.3	
Os07g0565400 KinaseSRF3 (STRUBBELIG - RECEPTOR FAMILY 3); SRF8	**SRF8_F**	GCATGAGCCAGAGTTTAGGC	63.8	237
	SRF8_R	GTTCGCTGCTTGAACTTTCC	63.8	
Os04g0587100 Pectin esterase inhibitor	**PecI_F**	GGCCATCGACTACCCCTACT	63.9	170
	PecI_R	GCATCTTCTCCTCCTTGTGC	63.9	
Os10g0551200 SCARECROW-like protein	**Scl1_F**	GAGGAGGAGGAGGAGGAAGA	63.8	192
	Scl1_R	GTGTTGGAGGAGGAAGTTCG	63.6	
Os01g0247900 AWPM 19	**AWPM_F**	TCAGTCTCGACAGACGCAAC	64.4	242
	AWPM_R	ACGTCTGCGTCTTCACCTTT	63.8	
Os03g0692500 galactose-binding lectin family protein	**Gal_F**	GCTGGACAGAGGAACAGAGG	64.1	198
	Gal_R	AATGTCAACATCGCCATTCA	64.0	
Os12g0626200 Auxin responsive SAUR protein family protein	**AuxSAUR_F**	AGTACGGCTACGACCACCAC	62.0	195
	AuxSAUR_R	CCACAAAGTTCTCCGAGCTA	63.9	
OsAffx 32313.1 A1 Oryza sativa Indica Group isolate 93-11 chloroplast	**32313_F**	TTTATGTATCCGCGTTGCTG	63.5	169
	32313_R	GCGTTCATTTGCCTCAAACT	64.0	
Os07g0624600 Similar to Trehalose-6-phosphte phosphatse	**T6PP_F**	GAAATGAGAGAGGCGGTGAG	63.9	183
	T6PP_R	TGCCTTCATGTTGTGGTTGT	64.1	
Os03g0702500 UDP-glucuronosyl/ UDPglucosyltransferase family protein	**UDPG_F**	AGGAAGAGGGGAAGACGTTC	63.5	187
	UDPG_R	TTGGCTAGCTTTCACCGAGT	63.8	
Os01g0220100 Cellulase	**Cellulase_F**	AACGTGCTCTACGCTGAGGT	64.0	177
	Cellulase_R	GGAGCTACGGAAGACGAGTG	63.9	
Os05g0163700 Acyl-coenzyme A oxidase 4	**ACX4_F**	GCCTGTGCAAGCTGTATGAA	64.0	183
	ACX4_R	ACGAGAAGATTGGCTCCAGA	63.9	

2.4.5 *In Situ* hybridisation analysis

I. Fixation, dehydration and embedding

Rice plants with leaf 5 (Lf5) at P3 stage, which were transferred from high light (HL) to low light (LL) for 6 hours, were collected and used for *in situ* hybridisation analysis. The 6 hours LL and 6 hours HL were the 2 groups of the plants used in this study. The rice plants were then cut into a piece of 1 cm flanking the position of the shoot apical meristem (SAM) and fixed on ice in a scintillation vial in a fixative solution containing 4% (v/v) formaldehyde, 5% (v/v) glacial acetic acid and 50% ethanol. Briefly, the tissue samples in the fixative were placed under vacuum for 15 minutes repeatedly for 3 times before replaced with fresh, cold fixative solution and left at 4°C for overnight. The fixative was then removed and replaced with cold 50% (v/v) ethanol, then incubated at 4°C for 30 minutes. Then, the samples were incubated at 4°C through a series of graded ethanol solutions at a concentration of 60%, 70%, 80%, 90% and 100% for 30 minutes/ step. The samples were transferred to room temperature (RT) before incubation in 100% ethanol with 3 times replacement of the fresh ethanol. The ethanol was then removed and replaced with 25% (v/v) Histoclear/ 75% (v/v) ethanol before incubation at RT for 1 hour. The samples were processed at RT through 50% (v/v) Histoclear/ 50% (v/v) ethanol, then 75% (v/v) Histoclear/ 25% (v/v) ethanol and 100%(v/v) Histoclear (Fisher, UK) with 1 hour incubation/ step. The samples were further incubated in fresh 100% (v/v) Histoclear for 1 hour at RT. All the aqueous solutions used in this procedure were sterile/ autoclaved.

On the next day, 10-15 chips of Paraplast Extra (Sigma, USA) were added into the samples vial and incubated overnight at RT. The vial was then placed at 40°C for 1 hour, so that all the paraffin dissolved and then more chips were added before incubation for 3 hours at 40°C. Paraffin chips were further added and left for 3 hours at 40°C before moving into a 58°C oven (Griffin-Grundy, UK) for 1 hour incubation. The mixture of Histoclear and paraffin was poured off and replaced with the pure molten paraffin before an overnight incubation. The paraffin was then replaced with fresh molten paraffin 2 times a day for 3 days. The samples suspended in the molten paraffin were pour into a labelled aluminium foil mould which was then filled up to reach a

final depth of 5-8 mm and left for cooling down and set for 3 hours. For mounting, the paraffin embedded leaf samples were removed from the mould and the individual samples were cut and trimmed to create a true trapezoid before attaching to a paraffin block using some molten paraffin. The samples were transverse-sectioned at 5 µm using a microtome (Leica RM2145, Leica, Germany) with a Low profile disposable blade 819 (Leica, Germany) and mounted onto Polysine slides (Thermo Scientific, USA) using sterile UHP-water. The slide was then placed on a 40^{o}C hot plate (Leica HI1220, Leica Germany) for 10 minutes and left to dry for overnight.

II. RNA probes synthesis

The RNA probes were synthesised via pBluskript II SK (-) plasmid (Figure 2.3) construction before in vitro transcription and labelling with digoxigenin-substituted nucleotide (DIG-UTP). Briefly, cDNA, generated from RNA extracted from the 6 hours HL rice leaves, was used as a template for PCR reactions. The PCR amplifications were carried out using *Pfu* DNA polymerase (Promega, USA) in 50 µl reactions that was composed of 5 µl of 10x *Pfu* DNA polymerase buffer with $MgSO_4$, 2 µl of 10 mM dNTPss, 2 µl of 10 µM forward primer and 2 µl of 10 µM reverse primer, 1µg of cDNA and 0.5 µL of *Pfu* DNA polymerase (2 units/µl) and RNase-free water. Primers with KpnI and SacI recognition sitees added that were used in this study were designed using Primer3 (available at http://frodo.wi.mit.edu/). The primers sequences are listed in Table 2.2.

Table 2.2 Sequences and annealing temperature of primers used in riboprobe synthesis

Gene	Primer Name	Sequence (5'→3')	Tm (°C)	Annealing Temp (°C)	Amplicon size (bp)
Os03g0178000 Elongation factor, eEFIa	**KpnI_eEFIa**	ATAGGTACCGTCATTGGCCACGTC	70.4	60°C	118
	SacI_eEFIa	ATAGAGCTCTGTTCATCTCAGCGG	66.8		
Os07g0565400 (STRUBBELIG-RECEPTOR FAMILY 3); SRF8	**KpnI_SRF8**	ATAGGTACCGCATGAGCCAGAGT	66.8	60°C	237
	SacI_SRF8	ATAGAGCTCGTTCGCTGCTTGA	67.3		
Os10g0551200 SCARECROW-like protein	**KpnI_Scl2**	ATAGGTACCATTGTCGTGTCACCT	64.4	58°C	181
	SacI_Scl2	ATAGAGCTCTTTCACGGGGAATCG	69.0		

The PCR conditions were as follows; initial activation of Taq DNA polymerase at 94°C for 3 minutes, and then 36 cycles of denaturation at 94°C for 30 minute, annealing at 60°C for 30 seconds and extension at 72°C for 1 minute followed a final extension step 72°C for 5 minutes. The PCR products were then digested with the appropriate restriction enzyme and purified via agarose gel extraction method. For agarose gel electrophoresis, the PCR products were mixed with 6x loading buffer (0.2% w/v bromophenol blue, 50% v/v glycerol) and then electrophoresed together with 5 µL Hyperladder I (Bioline) on 1% (w/v) agarose gels in 1x TAE buffer containing ethidium bromide (1 µg/ mL) under 90 V for 1 hour. 1 litre of 50x stock solution of TAE was composed of 242 g Tris base, 57.1 ml glacial acid, 100 mL of 0.5 M EDTA (pH 8.0) and 750 ml deionized water. The PCR products were visualised using a UV-transilluminator (UVP, USA), and the digital images were taken by UVidoc connected with UVitec digital camera (Uvitec, UK). The PCR products were then extracted from the gel and purified using the QIAquick Gel Extraction Kit (Qiagen, USA) following the manufacturer's protocol at room temperature. Briefly, the band of DNA fragment was excised from the agarose gel using a clean scalpel blade under a UV-transilluminator and then transferred into a pre-weighed microcentrifuge tube. 3 volumes of the buffer QG to the gel were added before incubation at 50°C for 10 min until the gel was completely dissolved. The dissolved gel solution containing the PCR products was then transferred to the QIAquick spin column before centrifugation at 13000xg for 1

minute, and then the flow-through was discarded. The column was washed with 750 µl buffer PE and centrifuged at 13000xg for 1 minute and an additional centrifugation for 1 minute was done. The column was then transfer to a fresh 1.5 ml microcentrifuge tube, 25 µl of nuclease-free water (Ambion, Invitrogen, USA) was added and then left to stand for 1 minute before elution by centrifugation at 13000xg for 1 minute. The purified PCR products were ligated to the KpnI/ SacI double-digested pBluskript II SK (-) plasmid using a 2:1 molar ratio of DNA insert:vector. 10 µl ligation reaction was consisted of 1 µl 10x ligase reaction buffer containing ATP and BSA, 0.5 µl T4 DNA ligase (1-3 units/ µl, Promega, USA), nuclease-free water, double-digested PCR products and double-digested pBluescript II SK (-) vector (2:1 molar ratio). The ligation reaction was incubated at RT for 4 hours.

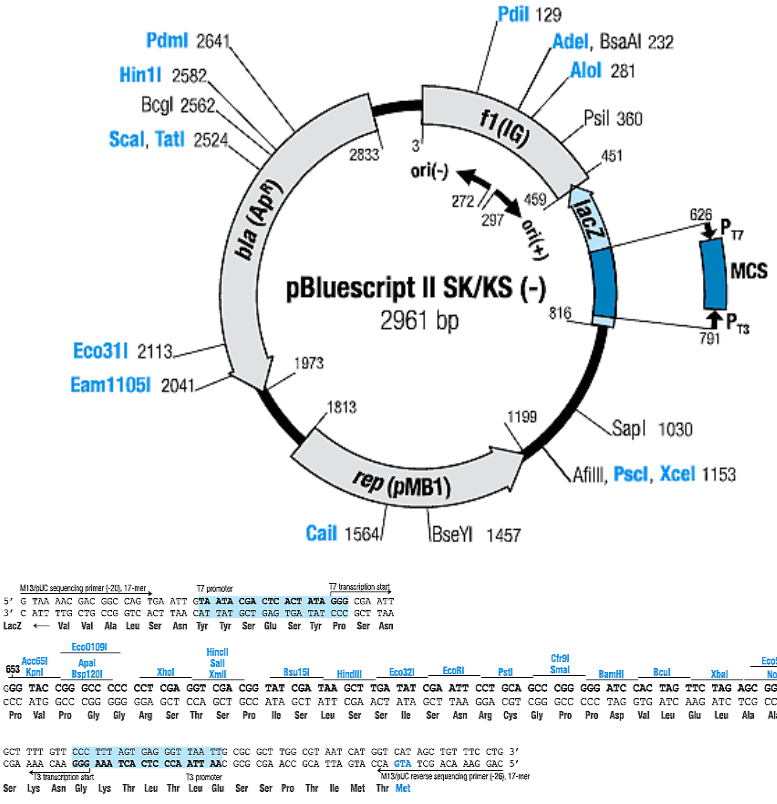

Figure 2.3 The diagram showing the restriction maps and the multiple cloning site of the pBluescript II SK (-). Taken from http://www.picstopin.com

Then, the recombinant plasmids were transformed into competent cells *Escherlichia coli* Top10 (One Shot® Top10 kits, Invitrogen, USA) by incubation of the 10 µl ligation reaction with 50 µl Top 10 *E. coli* on ice for 10 minutes and then heat-shock in 42°C water bath for 40 seconds before placing them on ice for 2 minutes. Then, 250 µl of pre-warmed S.O.C medium was aseptically added to the mixture before shaking incubation (Orbisafe shaking incubator, Sanyo, Japan) at 37°C, 200 rpm for 1 hour. The transformed *E. coli* were then spread on LB-agar selective medium (1% tryptone, 0.5% yeast extract, 10% NaCl and 1.7% agar) containing 100 µg/ml of ampicillin and incubated overnight at 37°C. Single colonies of the transformed *E. coli* were selected and used in colony PCR to screen for plasmid inserts. Briefly, the PCR amplifications were carried out using a small amount of the colony with BioTaq DNA polymerase (Bioline, UK) in 25 µl reactions that was composed of 2.5 µl of 10x NH_4 buffer, 1 µl of 50 mM $MgCl_2$, 1.5 µl of 10 mM dNTPs, 1 µl of 10 µM forward primer and 1 µl of 10 µM reverse primer, 0.25 µL of BioTaq DNA polymerase (5 units/ µl) and RNase-free water. The PCR reactions were performed using a Touchgene Gradient Thermal Cycler (Techne, UK) and the PCR conditions were as follows; initial activation of Taq DNA polymerase at 94°C for 5 minutes, and then 36 cycles of denaturation at 94°C for 1 minute, annealing at 60°C for 30 seconds and extension at 72°C for 1 minute followed a final extension step 72°C for 7 minutes. The PCR products were electrophoresed on agarose gels in 1x TAE buffer containing ethidium bromide (1 µg/ mL) under 90 V for 1 hour to check for the correct size of the insert DNA in the recombinant plasmids. For plasmid extraction, the selected transformed *E. coli* was inoculated in 5 ml LB-broth (1% tryptone, 0.5% yeast extract and 10% NaCl) and then incubated overnight in an orbital shaking-incubator (Orbisafe, SANYO, Japan) at 37°C, 200 rpm. The recombinant plasmids were then extracted from *E. coli* using QIAprep spin miniprep kits (Qiagen, USA) following the manufacture protocol. Then, DNA sequences of the recombinant plasmids were confirmed and ascertained the orientation of the inserts by automated DNA sequencing performed by the Genetics Core Facility at the University of Sheffield (http://www.shef.ac.uk/medicine/research/corefacilities/genetics.html).

The recombinant plasmids were used for synthesis of sense and anti-sense riboprobes using T7 and T3 RNA polymerase respectively. Briefly,

5 µg of the plasmids were digested with a recombinant enzyme, KpnI for anti-sense probes or SacI for sense probes. The digested plasmids were checked by agarose gel electrophoresis and then purified using phenol/ chloroform extraction method. The purified digested plasmids were then precipitated using 1/10th volume of 3M sodium acetate pH 5.2 and 2 volumes ethanol and centrifugation at 12,000xg for 2 minutes. The precipitated DNA were washed with 70% ethanol and air-dried before dissolving in 10 µl nuclease-free water. Then the linearised plasmids were used as a template for *in vitro* transcription reactions (Roche, Germany) using a 20 µl reaction mixture containing 1 µg linearised template DNA, 2 µl 10x transcription buffer, 2 µl DIG RNA labelling mix (Digoxigenin-UTP), 1 µl RNase inhibitor (40 units/ µl), 2 µl T3 or T7 RNA polymerase (20 units µl) and nuclease-free water. The in vitro transcription reactions were incubated at 37^{o}C for 2 hours before 1 µl RNase-free DNase I recombinant (Roche, Germany) was added and left for incubation at 37^{o}C for 15 minutes. 2 µl of 0.2M EDTA was then added and mixed followed by 2.5 µl of 4M LiCl and 75 µl absolute ethanol before incubation at -20^{o}C for overnight. Then centrifugation at 12000xg for 25 was performed and the pellets were collected and washed with cold 70% ethanol. The riboprobes pallets were air-dried and dissolved in 50 µl of 50% (v/v) formamide. 2 µl of the riboprobes were run on a 1% agarose gel in 1x TAE buffer.

III. Hybridisation

For pre-hybridisation, the slides of transverse-sectioned rice plants were mounted in a sterile glass holder and processed through a series of solutions in a volume of 200 ml contained in sterile glass dishes. Briefly, the slides were immersed in 100% Histoclear for 10 minutes (2 times) followed by 100% ethanol for 1 minute then 90% ethanol, 80% ethanol, 60% ethanol and 30% ethanol serially for 1 minute/ each step, then washed in sterile water for 5 minutes. The slides were then incubated in 2x SSC (1x SSC contains 150 mM NaCl, 15 mM $NaHCO_3$ pH 7.0) for 20 minutes before transfer to a glass dish containing pre-warmed 100 mM Tris and 50 mM EDTA, then proteinase was add at a final concentration of 1 µg/ µl before incubation at 37^{o}C for 30 minutes. The slides were then transferred to incubate for 2 minutes in phosphate buffer saline (PBS) pH 7.4 (Sigma, USA) containing

2mg/ ml glycine followed by 2 times washing with PBS for 2 minutes and then incubated in 4% formaldehyde in PBS for 10 minutes. The slides were washed 2 times in PBS before transfer to incubate in 0.1 M triethanolamine adjusted pH 8.0 with conc. HCl for 10 minutes before addition of 1 ml acetic anhydride and a further 10 minutes incubation with stirring. The slides containing sections were then washed 2 times in PBS for 5 minutes before transfer through 30% ethanol, 60% ethanol, 80% ethanol, 90% ethanol and 100% ethanol serially for 1 minute/ each step, and then final washed in 100% ethanol before incubation in a glass dish containing a small amount of 100% ethanol at the bottom at 4^{o}C for 2 hours.

The slides were then removed from the ethanol glass dish and air-dried for 20 minutes. The anti-sense and sense probes used for hybridisation were prepared in 3 dilutions by dilution 1, 5 or 10 µl of stock probes with 50% formamide to make a final volume of 30 µl. The 30 µl probes were heated a 80^{o}C for 2 minutes and then placed on ice before mixing with 120 µl hybridisation buffer (1600 µl, for 12 slides, was composed of 200 µl of 10x salt buffer (100 mM Tris pH 7.5, 10 M EDTA, 3M NaCl), 800 µl Formamide (Amresco, USA), 400 µl 50% dextran sulphate (Amresco, USA), 20 µl 100x Denhardts (Amresco, USA), 20 µl RNase-free tRNA (Roche, USA) and 140 µl sterile nuclease-free water). The mixture of probe and the hybridisation buffer was then dropped onto the sections coated on the slide and covered with a cover slip. The slides were placed in a sealed box and incubated at 50^{o}C for overnight. Washing and signal visualization step were started the next day by removing the cover slips by rinsing with 5 ml of 0.2xSSC pre-warmed in a 55^{o}C water bath and the slides were immediately immersed and incubated in 0.2xSSC at 55^{o}C for 30 minutes, 2 times and further incubation in 0.2xSSC at 55^{o}C for 60 minutes, 2 times. Roche blocking buffer (10% Roche blocking reagent in a buffer containing 100 mM Tris pH 7.5, 150 mM NaCl) was added to the sections before incubation for 40 minutes with gently shaking. The blocking buffer was replaced with BSA blocking buffer (5 g bovine serum albumin in 500 ml of a buffer containing 100 mM Tris pH 7.5, 150 mM NaCl, 15 ml 10% Triton X 100) before a further incubation with shaking for 40 minutes. The slides were removed from the BSA blocker and dried on a clean paper before 150 µl of 1/1250 diluted anti-DIG Antibodies (Roche, USA) was

overlaid on the individual slide and covered with a cover slip followed by incubation at RT for 90 minutes. The coverslips were slid off and the slides were placed in with 50 ml BSA blocker for incubation at RT for 15 minutes, with 4 times replacement of fresh BSA blocker. Then, the slides were immersed in a glass dish containing Developing buffer (100 mM Tris pH 9.5, 50 mM $MgCl_2$ and 100 mM NaCl) and incubated at RT for 10 minutes, 2 times. Then, the slides were removed from the container and gently wiped to remove the excess buffer before 150 µl Developing Reagent (1 ml Developing buffer, 2.2 µl 4-nitroblue tetrazolium chloride (NBT, Roche, USA)) and 1.6 µl 5-bromo-4-chloro-3-indolyl phosphate (BCIP, Roche, USA) were overlaid on the individual slide and then covered with a cover slip. The slides were incubated in the dark at RT for 2-3 days, and then the reactions were stopped with a stopping buffer (10 mM Tris pH 7, 1mM EDTA). Finally, the slides were air-dried and mounted under a cover slip using DPX mounting medium (Fisher, UK).

Chapter 3 | Response of rice leaf morphology to irradiance

3.1 Introduction

One of the most important factors crucial for plant growth and development is the level of irradiance, a major factor determining the CO_2 assimilation rate of individual leaves (Nobel et al., 1993). Leaf anatomy is a key factor leading to differences in light use efficiency, thus influencing net leaf photosynthesis. Leaf anatomy structure has to optimise absorption and conversion of the photosynthetically active part of the spectrum (400-700 nm) for the generation of chemical energy via photosynthesis. In order to maximize this process, it is believed that light should reach all chloroplasts in the leaf (Terashima et al., 2011). However, not only light, but also CO_2 and H_2O are essential for photosynthesis and the supply of these substrates to each chloroplast and the transport of end products out of the individual leaves are crucial for photosynthesis. Therefore, morphology and histology are fundamentally important for leaf function. This chapter describes how rice leaf morphology responds to changing light regime and reports on a series of experiments to investigate the role of leaf developmental stage in this response.

Leaf structure, shape and cell distribution are genetically determined but change, within limits, with prevailing growth conditions allowing adjustment to the environment. Leaf mesophyll structure (the number and density of the mesophyll cell layers) plays a key role in light capturing process for photosynthesis (Lawler, 1993). Variation in light conditions in nature leads to modification of leaf development. It has long been known that plants acclimate to prevailing irradiance by developing sun and shade leaves. Sun leaves are thicker, smaller, have a higher level of photosynthetic components per unit leaf area and a higher light-saturated rate of photosynthesis compared to shade leaves (Boardman, 1977; Bolhar-Nordenkampf and Draxler, 1993; Lambers et al., 1998; Terashima et al., 2001; Yano and Terashima, 2001; Terashima et al., 2011). Leaf anatomy is closely related to photosynthesis, since it contributes to the maintainance of CO_2 concentration in chloroplast stroma, one of the key factors of photosynthesis. It is known that RubisCO, which is able to catalyse either carboxylation or oxygenation reaction, has a low maximum rate of CO_2 fixation, low affinity to CO_2 and also RUBP carboxylation

is competitively inhibited by RUBP oxygenation, which is one of the steps in photorespiration, a waste-energy process (Lambers et al., 1998; Terashima et al., 2011). As a consequence, if the CO_2 concentration in the chloroplast stroma is low, the carboxylation rate will decrease. On the other hand, the oxygenation rate will increase with the wasting of light energy and other resources, i.e., water and nitrogen. One of the key structural features of the leaf that influence CO_2 concentration in chloroplast stroma is mesophyll conductance (g_m) or leaf internal conductance, the conductance for CO_2 diffusion from substomatal cavity to the chloroplast stroma where RubisCO is located. As a low g_m limits photosynthesis and since the diffusion rate of CO_2 in liquid phase is smaller than in the gas phase (Hall et al., 1993), increasing the mesophyll surface area exposed to the intercellular spaces (S_{mes}) should have an advantage by increasing the area for CO_2 dissolution and the effective pathway for CO_2 diffusion, thus photosynthesis. An increase in g_m with greater S_{mes} is positively related to an increase in the total surface area of chloroplasts exposed to the intercellular space (S_c) (Evan and Loreto, 2004; Terashima et al., 2006), since the greater S_{mes} provides more space for the distribution of chloroplasts at the mesophyll cell surface. However, leaves need a considerable amount of RubisCO per leaf area for phosynthesis, thus the ratio of RubisCO/ S_c should be kept small to keep the CO_2 concentration in the chloroplast stroma at a high level. To achieve higher maximum photosynthetic rate at light saturation (P_{max}), sun leaves should have more RubisCO per unit leaf area than shade leaves, and this is consequently supported by a greater S_{mes} which is prerequisite for the larger S_c. This could be an explanation why sun leaves are thicker than shade leaves (Terashima et al., 2011)

The difference in leaf thickness between sun and shade leaves mainly results from adaxial/ abaxial elongation and/ or an increase in layer number of palisade cells in the mesophyll of sun leaves (Hanson, 1917; Ballantine and Forde, 1970; Yano and Terashima, 2001; Yano and Terashima, 2004). Due to the reduction in mesophyll thickness fewer chloroplasts are found in shade leaves (Lambers et al., 1998). Two-cell layered palisade tissue was observed in sun leaves of *Chenopodium album* L. as a result of a change in cell division orientation (Yano and Terashima, 2001; Yano and Terashima, 2004). It is believed that, in sun-type *C. album,* the anticlinal and periclinal cell division

that occur simulatanously during leaf development makes the two-cell layered palisade tissue. It has been observed that sun leaves have a larger mesophyll cell size than shade leaves in *Lolium* genotypes (Wilson and Cooper, 1969), whereas in soy bean, leaves growing under high light intensity either have 3-4 layers palisade mesophyll or a larger spongy mesophyll than low light-grown leaves which have two layers of the mesophyll cells (Ballantine and Forde, 1970). Thus, the cellular mechanism by which altered leaf thickness is achieved may vary depending on species. The level of irradiance also affects stomatal density and stomatal index. Thus, sun leaves tend to have higher stomatal density than shade leaves within a smaller leaf blade (Givnish, 1988; Bolhar-Nordenkampf and Draxler, 1993; Lake et al., 2001). Moreover, there are also reports that the size of stomata of shaded plants is smaller than in sun plants (Wilson and Cooper, 1969; Hubbart et al., 2012).

With respect to rice, it has been reported that thickening of rice leaves in response to high irradiance is a result of mesophyll cell enlargement, not by increasing cell number (Murchie et al., 2005). The increase in rice leaf thickness is also found to be associated with a reduction in leaf area. Murchie *et al*. (2005) transferred low-light grown leaves to high light conditions at progressively earlier points from when the leaves were fully expanded to see if there was any restriction on acclimation to high light intensity of the leaves with respect to leaf thickness and cell size. They found that the induction of further cell expansion by high light intensity did not happen if the leaves were already emerged from leaf sheath. Therefore, low-light grown leaves were unable to achieve high-light leaf morphology if exposed to high irradiance after emergence from the leaf sheath. They suggested that the reason for this might be the termination of cell elongation which occurs before emergence of a leaf from the surrounding leaf sheath. Their findings suggested that acclimation to irradiance via leaf structural changes only happens before the emergence of the rice leaf blade. It is unclear from this experiment whether leaves developing within a sheath can perceive alterations in irradiance or whether the altered thickness response was due to a signal perceived by older leaves (exposed to the environment) and somehow transmitted to the developing leaves, although available data supports the idea that older leaves can perceive and transmit such a signal (see below). This study leaves open the

question of exactly at which stage of leaf development control of the rice leaf thickness occurs. An aim of the experiments reported in this chapter is to more precisely define the developmental window during which rice leaf thickness can be changed in response to altered irradiance.

Perception of the light environment is a key step for plants to establish appropriate leaves that are adapted to irradiance. Although there are questions as to the mechanism involved, several studies have shown that light quantity is a stimulus that has a greater impact on leaf thickness and differentiation than light quality (Kim et al., 2005; Lopez-Juez et al., 2007; Ferjani et al., 2008). As to which parts of the plant are involved in light recognition, much is still unclear. The shoot apical meristem (SAM) is protected from environmental risks including severe light stress, by being shielded within the surrounding bud. Exactly how much light gets through to the SAM is unclear, but the general consensus is that other parts of the plant that are directly exposed to prevailing irradiance sense the light and send signal(s) to the SAM so that the young leaves adapt their form accordingly. Recent investigations support the hypothesis of a long-distance signal from mature leaves to younger developing leaves (Lake et al., 2001; Yano and Terashima, 2001; Lake et al., 2002; Thomas et al., 2004; Ferjani et al., 2008). The study of Yano and Terashima (2001), for example, demonstrated the presence of a signal from mature leaves as they applied a partial shading treatment to *C. album* and observed that, even though a young developing leaf of high light grown plants was shaded, it also produced two-cell layered palisade tissue which was similar to leaves grown continually under high light intensity. A study in *Arabidopsis thaliana* (Lake et al., 2001) reported that light intensity and CO_2 level perceived by mature leaves also affected stomatal development in young developing leaves. There are several candidate long-distance signals that might be the key regulators for adaptation to light environment in plants including RNAs, peptides, sugars, phytohormones, and redox-sensing compounds (Karpinski et al., 1999; Kim et al., 2005; Coupe et al., 2006), however there is no conclusive evidence to support the identity of any of these as the endogenous signal involved in long-distance regulation of early leaf development.

3.2 Aims

1. To identify the developmental stage at which control of leaf thickness occurs in response to altered light regime in rice.

2. To study changes in rice leaf morphology in response to altered light regime.

3.3 Brief methodology

Rice plant growth conditions are discussed in detail in Chapter 2. A brief summary of methods used in the study of rice developmental stage and leaf morphology are described below. Mean and standard deviation from different treatments were analysed using ANOVA and Tukey's post hoc test. Leaf 5th was the target leaf for analysis in the experiments.

3.3.1 Leaf plastochron index

The 3rd leaf (Lf3) of rice plants was used as a proxy to establish a plastochron index relating to the developmental stage of the 5th leaf (Lf5). We considered Lf3 to have emerged when its tip appeared above the preceding leaf 2 sheath and then measured its length over time. A number of rice plants with differences in length of Lf3 growing either under high light (HL) or low light (LL) conditions were dissected under a stereo-microscope to remove all successive leaves to explore the developmental stage of the Lf5 inside. We used Itoh et al., (2005) as a reference to identify rice leaf developmental stages.

3.3.2 Leaf size

Leaf blade lengths were measured from leaf tip to collar, the boundary between leaf blade and sheath. Maximum width of leaf blades was measured and averaged from two different positions at the middle part of the leaf. Leaf areas were determined by leaf blade scanning and the scanned images of leaf blade were processed and analysed using ImageJ.

Leaf absolute extension rate at time j (AERj) over two time points was calculated by using the equation; $AER_j = (l_j - l_{j-1}) / (t_j - t_{j-1})$, where l is leaf

length, t is time, and l_j and l_{j-1} are measurements at times t_j and t_{j-1}, the previous time point.

3.3.3 Leaf thickness

For leaf thickness measurements, the middle part of fully expanded Lf5 samples were cut, fixed and dehydrated before embedding in Technovit 7100. The leaf samples were sectioned at 2 μm thickness and stained with toluidine blue. The stained leaf sections were observed using a light microscope at 20x magnification. Images of the leaf sections were taken for leaf thickness measurement using ImageJ. The line selection tool of the ImageJ was used in leaf thickness measurement with length calibration by using the scale bar indicated in the images. Two separate measurements of leaf thickness were taken (at minor veins and at bulliform cells).

3.3.4 Stomatal density

Leaf segments were taken from the middle part of leaf blades before fixing and bleaching steps. Samples were treated with chloral hydrate/glycerol solution before observation using differential interference contrast microscopy. For stomatal counting of both abaxial and adaxial surface, at least 3 fields of view captured in regions across the leaf width and were used in epidermal cell file width and measurement using ImageJ. The areas between two minor viens of the rice leaves were selected for the stomatal counting. The images were also used in the analysis of guard cell and supporting cell complex size. For stomatal density, all stomata in each field of view bounded by two minor veins were counted. For stomatal size, at least 10 stomata/field of view were counted, with data captured from stomata in each row of cells containing stomata.

3.3.5 Transfer experiments

In order to analyse responses in rice leaf morphology to light regime, we applied different light intensities to developing plants transferred between light regimes at specific stages of Lf5 development. For transfer experiments, rice seeds were sowed under HL conditions and transferred to LL when Lf5 of the rice seedlings was at P1, P2, P3, P4 or P5 stage (and vice

versa for the rice plants that were sowed under LL condition and transferred to HL). The transferred plants were left to grow in the new light regime until Lf5 maturity before further analysis. Controls involved rice plants maintained under HL and LL throughout the experiment.

3.4 Results

3.4.1 The study in rice leaf morphology and development

A mature rice leaf is strap-like and divided into three main parts along the proximal–distal axis, as shown in Figure 1.2. The first part of the leaf is the blade, the major site of photosynthesis. The leaf sheath is the proximal region encasing the shoot apex and younger leaves. The third part is the boundary between the leaf blade and sheath which consists of three distinct parts: the lamina joint (collar), the ligule and the auricle.

A new rice leaf forms from the encased SAM and eventually emerges from the leaf sheath of the preceding leaf. The first 4 developmental stages (P1, P2, P3, and P4) occur prior to leaf emergence (Itoh et al., 2005). The P5 used in this study represents the stage after P4, as the leaf emerges from the surrounding sheath. A transverse-section of the stem of a young rice plant (Figure 3.1) shows leaves at the different P-stages surrounding the central SAM.

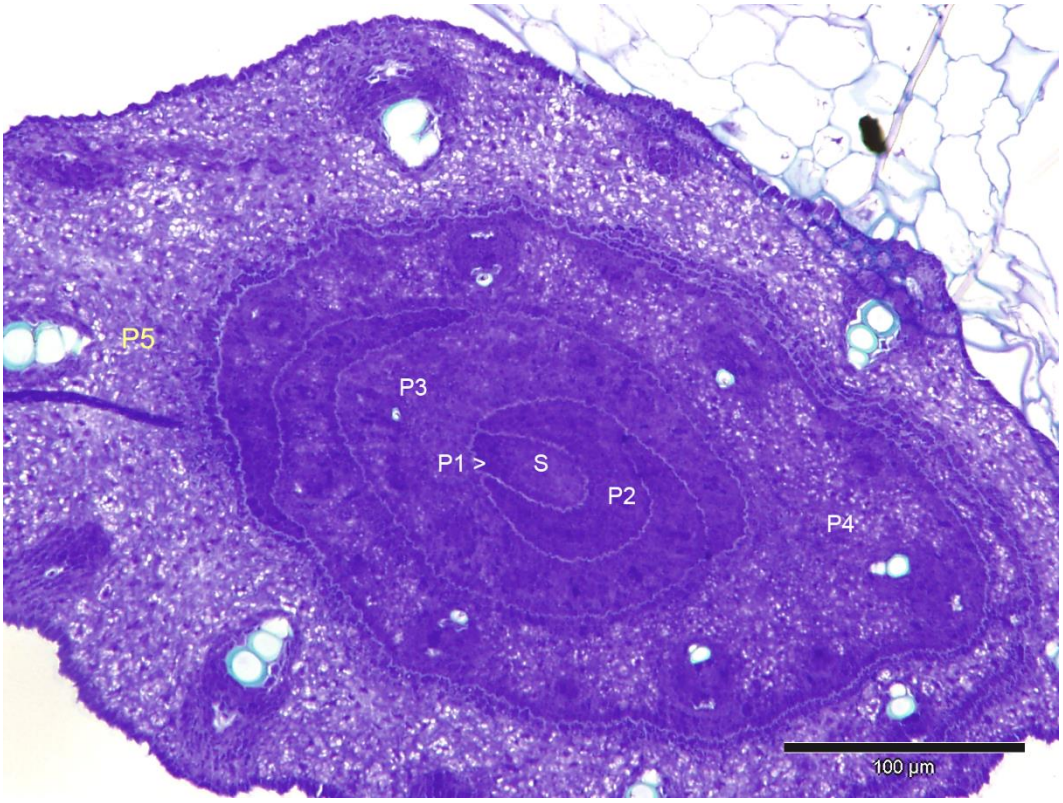

Figure 3.1 Transverse-section of a young rice plant stem. S represents SAM, P1-P5 indicate developmental stage of each leaf.

An analysis of rice leaves grown under either high or low irradiance showed that rice leaves reach different sizes depending on the light regime under which they are grown and which leaf is being studied (Figure 3.2, 3.3). For example, the first leaf (leaf 1) was the smallest fully-expanded leaf in all rice plants. The results in Figure 3.2 show that the fully expanded leaf blades of LL-grown leaves were longer and wider than HL-grown leaves. Thus, the mean maximum length of mature Lf5 growing under HL and LL conditions was 188.16 mm (S.D. $\pm$ 27.88 mm) and 230.60 mm (S.D. $\pm$ 17.15 mm), respectively. Similarly, the mean width of mature LL grown Lf5 was 5.91 mm (S.D. $\pm$ 0.37 mm) which was 0.60 mm (S.D. $\pm$ 0.22 mm) wider than the mean width of HL grown Lf5. I also observed that there were differences in growth rate between HL and LL grown leaves. The first leaf (L1) of HL grown rice plants emerged approximately 6 days after sowing and 7 fully expanded leaves were generated 28 days after sowing while it took around 34 days for LL plants to achieve the 7 leaf stage (Figure 3.2 A, B). These data were also used to calculate the time taken to 50% of full leaf extension (LE_{50}, Table 3.1). The results indicated that high irradiance resulted in a significantly lower LE_{50} suggesting a higher extension rate of the high light-grown leaves under ambient CO_2 level. Leaf blade width of the rice plants growing under different irradiance was also different with differences in leaf width between the different leaf numbers of the same rice plant (Figure 3.3 A, B). The LL leaves were relatively wider than HL leaves. The absolute extension rates of leaves were analysed to confirm the previous study of Murchie et al. (2005) which suggested that rice Lf 5 is a good representative for studying leaf acclimation to irradiance. The absolute extension rates of rice Lf5 growing either under HL or LL was similar to those observed in both earlier (Lf 4) and later (Lf6 and Lf7) formed leaves, i.e, showed a consistent growth curve similar to other leaves (Figure 3.4 A, B). Lf5 was used as the target leaf for analysis in subsequent experiments.

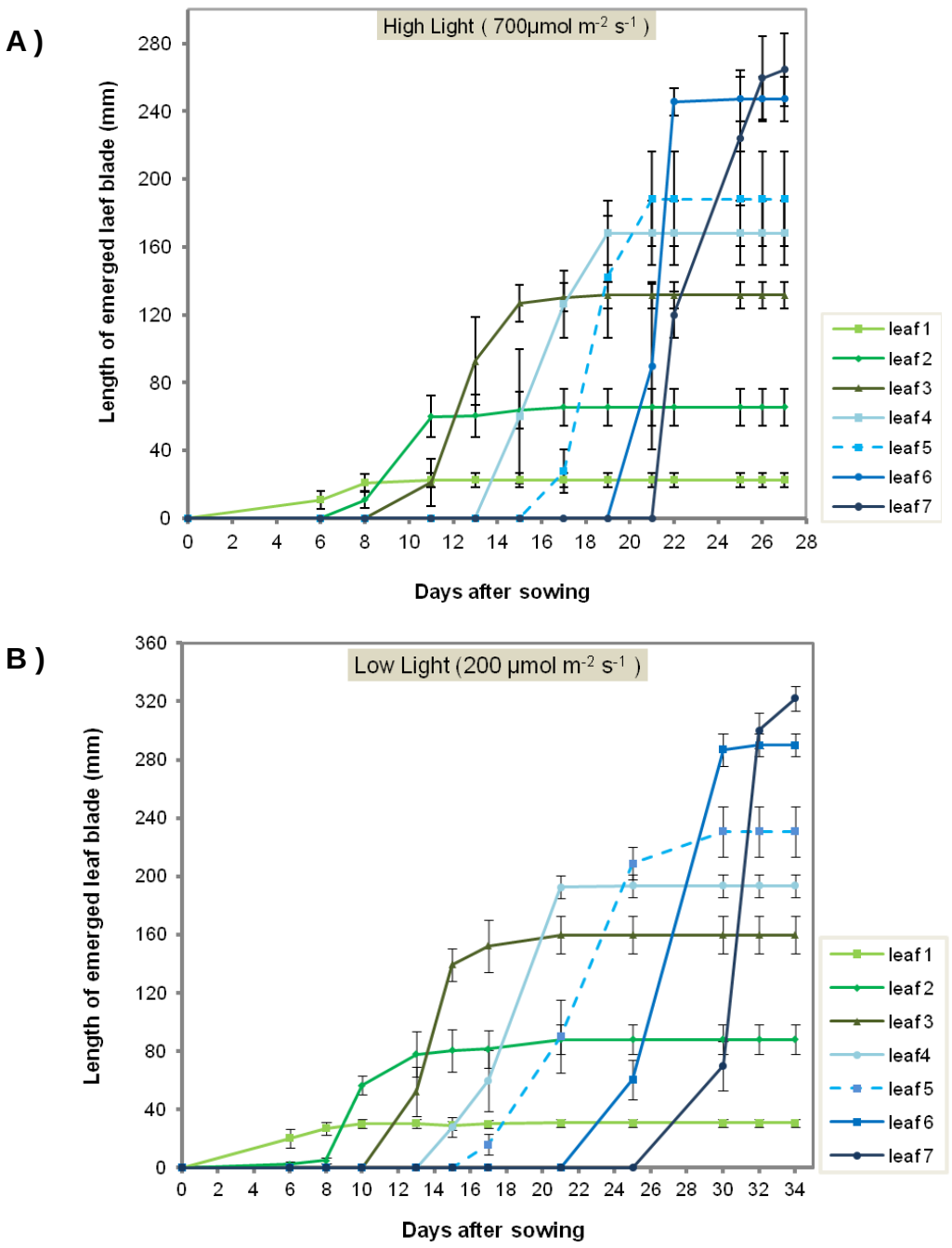

Figure 3.2 Leaf blade length of rice growing under **A)** high irradiance (700 µmol m^{-2} s^{-1}) and **B)** low irradiance (200 µmol m^{-2} s^{-1}). Error bars indicate standard deviation; n=10. Different leaves are indicated in different colours, as shown in the inset.

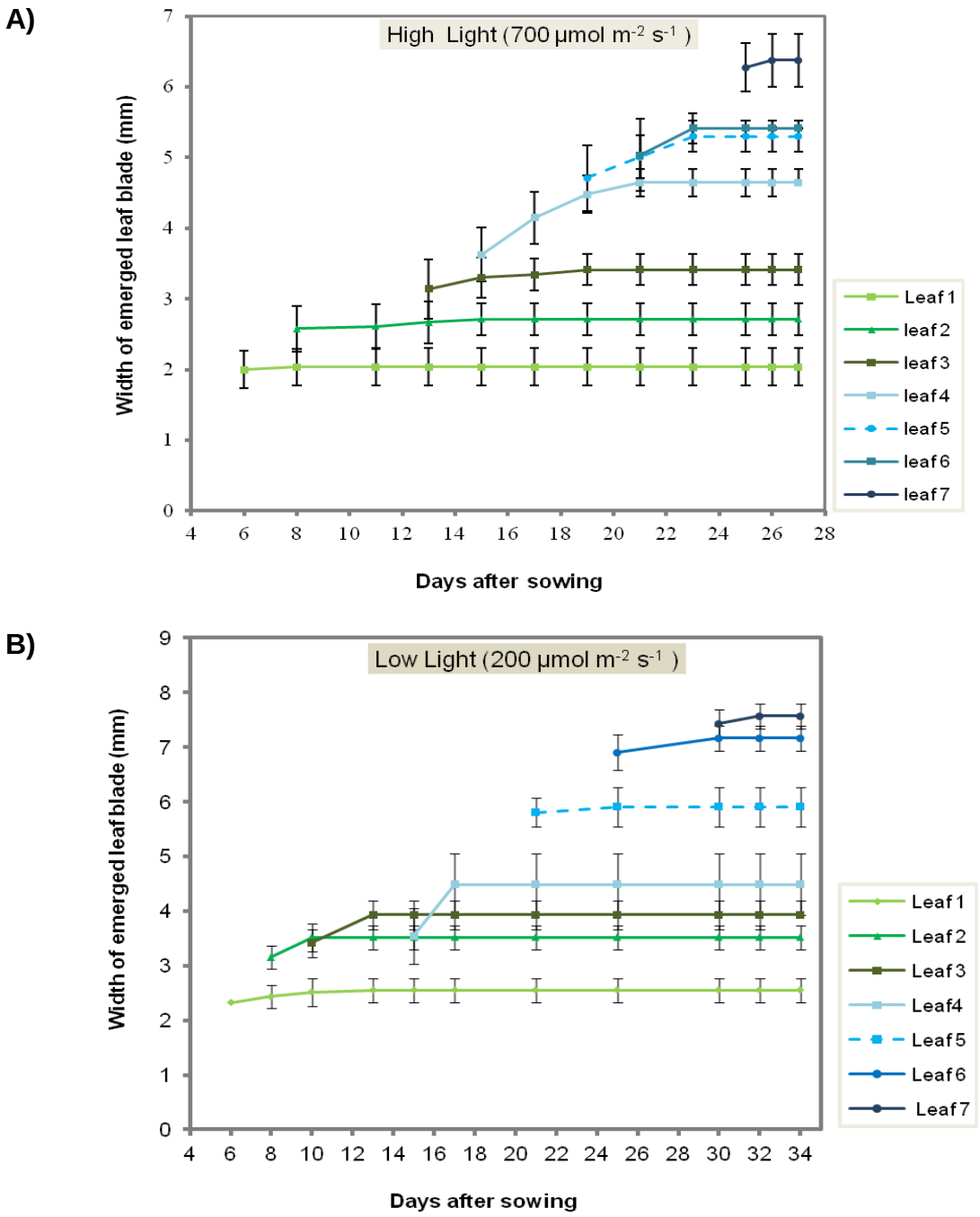

Figure 3.3 Leaf blade width of rice growing under **A)** high irradiance (700 µmol m^{-2} s^{-1}) and **B)** low irradiance (200 µmol m^{-2} s^{-1}). Error bars indicate standard deviation; n=10. Different leaves are indicated in different colours, as shown in the inset.

A)

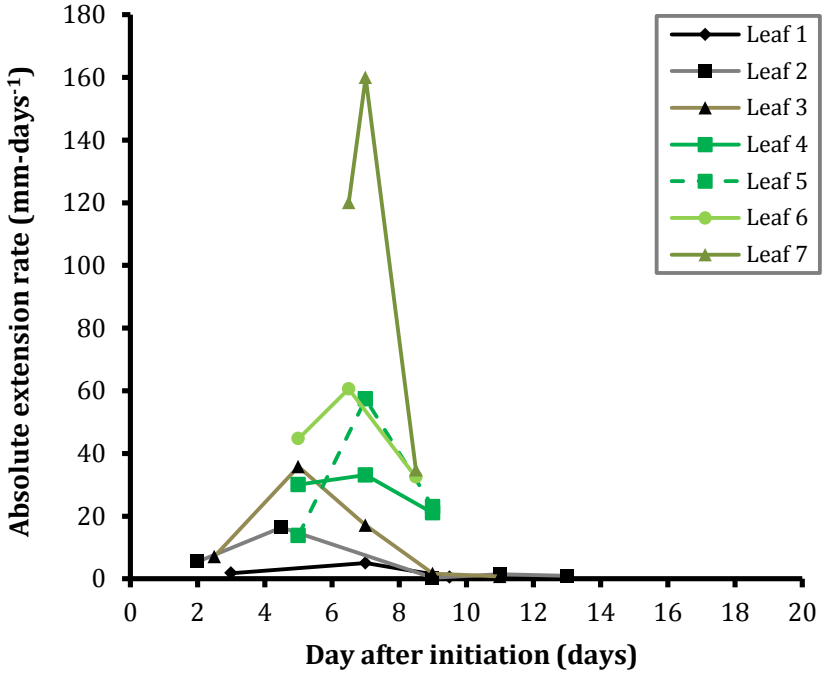

B)

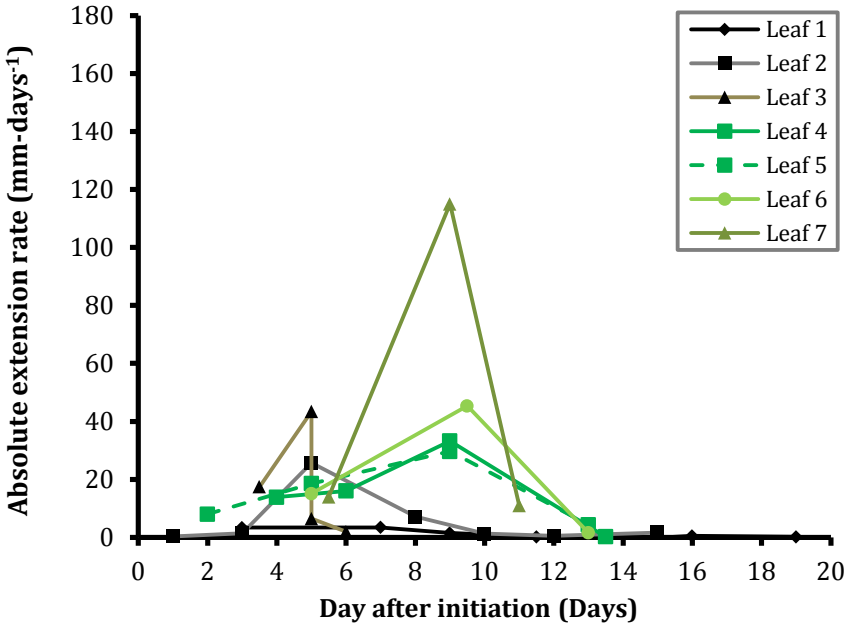

Figure 3.4 Absolute extension rates of rice leaf growing under **A)** high irradiance (700 µmol m^{-2} s^{-1}) and **B)** low irradiance (200 µmol m^{-2} s^{-1}). Different leaves are indicated in different colours, as shown in the inset. n=10.

Table 3.1 Days (days after sowing) taken to 50% full leaf extension in leaf 1, 2, 3, 4, 5, 6 and 7. LE_{50} was calculated from the leaf blade length data in Figure 3.2. For each leaf, identical letter indicates no significant-difference between treatments for a leaf stage (one-way ANOVA, $P < 0.05$). Means ± standard error of the means are given, n=10.

Light condition	Days to 50% full extension (LE_{50})						
	Leaf 1	Leaf 2	Leaf 3	Leaf 4	Leaf 5	Leaf 6	Leaf 7
HL	6.22 ±0.16[a]	8.51 ±0.27 [a]	9.54 ±0.31 [a]	16.32 ±0.13 [a]	18.23 ±0.25 [a]	21.72 ± 0.42 [a]	24.24 ± 0.68 [a]
LL	4.55 ±0.32[b]	9.19 ±0.21 [a,b]	14.62±0.18[b]	18.21 ±0.28 [b]	22.76 ±0.31 [b]	26.87 ± 0.52 [b]	31.54 ± 0.33 [b]

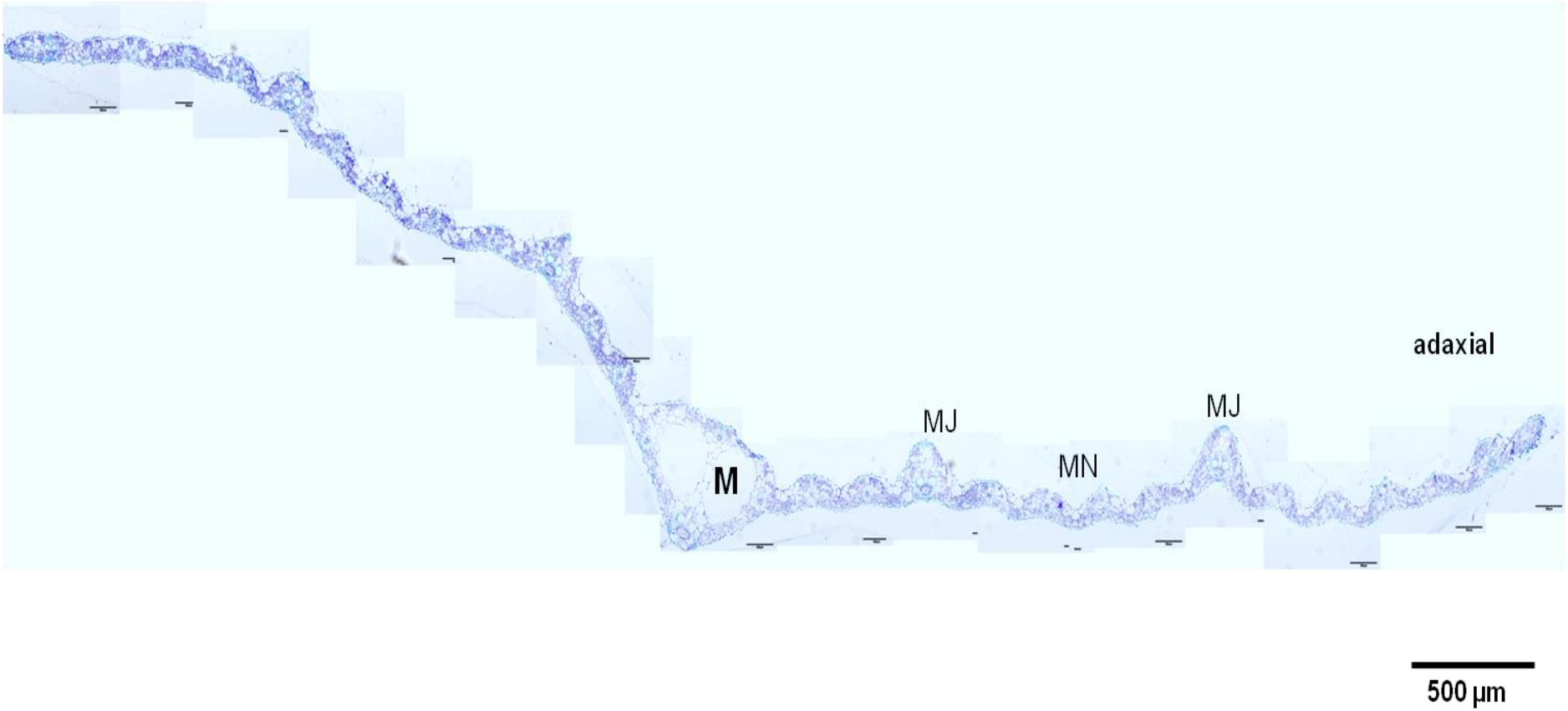

Figure 3.5 A full width cross section of fully expanded rice Lf5 showing a midrib (M), and the repeating pattern of major veins (MJ) and minor veins (MN) extending toward both of the leaf margins.

Cross sections of rice IR 64 leaves revealed the 4 different types of tissue arranged across the leaf: the epidermis, vascular tissue, chlorenchyma and bulliform cells. The chlorenchyma cells (defined as parenchyma cells containing chloroplasts) are the major part of the rice leaf mesophyll layer. Figure 3.5 shows a full width cross section of Lf5. There were approximately 6 major veins, 20 minor veins and 32 bulliform cells regions per mature rice Lf5 (data not shown). The bulliform cells are situated at the adaxial side of the leaf and arranged in vertical rows between vascular bundles. The midrib (mid vein), major veins, minor veins were 3 distinct types of the vascular bundles classified in the leaves (Figure 3.6). The midrib is the largest vascular bundle and is found in the centre of the leaf, flanked by major and minor veins extending towards both of the leaf margins.

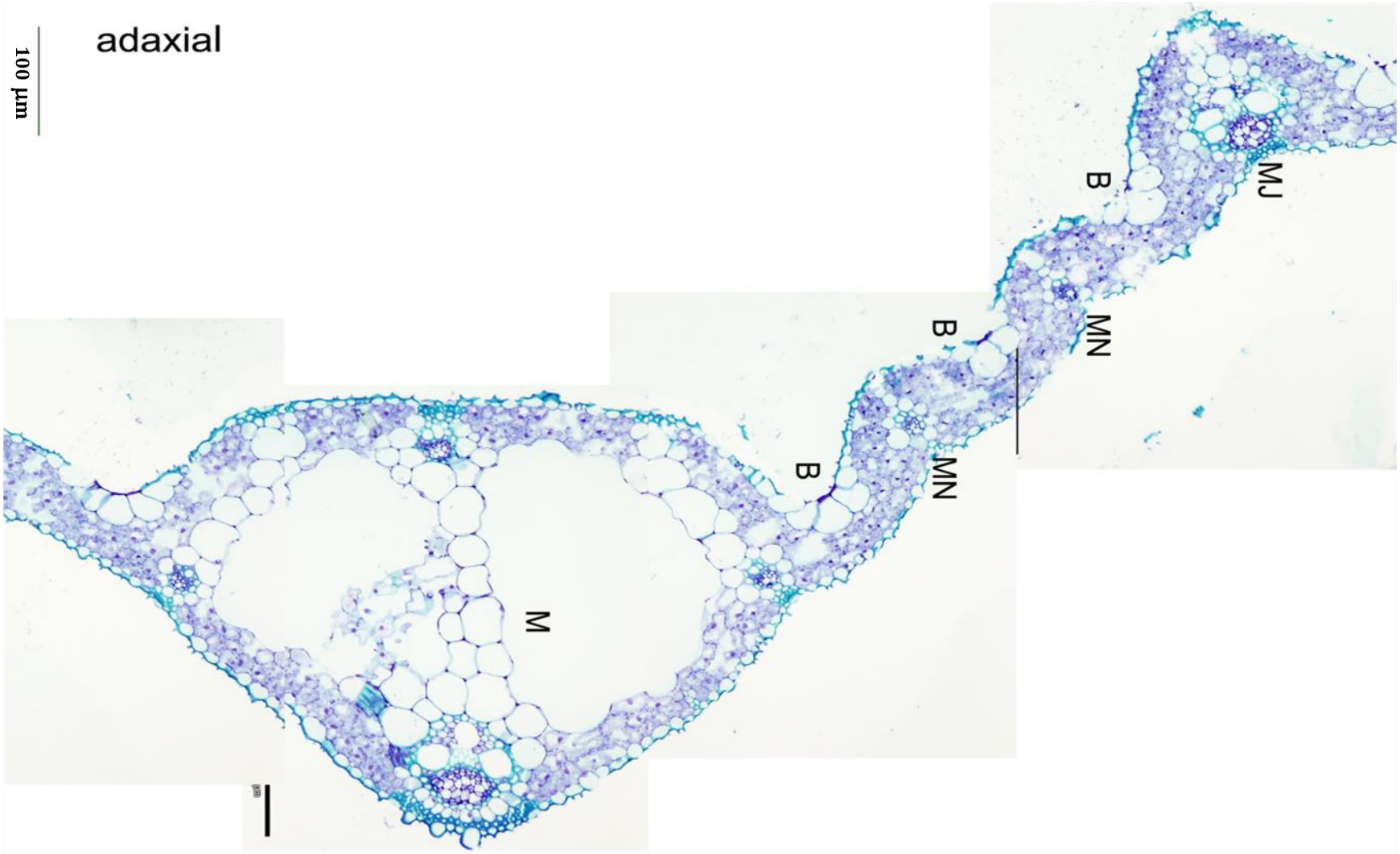

Figure 3.6 Cross section of a rice leaf showing midrib (M), major vein (MJ) and 2 adjacent minor veins (MN); B, bulliform cells.

3.4.2 Using Lf3 length as a proxy for staging Lf5 development.

Development of a new rice leaf arises inside the sheath of the preceding leaf. To allow transfer of plants to a different irradiance at specific stages of Lf5 development, I needed to find a proxy that could be linked to Lf5 development. Micro-dissection of a number of young rice plants of different ages allowed me to distinguish and define the sequence of plastochron stages for Lf5 (Figure 3.7). At P1 stage the leaf primordium is a crescent-shaped primordium recognised as a small protrusion surrounding the SAM. At P2 stage the leaf primordium is hood-shaped with length (measured from tip to the base of SAM,) of around 90-150 µm. A P3 stage leaf primordium is conical shaped and longer than the P2, with measured lengths of P3 leaf being 250 µm to 1.5 mm. At the P4 stage elongation of leaf blade occurs, and the boundary between leaf blade and sheath can be observed. Lengths of P4-stage leaf primordia observed in the present study were between 7.5 mm to 2 cm.

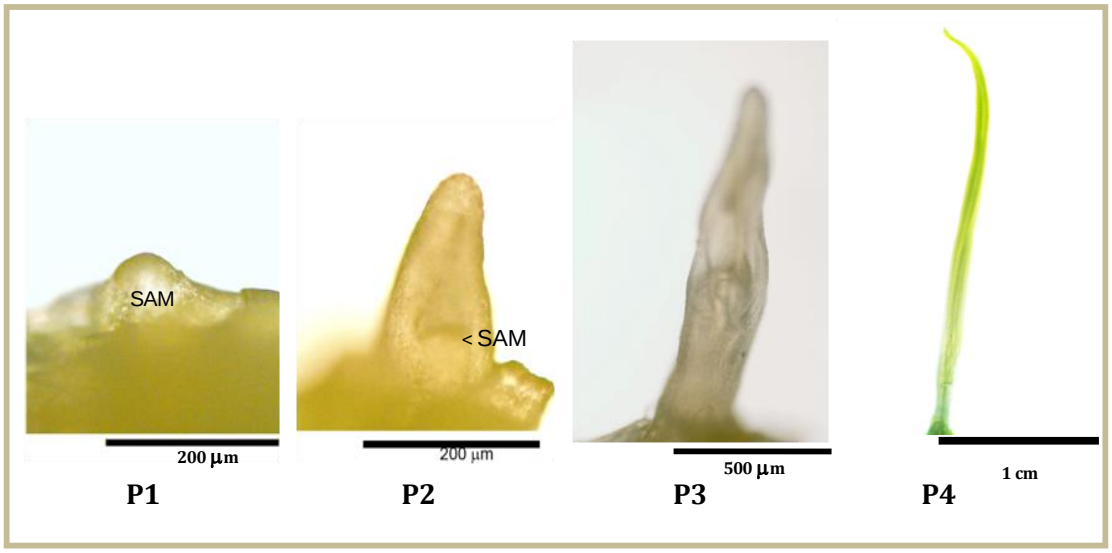

Figure 3.7 Dissection of rice plants showing different morphologies of leaf primordia at different plastochron stages (P1, P2, P3 and P4).

By dissecting a series of plants and measuring the lengths and plastochron ages of Lf5, we found that the length of leaf 3 (Lf3) could be used as a proxy for Lf5 plastochron stage. For HL-grown leaves, the Lf5 primordium

was at P1 stage when the length of Lf3 was in the range of 4 to 22 mm (Figure 3.8A). When the Lf3 had extended out further from the sheath of Lf2 (25-76 mm in length), Lf5 was at P2 stage (Figure 3.8B). P3 and P4 stage of Lf5 primordium were identified when the Lf 3 length was in the range of 77-112 mm and 120-150 mm, respectively (Figure 3.8C, D). The relationship between Lf3 lengths and Lf5 plastochron stages of LL-grown leaves was different from HL leaves (Table 3.2, Figure 3.9). Thus, the rice plants growing under LL conditions have a broader range of Lf3 lengths relating to each Lf5 developmental stage, and the LL leaf development takes longer than for HL leaves, i.e., the growth rate of LL leaves is lower. The relationship of Lf3 length and Lf5 plastochron stage was used to estimate Lf5 development in subsequent experiments.

Table 3.2 Relations of Leaf 3 length and Leaf 5 plastochron stages in rice growing under high and low irradiance conditions.

Light condition	Leaf 3 length (mm)	Leaf 5 P-stage
HL	4 - 22	P1
	25 - 76	P2
	77 - 112	P3
	120 - 150	P4
LL	10 - 30	P1
	35 - 73	P2
	80 - 140	P3
	170 - 190	P4

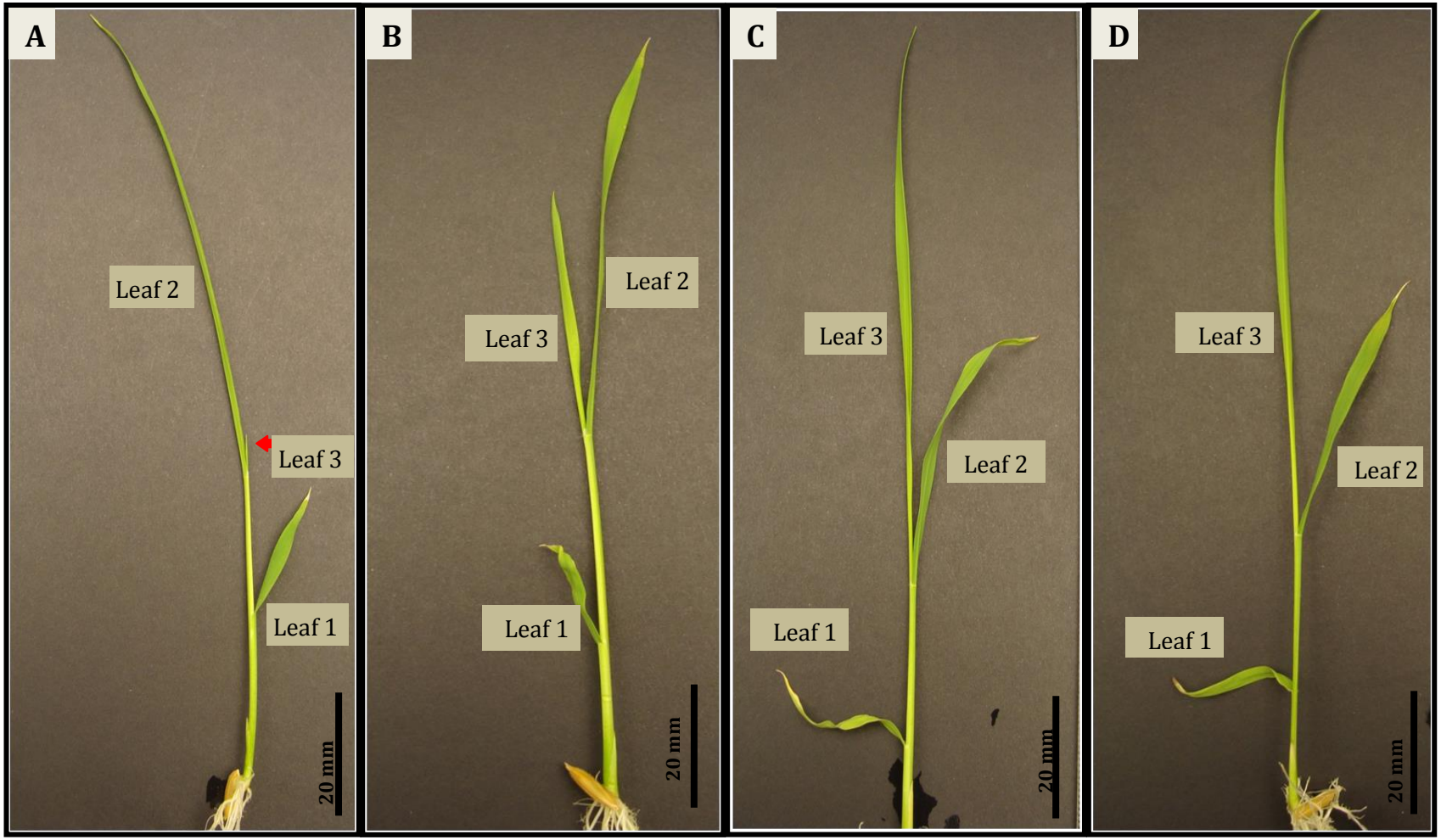

Figure 3.8 Young rice plants showing the length of the 3rd leaf equivalent to leaf 5 developmental stages P1 (A), P2(B), P3 (C) and P4 (D).

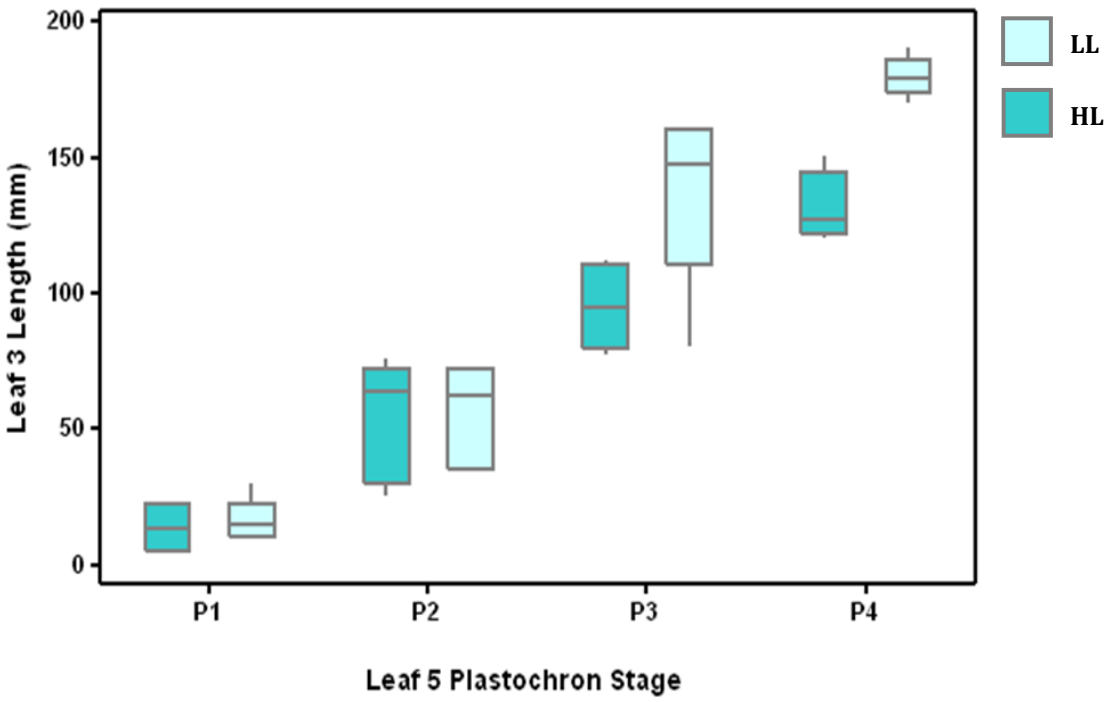

Figure 3.9 Relationship of leaf 3 length (mm) and leaf 5 plastochron stage of HL and LL–rice leaves. The interquartile box represent the range of data (n=26 for HL, n= 25 for LL) with median line indicated. The bottom of the box is the first quartile (Q1) and the top is the third quartile (Q3) value.

3.4.3 The response of leaf thickness to altered irradiance at different developmental stages of Lf5

The rice leaf sections shown in Figure 3.10 show the differences in leaf thickness of rice plants grown under HL and LL conditions. The mean leaf thickness of HL grown Lf5 measured perpendicular to the leaf plane (from adaxial to abaxial suface) at the minor veins was 72.2 μm, which was significantly thicker (p<0.01) than mean LL leaf thickness at minor veins (59.7 μm). Similarly, the mean thickness measured at bulliforms cell of HL grown Lf5 was 67.4 μm while for LL grown-Lf5 it was 51.5 μm (Figure 3.11A). Although, the mesophyll cells in HL grown leaves appeared larger than LL grown leaves (Figure 3.10), further analysis needs to be performed in order to confirm this observation. However, there was no significant difference in mesophyll cell number measured from adaxial to abaxial surface (both at minor veins and bulliform cells) between HL and LL leaves (Fig 3.11B).

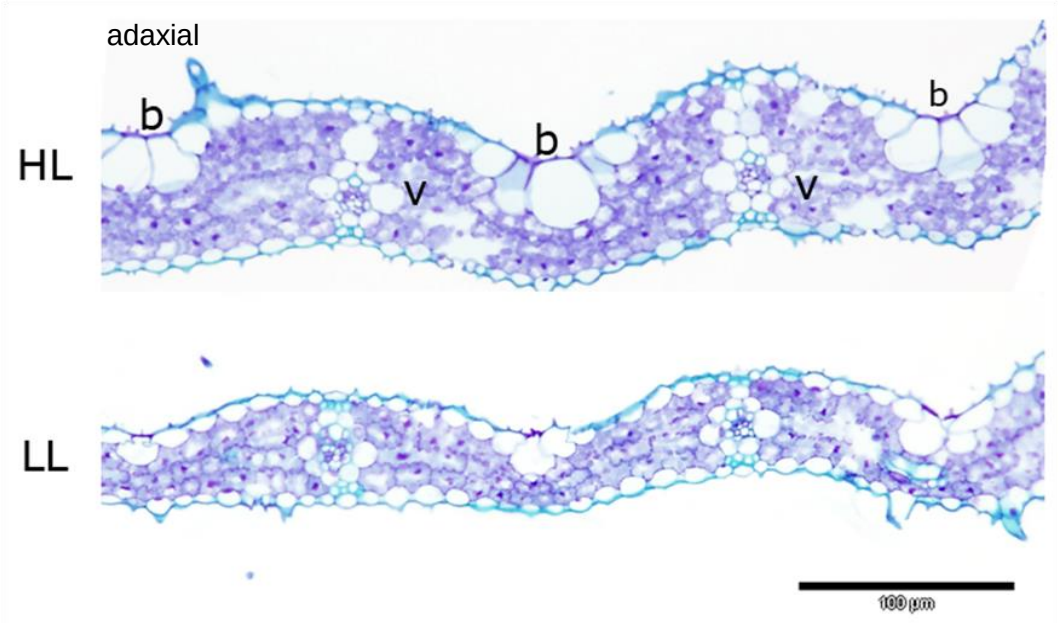

Figure 3.10 Cross-sections IR64 rice leaf showing differences in leaf thickness between high light (HL) and low light (LL) leaf. V= minor vein, b=bulliform cells. Scale bar = 100 μm.

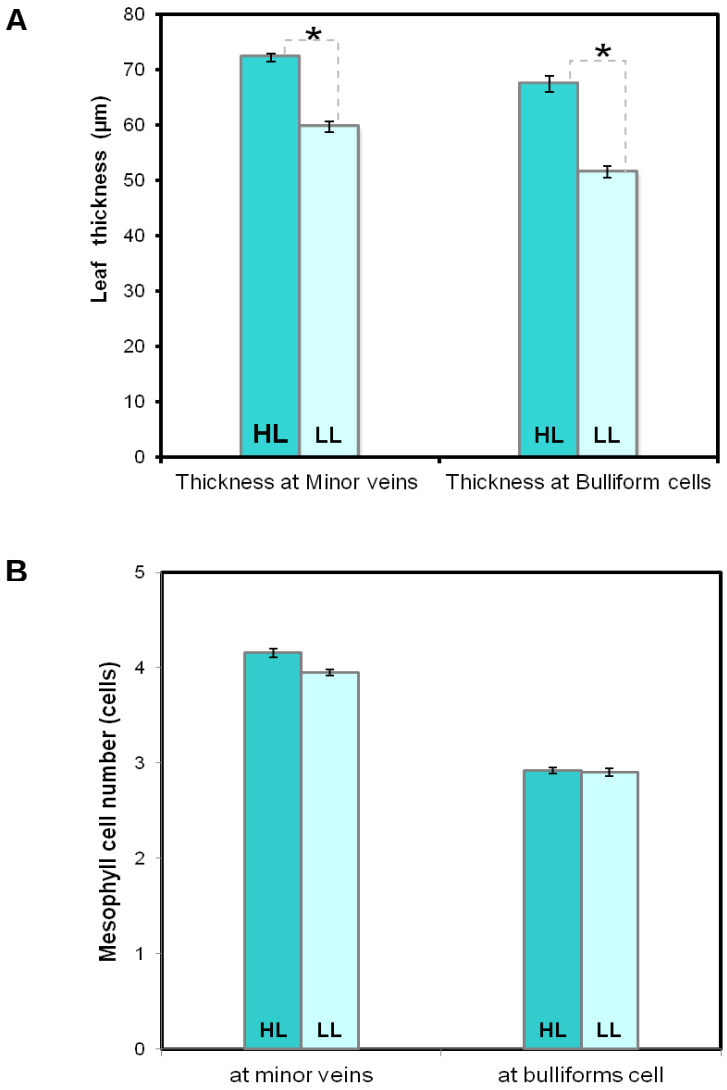

Figure 3.11 (A) Means of leaf thickness measured at the position of minor veins and bulliforms cell at maturity of Leaf 5 grown under high light (HL, n=5) and low light (LL, n=5). Error bars illustrate standard eror of the mean. T-test indicates a significant difference (p<0.01) between treatments (asterisk). **(B)** Means of mesophyll cell number measured from adaxial to abaxial surface of mature HL grown-Lf5 (n=5) and LL grown-Lf5 (n=5), both at bulliforms cells and the area in between two minor veins, with at least 7 positions of minor veins and bulliforms cell/ sample. Error bars illustrate standard error of the mean. T-test indicates no significant difference between sample classes.

3.4.4 Using transfer experiments to identify the developmental stage at which control of leaf thickness occurs

In order to investigate the developmental window of reponsiveness of Lf5 thickness to altered irradiance, I performed a series of transfer experiments in which plants grown under one irradiance were transferred to another irradiance at specific stages of Lf5 development (as assayed by Lf3 length). The data in Table 3.1 were used as a reference for the transfer of the plants from one light regime to another. Leaf thickness of fully expanded Lf5 was measured at both minor vein and bulliforms cell from rice plants which were transferred from HL condition to LL condition at different plastochron stages of Lf5 (Figure 3.12) and vice versa for the LL condition (Figure 3.13). Considering P5-stage transferred Lf5, the final leaf thickness was characteristic of a leaf grown continually under the initial light conditions (Figure 3.12 and 3.13), i.e, if a plant was grown in HL until Lf5 was at stage P5 then transferred to LL, the mature Lf5 had a thickness characteristic of a Lf5 grown continually under HL. Rice leaf at P5- stage approximately corresponds to the emergence of the leaf tip from the preceding leaf sheath. On the other hand, if the rice plant was transferred at earlier plastochron stages of Lf5 (P2, P3 or P4), the leaf thickness adapted to the later light intensity and a thinner (shade-type) or a thicker (sun-type) mature leaf was generated when the plant was transferred from HL to LL or LL to HL, respectively. Surprisingly, when the transfer was performed at P1, the earliest plastochron age, the final leaf thickness was characteristic of a leaf grown continually under the initial conditions, not the later conditions under which the transferred leaf spent the vast majority of its development (Figure 3.12, 3.13). Thus there is a phase in developmental time (P2 to P4 stage) when rice leaf thickness responds to the prevailing irradiance, but prior to this window of development final leaf thickness is set by the irradiance at leaf inception. These data are consistent with the hypothesis that leaf thickness is set at inception but can be altered during a defined developmental window (P2-P4) dependent on a change in irradiance-related signal rather than detection of an absolute level of signal linked to irradiance level.

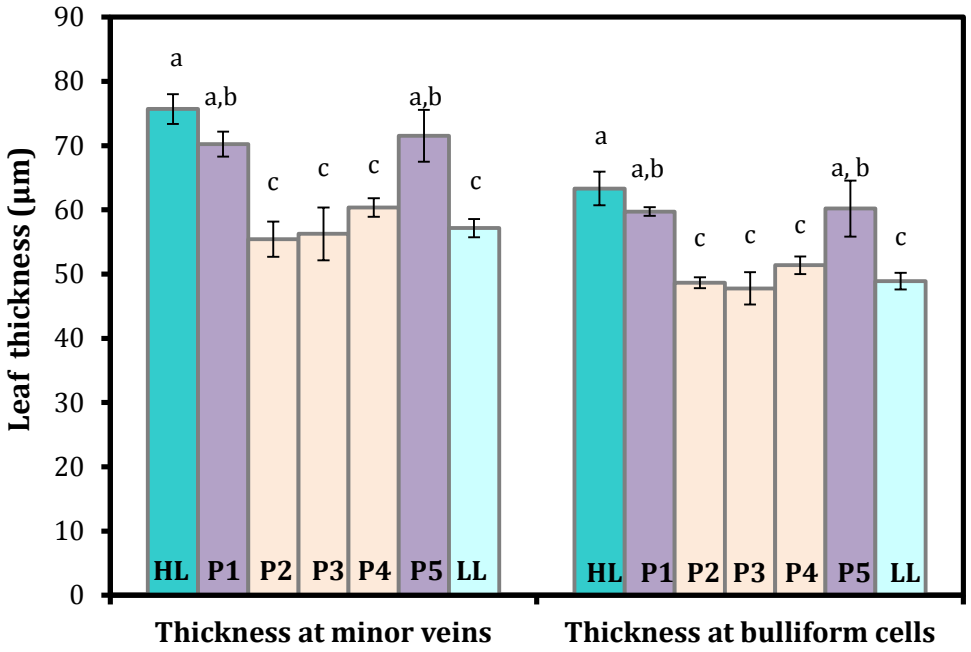

Figure 3.12 Means of leaf thickness measured at the position of minor vein and bulliforms cell at maturity of Leaf 5 grown under HL and transferred to LL at different developmental stages (P1, P2, P3, P4, P5). Identical letters above a bar indicate no significant difference (p<0.05) between treatments (Tukey's test, n = 8). Error bars indicate standard error of the mean.

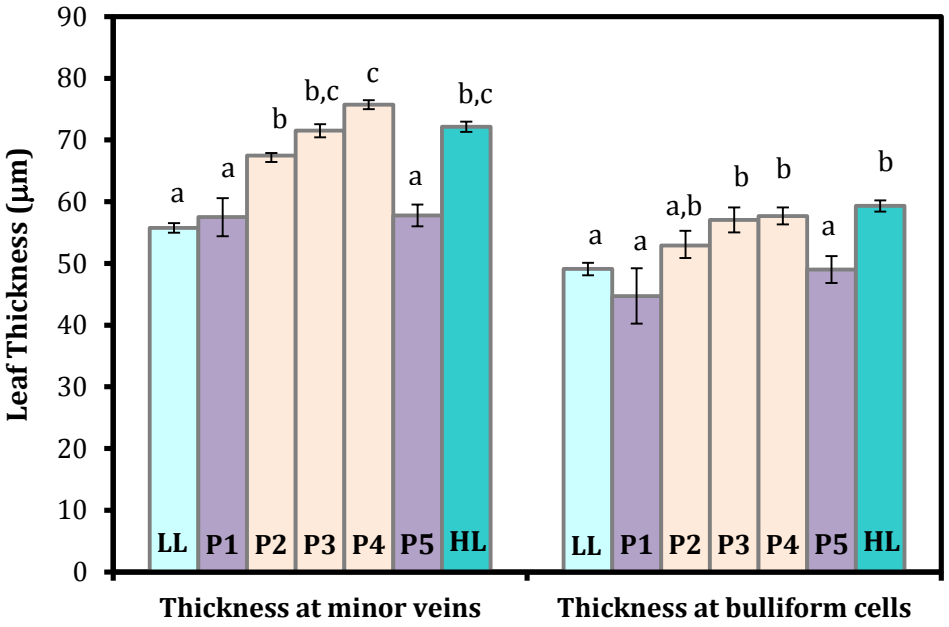

Figure 3.13 Means of leaf thickness measured at the position of minor vein and bulliforms cell at maturity of Leaf 5 grown under LL and transferred to HL at different developmental stages (P1, P2, P3, P4, P5). Identical letters above a bar indicate no significant difference (p<0.05) between treatments (Tukey's test, n = 8). Error bars indicate standard error of the mean.

3.4.5 The response of stomatal patterning to altered irradiance at different developmental stages of Lf5

The level of irradiance can affect not only leaf thickness but also stomatal density and stomatal index (Givnish, 1988; Lake et al., 2001; Thomas et al., 2004; Coupe et al., 2006; Araya et al., 2008). To investigate the potential influence of altered light regime on stomata formation in the experiments described in 3.4, I observed a number of prepared leaves using differential interference contrast microscopy (Figure 3.14 and 3.15). The results in Figure 3.16A indicated that although LL-grown Lf5 tended to have higher stomatal densities both on the adaxial and abaxial surfaces than other treatments, these differences were not statistically significant, with both LL and P1-transferred leaves having a stomatal density similar to HL-grown Lf5. However, stomatal densities, both on the adaxial and abaxial surfaces, in P3 and P5-transferred leaves were significantly lower than those observed in LL grown leaves ($p<0.05$). Although, the size of stomata in LL- grown Lf5 generally was smaller than that observed in HL or the HL-transferred leaves (Figure 3.16B), this difference was not statistically significant. Analysis of epidermal cell file width in rice leaves revealed that stomata-containing epidermal cell files were significantly wider than non-stomata cell files in all treatments ($p<0.05$). Moreover, there was a tendency for LL grown leaves to have narrower epidermal cell files than HL or HL-transferred leaves (Figure 3.16C). It is possible that the stomatal size will be influenced by file width, thus the results in Figure 3.16C may account for some of the tendencies in stomatal density and size observed in Figure 3.16A and B, but not for the distinct P3 and P5-transferred leaf stomatal densities observed in Fig 3.16A and B. Irrespective of the variation observed within and between different treatments, the stomatal characteristics of P1-transferred Lf5 were very similar to those observed in the control HL-grown leaves. However, considering the leaf area, leaves transferred from HL to LL at the P1 stage had an area significantly larger than HL-grown leaves ($p<0.05$) and were similar in area to LL-grown leaves (Figure 3.16D).

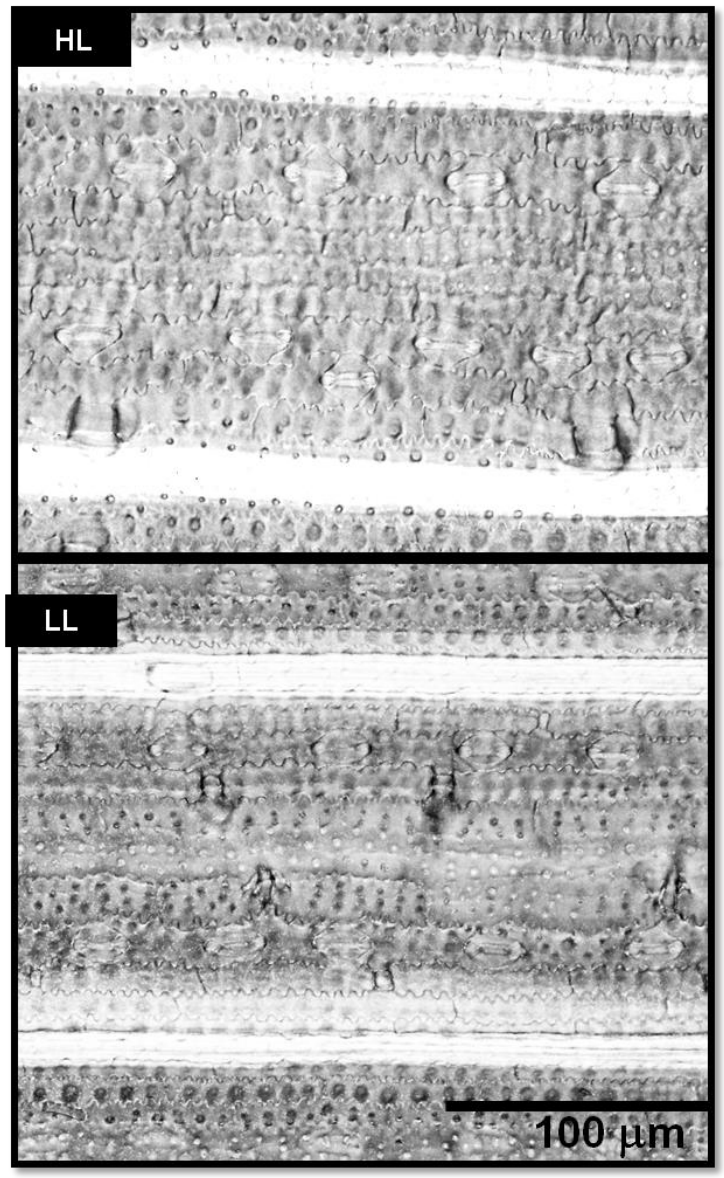

Figure 3.14 Images of epidermis of mature Lf5 grown under high light (HL) and low light (LL) conditions. Scale bar = 100 μm.

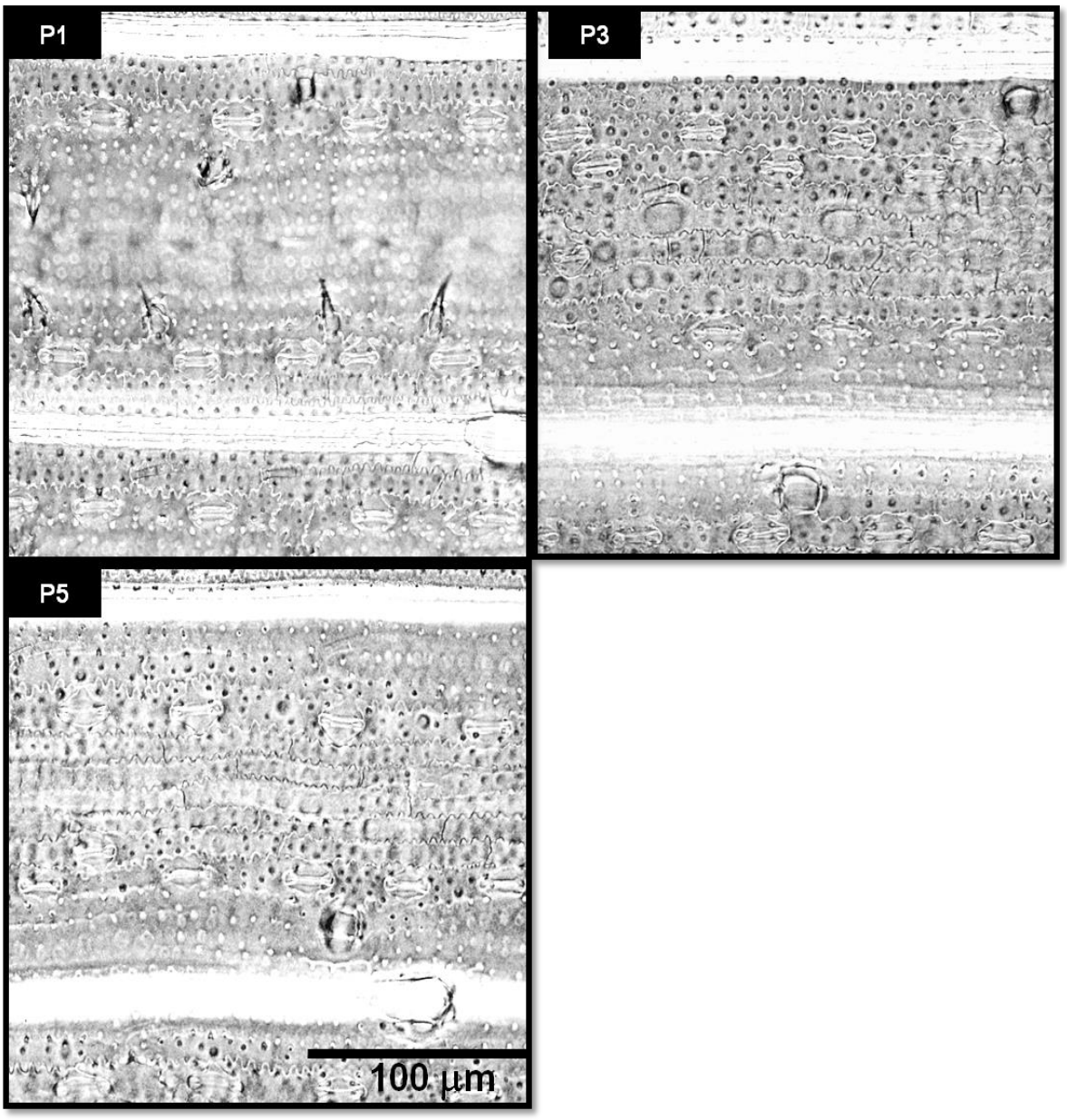

Figure 3.15 Images of epidermis of mature Lf5 grown under high light (HL) and transferred to low light (LL) at P1-, P3- or P5-stage of leaf development. Scale bar = 100 µm.

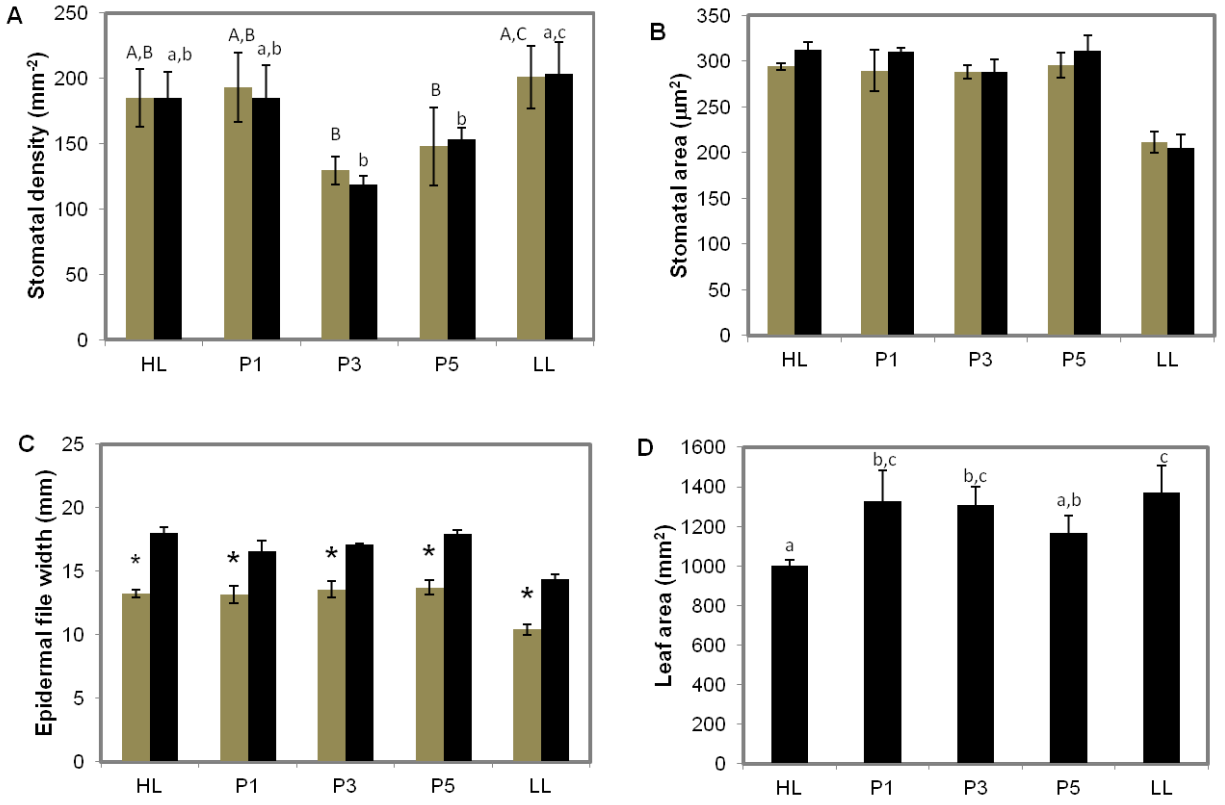

Figure 3.16 (A) Stomatal density in mature Lf5 grown under HL and were transferred to LL at different developmental stages. Brown columns, abaxial; Black columns, adaxial. Error bars show standard error of means (SEM). For each comparison (capital letters for abaxial comparison and small letters for adaxial comparison), identical letters above a column indicate no significant difference between treatments (Tukey's test; $p<0.05$. ANOVA indicated a significant difference between the sample classes ($p<0.05$, n≥ 4, with at least 10 stomata in 3 fields of view/sample). **(B)** Stomatal complex size in mature Lf5 grown under HL and were transferred to LL at different developmental stages. Error bars = SEM. Brown columns, abaxial; black columns, adaxial. ANOVA indicates no significant differences between the sample classes (n≥ 3, with at least 10 stomata in 3 fields of view/ sample). **(C)** Epidermal cell file width in non-stomata-containing files (brown columns) and stomata-containing files (green columns) in mature Lf5 grown under HL and were transferred to LL at different developmental stages. Error bars = SEM. T-tests indicated a significant difference ($p<0.05$) between the file widths within each treatment (asterisk); n≥ 3, with at least 6 files in 3 fields of view/ sample. **(D)** Leaf area of mature Lf5 grown under HL and were transferred to LL at different developmental stages. Error bars indicate standard deviation.Identical letters above a column indicate no significant difference ($p<0.05$) between treatments (Tukey's test, n=5).

3.5 Discussion

The main aims of this chapter were to study changes in rice leaf morphology and identify the developmental stage at which control of leaf thickness occurs in response to altered light regime. The results presented in this chapter indicate that there is a developmental window during which IR64 rice leaves show a response to altered light regime via a change in leaf thickness. The fact that a new rice leaf develops from a meristem encased within leaf sheaths of subtending leaves was a major challenge in this study. The classification of leaf developmental stages by means of plastochron age (P-stage) and using the emergent length of another leaf as a proxy for prediction of leaf developmental stage were crucial to the experimental approach.

The developmental window when rice leaf thickness can be set in accordance to prevailing light condition is between the P2 to P4 stage. As stated previously, it has been reported that low-light grown leaves transferred to high-light conditions did not achieve a high-light leaf morphology if the leaves had already emerged from leaf sheath. Thus, rice leaf thickness was set prior the emergence of the leaf blade, even though the exact stage when the setting occured was unclear (Murchie et al., 2005). My study has successfully identified the developmental window when rice leaf thickness can be set by irradiance. A surprising observation was that leaves transferred at the P1 stage (the earliest visible stage of leaf development) did not respond to altered irradiance by appropriate adjustment of their final thickness. At initiation cells within a leaf are undergoing co-ordinated growth and division. By the P4 stage cell division has been reported to be almost finished, with subsequent cell growth occurring without accompanying division. This termination of cell division occurs before the leaf emerges from the surrounding leaf sheath. (Itoh et al., 2005; Murchie et al., 2005). This might be the reason why the P5-transferred leaves did not respond to the alteration of irradiance.

As highlighted in previous work, grass leaves, such as rice, are produced repetitively from the meristem at the base of the plant within leaf sheaths of subtending leaves, therefore the leaf sheath not only protects the developing

leaves from external humidity and CO_2 but also restricts the amount of light they are exposed to. Taken all these facts and my results that leaf thickness was pre-set during a developmental window prior to leaf emergence and not determined by the post-emergence light intensity, it is possible that leaf thickness may be regulated by signals sent from other exposed parts of the plant. Previous studies on sun and shade leaf development have revealed that the differentiation of a new leaf primordia into sun or shade type can be remotely regulated by mature leaves which are fully exposed to the actual light environment (Lake et al., 2001; Yano and Terashima, 2001; Lake et al., 2002; Thomas et al., 2004; Coupe et al., 2006; Ferjani et al., 2008). Yano and Terashima (2004) studied the development of sun and shade leaves in *C. album* by focusing on the division of palisade cells over developmental time (leaf plastochron index; LPI) staging from LPI-1 to LPI-10. They found that the developmental stages where the difference in palisade thickness of sun and shaded leaves can be observed started from LPI-3. In addition, the developmental processes during the early stage (LPI-1) of sun leaves were similar to those of shaded leaves, except for the higher rate of periclinal palisade cells division observed in the sun leaves. They concluded that the periclinal cell division taking place earlier and at the expense of anticlinal division found in sun type leaves caused the formation of two cell- layered palisade tissue. This suggests long distance signalling regulates the orientation of cell division and the differentiation of sun and shade leaves in the apex. Although I did not investigate the nature of the signal in this context, it is important to consider how the long-distance signalling can systematically control leaf type. One possibility is that the systemic signal moves from mature to developing leaves through the vascular system of the plant. Considering that the differentiation of vascular bundle in rice leaves starts during the P2-stage of leaf development (Itoh et al., 2005), the lack of a vascular system in P1 leaf primordia may be a reason why the P1-transfered leaves do not respond to the change in plant irradiance. In addition, the fact that the P1 transferred leaves did not respond to the low or high irradiance to which the plants were exposed suggests that leaf thickness change might require a

change in irradiance-related signal rather than the measurement of some absolute level of signal. Assuming that, low irradiance leads to a signal in the exposed leaves which is then transported to the young developing leaves, this signal will be continually generated. A system in which the responding leaf perceives a change in level of the signal would explain my observations.

There are some candidate molecules that might be related to the long distance signalling system, e.g., phytochromes, cryptochromes and phototropins that are used in detection of changes in either light quality or quantity (Devlin et al., 1999; Quail, 2002; Franklin et al., 2003; Franklin and Quail, 2010). It has been long known that the red/ far- red light ratio is sensed by phytochrome which regulates a group of light responsive genes controlling many photomorphogenetic processes. Mutation analysis in rice shows that phytochrome B influences leaf area and stomatal density (Liu et al., 2012). The mature leaves of *phy*B mutant rice had larger epidermal cells and lower stomatal density than the wild type leaves. In addition, it is suggested that mutation of *phy*B induces higher expression levels of both ERECTA and EXPANSIN genes, resulting in the larger epidermal cells. Interestingly, the present results indicate that the mature high light- grown Lf5 was thicker than those of the low light-grown leaves by having a larger mesophyll cell size, however further analysis is required. Therefore, it is reasonable to doubt that phytochrome B affects the control of leaf thickness in rice.

Although we do not yet fully understand how the size of either plant cells or organs are controlled, cell division and cell growth are the two possible processes which contribute to the size control during organogenesis (Marshall et al., 2012). Furthermore, some transcription factors and co-activators such as ANGUSTIFOLIA (AN) and GROWTH-REGULATING FACTOR (GRF) are involved in the regulation of cell size (Kim and Kende, 2004; Horiguchi et al., 2005; Lee et al., 2009). Mutational analysis in *Arabidopsis thaliana* shows that leaves of an *AN* mutant were thicker and narrower than those of wild type (WT) (Tsuge et al., 1996). Interestingly, palisade cells of the *AN* mutant leaves exhibit enhanced elongation in the leaf-thickness direction and a greater

number of cell layers than those of WT, which is similar to the characteristic of sun leaves in some plants (Yano and Terashima, 2004). Considering all these findings, it can be said that the control of leaf thickness in rice is related to a signal controlled by the alteration in light intensity that is sensed by an unknown receptor in mature leaves and the signal transferred to the developing leaves, where the orientation of cell division and growth are determined accordingly.

As mentioned in the introduction, stomatal density and size are leaf characteristics that can be adjusted when plants acclimate to irradiance and CO_2 level. The result in here indicated that stomata in rice leaves growing under LL and ambient CO_2 condition were smaller than those growing under high light, supporting the recent investigation by Hubbart et al. (2013). In the experiments reported here, I found a significant difference in stomatal density only when rice plants were transferred from HL to LL at P3 and P5 stage of Lf5. The reason for this might be that epidermal differentiation (including stomata) only starts in the P3 stage and is completed by the P5 stage (Itoh et al., 2005). It is noteworthy that there was no significant difference in stomatal density and area between adaxial and abaxial surface of the leaves under the ambient CO_2 used in this study. This supports the idea that abaxialisation in modern rice is not obvious due to it having been bred to become more erect (Hubbart et al., 2013), so the stomatal density on the adaxial and abaxial sufaces is almost equal. In addition, there is an arrangement of epidermal cells in the rice leaf so that it is differentiated into stomata-containing and non-stomata cell files. We observed irradiance-dependent alteration in file width in this study. Moreover, the stomata-containing cell files were wider than the non-stomata ones. There is a possibility that stomatal size will be influenced by the file width. The work of Liu (2012) also indicates a reduction in either stomatal density or size in the *phyB* mutant leaves that might be influenced by the larger epidermal cells of the mutant leaves than those of WT. They proposed that the reduction in stomatal density and total leaf area in *phyB* mutant rice plants resulted in reduced transpiration rate per unit leaf area and improved drought tolerance. On the other hand, my data demonstrated an

inverse relationship between stomatal density and size, but reductions in leaf area were observed in the mature Lf5 grown under HL conditions. These might reflect an optimization which can affect leaf net assimilation rate. Considering these observations with the differences in leaf area between each treatment, our findings support the claim that final leaf shape and size are not always determined by the simple sum of behaviours of individual cells (Tsukaya, 2003). As the control of organ size remains unclear (Tsukaya, 2003; Fleming, 2006; Tsukaya, 2006; Powell and Lenhard, 2012), the control of stomatal density and size (which is also influenced by environmental factors) is likely to be complicated.

It can be summarised that the developmental window during which IR64 rice leaves show a response to altered light regime via a change in leaf thickness was first identified in this study. As described previously, leaf thickness is highly related to leaf photosynthesis, therefore how the alteration in leaf form, in response to light regime, affects rice leaf performance is interesting. Physiological studies underpinning the question were performed and reported in Chapter 4.

Chapter 4 | Does alteration in leaf form effect leaf performance?

4.1 Introduction

Photosynthesis is comprised of interconnected biophysical processes, such as the transportation of CO_2 through stomata and the leaf, and biochemical processes in the different compartments of chloroplasts, mitochondria, and the cytosol of the photosynthesising eukaryotic cells. The net CO_2 assimilation rate (*A*) of plants is determined by these processes (Sharkey et al., 2007). The potential CO_2 assimilation rate relies on the development of an effective metabolic system which is related to a complex function of interaction between the plant photosynthetic system and environmental conditions (Lawler, 1993). Generally, net CO_2 exchange of intact leaves depends on the balance between CO_2 uptake in photosynthesis and the release of CO_2 both by photorespiration and other processes, predominantly the TCA cycle. The three main biochemical activities underlying optimal photosynthetic performance are ribulose-1,5-bisphosphate carboxylase/oxygenase (RubisCO) activity, regeneration of ribulose bisphosphate (RuBP) and metabolism of triose phosphates (Taiz and Zeiger, 2010). These important metabolic steps, which require CO_2 as a substrate, take place in the palisade and spongy mesophyll cells of the leaf. Considering that CO_2 level supply to these cells is controlled by stomatal guard cells on the epidermis of the leaf and the extent of the sub-stomatal cavities, leaf anatomy may influence CO_2 uptake by its diffusive resistances, thus determining leaf photosynthetic rate (Farquhar and Sharkey, 1982; Reich et al., 1998; Nobel, 2009). This chapter considers the effect of alterations in leaf anatomy induced by different irradiance on leaf performance in rice.

Light is a vital resource for plant growth and reproduction, however it is an unpredictable resource that is spatially and temporary variable. Some plants have sufficient developmental plasticity to acclimate to a range of light regimes by producing a new leaf with a suitable set of biochemical and morphological characteristics that are best fit to a particular environment. The acclimation of photosynthesis and the optimisation of photosynthetic efficiency in leaves to irradiance is well documented (Anderson et al., 1995; Hikosaka

and Terashima, 1995; Murchie and Horton, 1997; Bailey et al., 2001). Plants develop sun or shade leaves when acclimated to different light regimes, as described in Chapter 3. Sun and shade leaves are not only distinct in leaf morphological characteristics i.e. sun leaves are thicker than shade leaves, but they also have some contrasting biochemical characteristics. For example, sun leaves have more RubisCO but a lower chlorophyll b/ chlorophyll a ratio and a lower total chlorophyll per reaction complex than shade leaves (Boardman, 1977; Givnish, 1988; Murchie et al., 2005; Taiz and Zeiger, 2010). Compared to sun plants, shade plants have greater chlorophyll a and b per unit volume of chloroplast and a higher chlorophyll b/a ratio due to the increase in light harvesting complex (LHC) protein (Anderson et al., 1995; Taiz and Zeiger, 2010). This has the effect of enhancing the maximal capacity for photon capture and the transfer of energy to the reaction centres (Lawler, 1993). In general, leaf photosynthesis is characterised by calculating the light saturated rate of photosynthesis (P_{max}) expressed on leaf area basis (Hikosaka and Terashima, 1995). Thus, sun leaves have a higher P_{max} and also greater nitrogen content than shade leaves (Hall et al., 1993; Murchie and Horton, 1997; Lambers et al., 1998; Murchie et al., 2005; Taiz and Zeiger, 2010). It is believed that the photosynthetic rate in sun leaves needs to be supported by thick leaves (Terashima et al., 2001) with a generous nitrogen investment that is required for photosynthetic enzyme biosynthesis (Boardman, 1977).

Photosynthetic enzymes are incorporated into chloroplasts. Since CO_2 diffusion in the liquid phase is very slow, the diffusion of CO_2 to the site of carboxylation, i.e. RubisCO enzyme, in the chloroplast stroma through the mesophyll , mesophyll conductance (g_m), can significantly limit photosynthetic rate (Flexas et al., 2008; Zhu et al., 2010). Recently, there is some evidence indicating that g_m is sufficiently small as to significantly decrease the CO_2 concentration at the chloroplast stroma (C_c) relative to the CO_2 concentration at the sub-stomatal internal cavity (C_i) (Flexas et al., 2008). Therefore, it is thought that the positioning of chloroplasts along the cell surface is important to optimise CO_2 conductance. Considering sun leaves, an increase in chloroplast number without thickening of the mesophyll layer would lead to

some chloroplasts not achieving sufficient CO_2 supply, as they would be at a distance from the cell surface. Positive correlations between photosynthetic capacity and either mesophyll surface area or leaf thickness have been reported (McClendon, 1962; Nobel et al., 1975; Jurik, 1986; Oguchi et al., 2003).

This chapter examines the relationship between leaf anatomy and photosynthetic capacity in rice IR64 plants after transfer between different irradiances at specific developmental stages. Given that the photosynthetic capacity can be determined by the amount of RubisCO content (Björkman, 1968), I hypothesised that the transferred rice plants grown under high irradiance conditions and which differentiated thicker leaves should have larger amounts of RubisCO protein and higher P_{max} than those grown under low irradiance conditions. Physiological studies on the response of assimilation rate to CO_2 concentration (A/C_i curve), light response curves, RubisCO concentration, and chlorophyll a/b ratio in rice plants grown under different light regime were determined. The correlations between rice leaf developmental stages when leaf thickness is set and the acclimation to different light regime were examined in this study.

4.2 Aims

1. To investigate the correlation between rice leaf anatomy and leaf performance after acclimation to different light regime.

2. To study the acclimation of photosynthesis to irradiance level in relation to rice leaf development.

4.3 Brief methodology

4.3.1 RubisCO protein analysis

Leaf discs (4.5 mm^2/disc) taken from mature Lf5 were ground to a powder in liquid nitrogen by using a pre-cooled micro-pestle and extracted with 50mM Tris-HCl (pH7.0), 10 mM MgCl2, 1mM EDTA, 5mM dithiothreitol, 5% (w/v) insoluble polyvinylpolypyrrolidone and 10% (v/v) glycerol. The crude

extracts were centrifuged at 15,000xg for 15 minutes, the supernatants collected, then protein concentration was estimated using the Bradford method. For estimation of RubisCO content, protein samples were separated by SDS-PAGE on a 12.5% (w/v) gel using standard Laemmli procedures, then stained with coomassie brilliant blue. Note that, a reference protein sample (from HL leaves) was loaded in each gel as a calibrator to ensure that the differences in protein concentration detected by this method are not the result from the gel staining process. The protein band intensity of the RubisCO large sub-unit was quantified in scanned gels using ImageJ. At least 6 gels were analysed per treatment.

4.3.2 Chlorophyll analysis

Leaf discs (5 discs/ leaf) were taken using a leaf borer and extracted 3 times with a total volume 1 ml of 80% Ethanol at 70^{o}C for 20 minutes. The crude extracts were centrifuged at 7000xg for 5mins and then the supernatant were collected. The supernatants from the three extractions (total volume 1 ml) were pooled and incubated in darkness for 1 hr before measurement using a UV-Vis spectrophotometer. The absorbance of chlorophyll a and b were measured at 665 nm and 649 nm, respectively. Leaf pigments were quantified using the following equations.

$$c_{\mathrm{a}} = 13.95\ \mathrm{A}_{665} - 6.88\ \mathrm{A}_{649}$$

$$c_{\mathrm{b}} = 24.96\ \mathrm{A}_{649} - 7.32\ \mathrm{A}_{665}$$

$$\boldsymbol{Chlorophyll\ a:b} = \frac{C_a}{C_b}$$

; Where chlorophyll a is c_{a}, chlorophyll b is c_{b}

4.3.3 Light response measurement

Photosynthetic CO_2 assimilations was measured at 28^{o}C, 400 µl l^{-1} CO_2 with 400 µmol s^{-1} flow rate using a Li-Cor 6400 portable photosynthesis

system connected with the Chamber/ IRGA. The range of PPFD values used in this experiment are listed in Table 4.1

Table 4.1 Order and light intensities used in analysis of photosynthetic responses to increasing light intensity.

Observation number	PAR ($\mu mol\ m^{-2}$)
1	0
2	100
3	200
4	500
5	1000
6	1500

4.3.4 CO_2 response measurement, The A/C_i curve

Photosynthetic CO_2 assimilation was measured at 28°C, 1000 µmol m^{-2} s^{-1}, with 400µmol s^{-1} flow rate using a Li-Cor 6400 portable photosynthesis system connected with the Chamber/IRGA. The range of atmospheric CO_2 used in this experiment are listed in Table 4.2

Table 4.2 Order and CO_2 concentrations used for fitting the $A/\ C_i$ curve .

Observation number	CO_2 concentration (μmol)
1	400
2	300
3	200
4	100
5	400
6	700
7	1000
8	1200

The net CO_2 assimilation response to the variation of CO_2 concentration as listed in table 4.2 were recorded and put into the PS-FIT A/Ci fitting curve model created in Microsoft excel file by C.J. Bernacchi, modified from Bernt Fischer's original design, available online at http://www.life.illinois.edu/ bernacchi/links.html. Photosynthetic parameters were calculated by the curve fitting model.

4.3.5 Analysis of carbon isotope discrimination

Leaf discs (4.5 mm^2/ disc) were taken from mature Lf5, 15 discs/ sample, and dried at 70^oC oven for 24 hrs, ground into smaller pieces before weighing, then loaded into an ANCA GSL 20-20 mass spectrometer for $^{13}C/^{12}C$ ratio analysis. Calibration using known PDB standards allowed total carbon and ^{13}C content to be obtained from each sample. At least 6 leaves were analysed/ treatment. The ratio of unknown to standard isotope distribution is $\delta^{13}C$, which can be calculated from

$$\delta 13C\ (‰) = \frac{\left({}^{13C}/_{12C}\right)\text{unknown substance} - \left({}^{13C}/_{12C}\right)\text{standard}}{\left({}^{13C}/_{12C}\right)\text{standard)}} \text{ x } 1000$$

4.4 Results

To investigate physiological performance in rice leaves showing altered leaf thickness after transfer from high light (HL) to low light (LL) conditions, physiological and biochemical analyses have been performed. The net CO_2 assimilation rate at increasing photon flux was measured from mature Lf5 growing continually under HL, LL and the leaves transferred from HL to LL at P1, P3 and P5 of Lf5 developmental stage. The light response curve (Figure. 4.1 A) of these 5 sample groups shows a statistically significant difference in response to increasing irradiance between HL and LL-grown leaves (p<0.05). The curve of HL leaves shows that the photosynthetic response to light reached saturation at PAR 1000 μmol m^{-2} s^{-1}, while that of LL-grown leaves and other

transferred leaves was at 500 μmol m^{-2} s^{-1} . In addition, all of the transferred Lf5 and the LL-grow leaves had a significantly lower CO_2 assimilation rate than the leaves grown continually under HL condition ($p<0.05$). This indicates that photosynthetic acclimation to low light irradiance occurred in the transferred leaves, including the P1-and P5-transferred leaves which exhibited relatively thick leaves (similar to HL-grown leaves results in Chapter 3).

Considering RubisCO content/ area (Figure 4.1 B), the concentration of RubisCO protein in mature Lf5 of P1-transferred leaves was not significantly different from either HL- or LL-grown Lf5. On the other hand, P3- and P5-transferred mature Lf5 displayed a lower amount of RubisCO protein than the leaves grown continually under LL conditions ($p<0.05$). Consequently, the value of total protein/ area extracted from the P1-transferred leaves was greater than other sample groups growing under LL, but this was not significantly different from either LL-grown leaves or HL-grown leaves (Table 4.3). It is noteworthy that the P3-transferred mature Lf5 had the lowest total protein/ area and lowest RubisCO content/ area (which can be linked to the thin leaf phenotype achieved when it was transferred to LL conditions as shown in Chapter 3). Although the Rubisco concentration results obtained from different gel comparisons were included in this analysis, a reference protein sample from HL leaves was used in all gels to avoid unequal gel staining signal in the different gels.

Analysis of chlorophyll a/b ratio (Table 4.3) also indicated that the P1-transferred mature Lf5 was intermediate between HL and LL grown leaves. The chlorophyll a/b ratios of the P3- and P5-transferred leaves were not significantly different from the LL leaves. These data indicate a biochemical acclimation to irradiance. There was no significant difference in total chlorophyll between the five sample groups (Table 4.3). These data indicate that the reduction in Chl a:b of LL-leaves and of the transferred mature Lf5 could be influenced by an increase in chlorophyll *b*.

Table 4.3 Physiological and biochemical parameters of mature leaf5 grown under high light (HL), low light (LL) condition, and leaves transferred from HL to LL at the different developmental P-stage.

Leaf Transfer	Chl a : b ratio	Total Chlorophyll	Protein/area (g m^{-2})	Vc_{max} (µmol m^{-2} s^{-1})	J_{max} (µmol m^{-2} s^{-1})
HL	3.23 ±0.04 **a**	3.20 ±0.09 **a**	8.09 ±0.57 **a**	92.31 ±9.70**a**	294.36 ±59.68**a**
P1	2.99 ±0.03 **b**	3.60 ±0.08 **a**	6.58 ±0.56 **a,b**	74.87 ±7.71**b**	247.55 ±39.38**b**
P3	2.81 ±0.02 **c**	3.27 ±0.10 **a**	4.60 ±0.33 **b**	63.76 ±5.59**b**	199.99 ±26.81**b**
P5	2.82 ±0.05 **c**	3.65 ±0.15 **a**	6.19 ±0.50**b**	80.15 ±10.63**a,b**	285.81 ±26.81**a,b**
LL	2.88 ±0.03 **b,c**	3.52 ±0.15 **a**	6.13 ±0.51**b**	69.58 ±14.22**b**	226.63 ±62.74**b**

All data are presented in Mean ± SE. In each parameter, different letters indicate significant difference (p<0.05,Tukey's test) between sample groups. Vc_{max} (the maximum rate of RubisCO for carboxylation) and J_{max} (the maximum rate of electron transport) derived from A/Ci curve analysis.

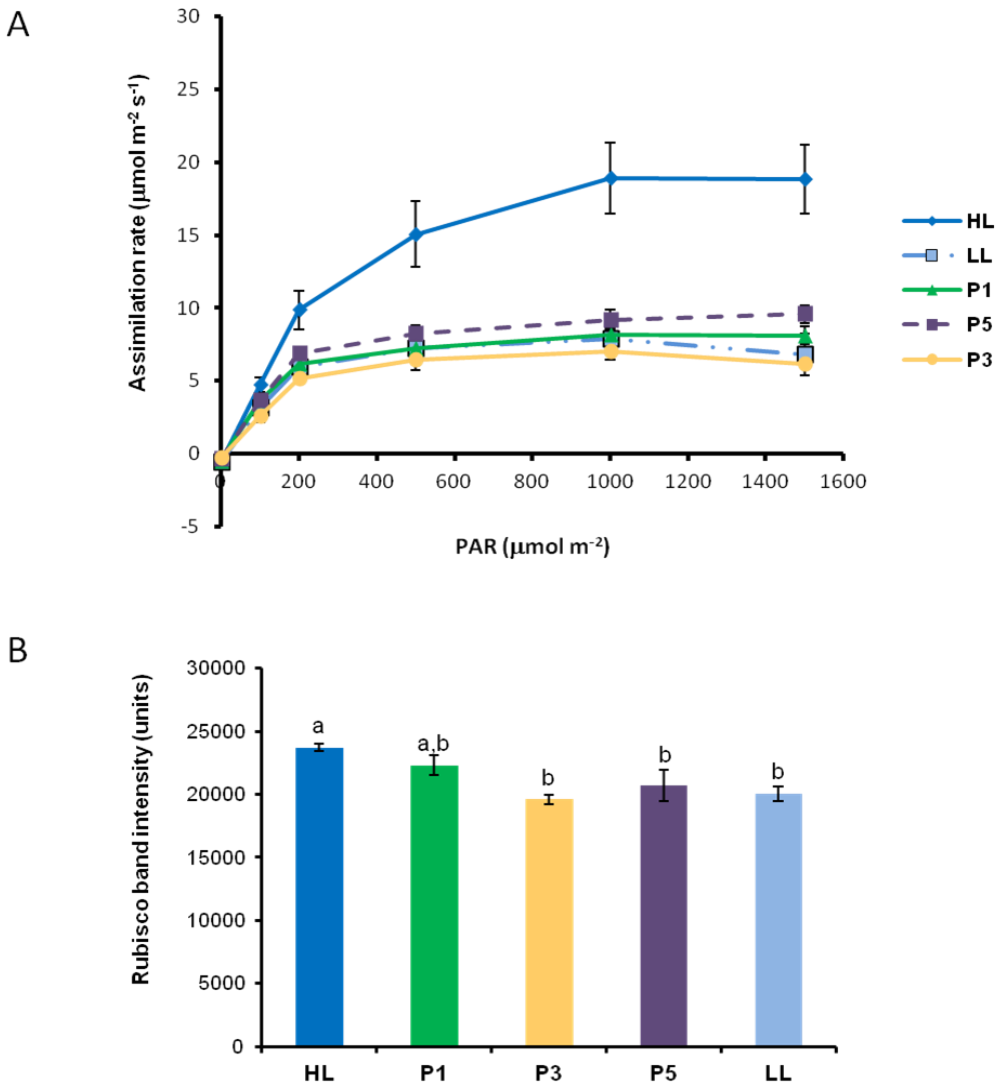

Figure 4.1 A) Light response curve of mature Lf5 grown under high light (HL), low light (LL) condition, and leaves transferred from HL to LL at the different developmental P-stage. P1, P3, P5 represents the leaves transferred at P1, P3, P5, respectively. Error bars indicate standard error of means. n=5. **B**) RubisCO large sub-unit/area in mature leaf 5 grown under HL and transferred to LL at different developmental stages (as stated in A). Identical letters in a column indicates no significant difference ($p<0.05$) between treatments (Tukey's test). Error bars indicate standard error of means. n≥7.

To investigate the effect of alteration in rice leaf thickness on leaf performance in response to irradiance, gas exchange analysis was performed to determine the response of the transferred leaves to different levels of atmospheric CO_2. The internal concentration of CO_2 (C_i) within the leaves has been calculated and plotted versus the observed CO_2 assimilation rate (A) using the *A*/*Ci* curve fitting model (Figure 4.2). Theoretically, there are three phases that can be visualised from the curves: the RubisCO-limited phase, the RuBP regeneration–limited phase, and the triose phosphate utilisation limited (TPU) phase. The maximum rate of carboxylation by RubisCO (Vc_{max}), the maximum rate of electron transport (J_{max}) and the dark respiration rate (R_d) were calculated and normalised to an equal temperature at 25^{o}C for all sample groups (Figure 4.3). The HL leaves showed a significantly greater Vc_{max}, Jmax and Rd than the other treatments (p<0.05). Although the Vc_{max}, J_{max} and Rd observed in the P1-, and P5-transferred mature Lf5 were slightly higher than LL leaves, these values were not significantly different (Figure. 4.3 A, B, C and Table 4.3).

The stomatal conductance of the transferred rice plants was also analysed. The results showed a similar pattern to the the other biochemical and physiological analyses in that the stomatal conductance (g_s) of P3-transferred mature Lf5 was lower than the other transferred plants (Figure 4.3 D). g_s of P5-transferred mature Lf5 was comparable to the HL- leaves and higher than LL-leaves, but these were not significantly different. Although the mean stomatal conductance of HL-leaves was greater than LL-leaves, this difference was not statistically different. These data are consistent with the results shown in Chapter 3 that there was no significant difference in stomatal density between the 5 treatments.

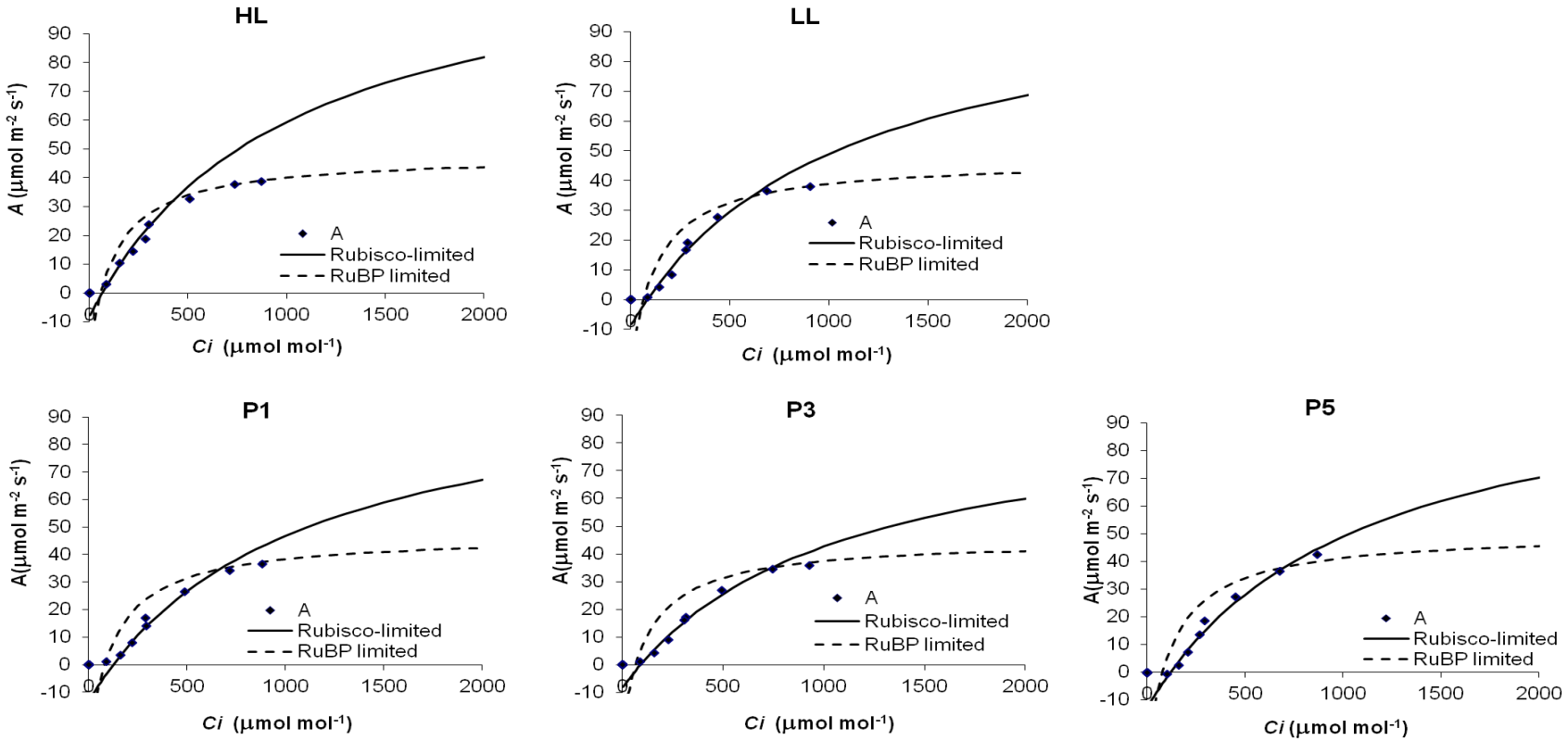

Figure 4.2 Selected A/*Ci* curves (net CO_2 assimilation rate; A, versus calculated internal CO_2 concentrations; C_i) from measurement of mature Lf5 grown under high light (HL), low light (LL) condition, and leaves transferred from HL to LL at the different developmental P-stage. P1, P3, P5 represents the leaves transferred at P1, P3, P5, respectively. Blue circles are the measured assimilation rate (*A*). Solid lines represent the estimated rate of carboxylation limited by RubisCO kinetics. Dashed lines represent the estimated carboxylation limited by RuBP-regeneration.

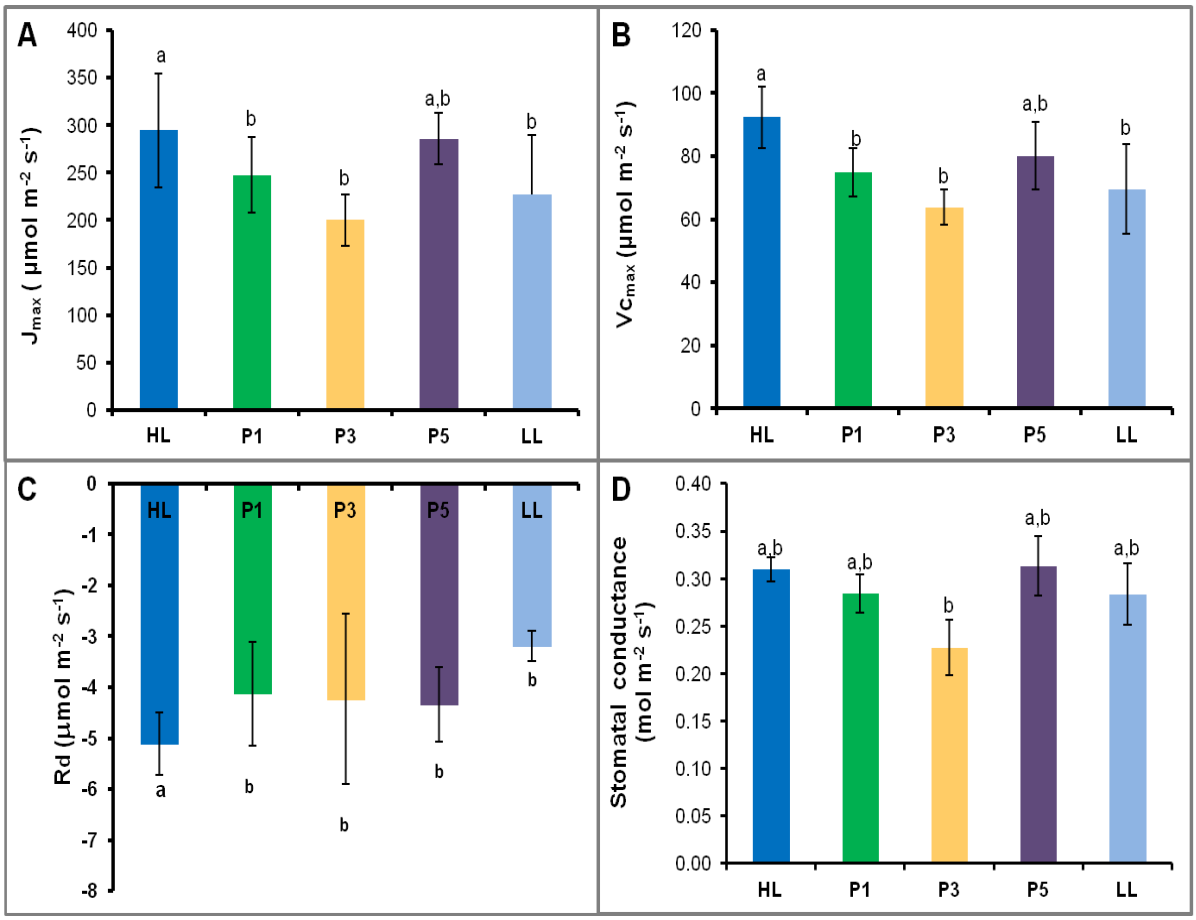

Figure 4.3 Biochemical parameters analysed from fitted *A*/*Ci* curve of mature Lf5 grown under high light (HL), low light (LL) condition, and leaves transferred from HL to LL at the different developmental P-stage. P1, P3, P5 represents the leaves transferred at P1, P3, P5, respectively. **A)** Maximum rate of electron transport (J_{max}). **B)** Maximum rate of carboxylation. **C)** Dark respiration rate, Rd. **D)** Stomatal conductance. Error bar indicates standard error of means. Identical letters indicate no significant difference (p<0.05) between treatments (Tukey's test). n≥6.

Photosynthetic discrimination against carbon isotopes was another measurement used to investigate leaf performance. The $^{13}C/^{12}C$ ratio provides important information about the flow of carbon, since it reflects the integrated CO_2 assimilation rate and stomatal conductance in plants over time (Lawler, 1993; Lambers et al., 1998). This analysis relies on the discrimination against $^{13}CO_2$ by RubisCO and the the slower diffusion rate of this carbon isotope compared to $^{12}CO_2$. In an open system, with unlimited supply of $^{12}CO_2$ and $^{13}CO_2$, RubisCO will preferentially fix $^{12}CO_2$ which is the lighter molecule, while in a closed system Rubisco will fix both $^{12}CO_2$ and $^{13}CO_2$ until no CO_2 is left. A low rate of CO_2 assimilation over time results in a large discrimination represented by a strongly negative $\delta^{13}C$ (Lambers et al., 1998).The ratio was determined in mature Lf5 grown under HL or LL conditions, and leaves transferred from HL to LL at the different developmental stages (P1, P3 and P5) by mass spectrometry (for more detail see 4.3.5). The ratio of unknown to standard isotope distribution is $\delta^{13}C$. The results (Figure. 4.4) indicated that the lowest $\delta^{13}C$ was observed in the P3-transferred leaves, consistent with the gas exchange results showing the lowest CO_2 assimilation in these leaves (Figure 4.2, 4.3). The HL leaves displayed the highest $\delta^{13}C$ which was significantly different from the others ($P<0.05$). Although the P1-transferred leaves were relatively thick and had a stomatal density similar to HL leaves, the $\delta^{13}C$ of the leaves was not significantly different from LL leaves. Although, carbon isotope discrimation is one of the most reliable method to estimate CO_2 concentration in the chloroplast (Terashima et al., 2011), it is difficult to conclude that all the carbon detected in here was fixed via photosynthesis only, as there could be some carbon fixed during leaf development.

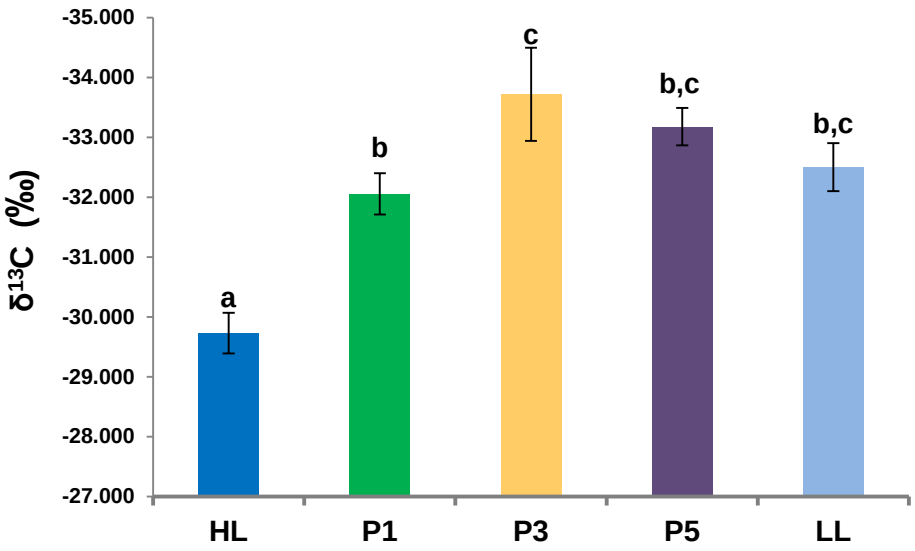

Figure 4.4 Analysis of carbon isotope discrimination measured from mature Lf5 grown under high light (HL), low light (LL) condition, and leaves transferred from HL to LL at the different developmental P-stage. P1, P3, P5 represents the leaves transferred at P1, P3, P5, respectively. $\delta^{13}C$ is the $^{13}C/^{12}C$ ratio of unknown to standard isotope distribution. Identical letters above a column indicate no significant difference ($p<0.05$) between treatments (Tukey's test, n= 5). Error bars indicate standard deviation.

4.5 Discussion

The correlation between rice leaf anatomy and leaf performance after acclimation to different light regimes was investigated in this chapter. It was shown in Chapter 3 that rice leaf thickness was set during leaf development. Alteration of light intensity during P2 to P4 stage of rice leaf development induced the differentiation of thick or thin leaves when the rice plants were transferred from LL to HL or HL to LL, respectively. I chose the P3-stage leaf primordium as a target group representing the developmental window where leaf thickness can be changed in response to different light regimes. The transfer experiments performed in this chapter were HL to LL transfer at P1, P3 and P5 stages of rice leaf 5 (Lf5). According to the results shown in Chapter 3, transfer of the rice plants at P1- or P5- stages of leaf development to a different irradiance condition was not sufficient to induce alteration in the leaf thickness. Considering transfer of rice plants from HL to LL, P1- and P5-transferred mature Lf5 were thicker than LL-grown leaves, and similar to HL-leaves.

The results presented in this chapter indicate that the maximum photosynthetic rates at light saturation (P_{max}) of P1- and P5- transferred mature Lf5 were lower than the HL-grown leaves and comparable to the LL-grown leaves. Whilst the P1- and P5-transferred leaves were thicker due to the earlier HL conditions, their photosynthetic responses were displayed as LL-acclimated leaves with all the physiological parameters that were suitable for LL conditions. On the other hand, the P_{max} of P3-transferred Lf5 was relatively low compared to LL leaves (Chapter 3, Figure 3.15). The lower P_{max} of the P3-transferred mature Lf5 was associated with their thinner leaves, lower RubisCO activity (V_{cmax}), electron transport rate (J_{max}), and lower dark respiration rate (R_d) when compared to all other sample groups. However, there was no significant difference in these biochemical parameters between the P5-transferred Lf5 and either HL-leaves or LL-leaves. These data indicate that present or recent light conditions are the major factor determining the physiological characteristics of mature leaves rather than leaf thickness.

Furthermore, the results presented in this study suggest that leaf development and physiological adaptation can be separated from each other.

I hypothesised that since leaves transferred from HL to LL at P1 and P5 stage had relatively thick mature leaves (chapter 3), they might accumulate a higher amount of RubisCO, thus potentially increasing P_{max}. The results presented in this chapter reveal that although the level of RubisCO protein in mature Lf5 of P1-, P3- and P5- transferred leaves correlated with leaf thickness, there were no statistically significant difference in the level of RubisCO between these transferred leaves and LL-leaves. The P1- and P5-transferred leaves showed a physiological performance that could not be distinguished from the LL grown leaves, indicating that my initial hypothesis was not supported.

In tree species, the investigation of plasticity of leaves to variation of irradiance via alteration in amount of RubisCO indicated a large reduction in RubisCO activity per unit leaf area when the plant seedlings were transferred from HL to LL (Paulilo et al., 1994). In rice, the study of Murchie et al. (2005) indicated no change in the level of RubisCO in fully expanded Lf5 transferred from LL to HL at the stage of leaf emergence, after full leaf extension. This result is consistent with the report that in rice leaves the synthesis of RubisCO is very high during leaf expansion and then declines at full leaf extension and becomes lower during senescence. It has been shown that the amount of RubisCO in a rice leaf reaches a peak just before leaf emergence and gradually declines after that (Suzuki et al., 2001). Since, RubisCO is the most abundant leaf protein in mature C3 plants, and accounts for 15-30% of total leaf nitrogen (N), a positive correlation between N-influx and RubisCO synthesis has been reported (Imai et al., 2008). It has also been shown that leaf N concentration is positively related to the light intensity experienced by the leaf (Werger and Hirose, 1991). Moreover, the genes encoding for RubisCO (*rbc*S and *rbc*L) are light activated genes which show large increases in their transcription and protein products when leaves are illuminated (Lawler, 1993). Taken all of these data together, it can be said that the alteration in irradiance

during rice leaf development can induce changes in the level of RubisCO to suit the prevailing light condition that is a prerequisite for acclimation to different light regime.

The decreased chlorophyll a/b (Chl a:b) ratio observed here were is also consistent with a shade acclimation response Lf5 of the transferred rice plants. Plants growing under low light intensity may have more chlorophyll *a* and *b* per unit volume of chloroplast and higher chlorophyll *b* due to increase in the light-harvesting complex (LHC) (Lawler, 1993; Lambers et al., 1998; Taiz and Zeiger, 2010). These mechanisms enhance photon capture and energy transfer to the reaction centre of photosynthesis in shaded plants. Transfer of rice plants from LL to HL after full leaf extension causes a decrease in chlorophyll *b level*, thus Chl a:b ratio increases (Murchie et al., 2005). Moreover, the decrease in chlorophyll *b* level is believed to help avoidance of photo-oxidation and over-excitation of chlorophyll protein complexes that can be regulated by degradation of the LHC. This is a chloroplast-level acclimation of rice leaves that occurs independently of leaf age (Murchie et al., 2005). The decrease in total chlorophyll and increase in Chl a:b ratio in mature leaves of tropical tree transferred from LL to HL has also been reported (Krause et al., 2004).

It has been reported that chloroplast biogenesis in rice occurs at the P4-stage where leaf blade elongation occurs (Kusumi et al., 2010). Chlorophyll content of the P4-leaf remains insignificant but increases as the leaf enters the P5 stage. Moreover, the photosynthetic machinery is also activated during the late P4 and P5 stage after leaves start to emerge (Kusumi et al., 2010). These results suggest that chloroplast-level acclimation probably occurs relatively late in rice leaf development. This is consistent with my findings that the P1-, P3- and P5-transferred mature Lf5 displayed a low Chl a/ b ratio (as did LL-leaves) when they acclimated to low light intensity. These data suggest that chloroplast-level acclimation is more plastic than leaf anatomical acclimation.

Although, leaf thickness is not the main factor determining physiological adaptation of a leaf, there is a strong correlation between leaf thickness and P_{max}. It is believed that, to achieve higher P_{max}, sun leaves should have more

RubisCO than shade leaves. Moreover, the increase in RubisCO level should be accompanied by a greater mesophyll surface area exposed to intercellular spaces per unit leaf area (S_{mes}) which is indispensable for a larger chloroplast surface area (S_c) to function (Terashima et al., 2006; Terashima et al., 2011). The reason for this is that a greater S_{mes} means increasing the area for CO_2 dissolution and the effective pathway for CO_2 diffusion, thus for photosynthesis. Maximising S_{mes} by increasing cell hight could be the reason why sun leaves are thicker than shade leaves (Terashima et al., 2001; Terashima et al., 2011). Mature leaves of *Chenopodium album* grown under LL showed higher P_{max} with increased S_c after they were transferred to HL at maturation. However, the higher P_{max} that the transferred leaves achieved was not as high as HL leaves, probably due to the fact that the open spaces along the leaf cell walls that accommodate the increase in chloroplast surface area of these LL grown leaves were not as great as in HL leaves (Oguchi et al., 2003). In conclusion, a suitable leaf thickness is required for photosynthetic acclimation to HL and sets the limits of the system early in development, but whether this potential is achieved depends very much on the environment in which the leaf is growing.

Chapter 5 | How is leaf thickness controlled by changing irradiance?

5.1 Introduction

Generally, plants produce an optimal leaf form to suit a given environment by principles of water use efficiency, temperature, and gas exchange. The thin, flattened lamina of leaves optimises function in capturing sunlight and facilitating gas exchange, enabling a compromise between leaf energy exchange, leaf temperature and photosynthesis. Therefore, the shape and size of a leaf are the key features related to function. The interaction between genotype and environmental influence has a crucial impact determining the shape and size of plant organs such as flowers and leaves (Powell and Lenhard, 2012). Although our understanding of the genetic regulation of organ size and shape is still fragmentary, it has been long known that the main cell processes affecting the growth of organs are cell proliferation and cell expansion. Expression of a number of genes regulates these processes, and thus influences the control of final organ size and shape. In addition, studies suggest the control of cell proliferation, and thus leaf morphogenesis, by a transcription factor/ microRNA based pathway (Palatnik et al., 2003).

Although leaf morphogenesis is under genetic control, there is a certain degree of flexibility which allows leaves to adapt their growth to fit the prevailing environment, such as irradiance, nutrient and water (Smith and Hake, 1992; Kim et al., 2005). As light, captured by chloroplasts in leaves, is the source of energy driving photosynthesis, modulation of leaf development is a crucial mechanism that plants use for surviving under various light conditions. As I described previously in Chapter 3, plants produce sun- or shade-type leaves when growing under high light or low light conditions, respectively. One of the most important anatomical characteristics that make sun leaves different from shade-leaves is leaf thickness, with sun leaves being thicker than shade leaves. It is believed that the differentiation of a leaf into sun or shade type is controlled remotely by mature leaves via a long-distance signalling system (Lake et al., 2001; Yano and Terashima, 2001; Thomas et al., 2004), although also control via a short-distance signalling system in leaf

primordia has been proposed (Ferjani et al., 2008). The reason why plants have developed these signalling systems could be due to the fact that a leaf primordium, especially leaf primordium of grasses such as rice, develops from a shoot apical meristem (SAM) protected and thus shaded inside the leaf sheath of the preceding leaves. Since important aspects of leaf shape are determined early in development, the plant requires a system by which the prevailing light environment (experienced by mature leaves) is signalled down to the early, developing leaves. Although, the exact light sensory mechanism and genetic mechanism leading to the systemic signal remain unclear, there are three main proposed steps required: a sensing of the irradiance intensity; transformation of the environmental information into a mobile substance(s); and induction of the expression of the genes that play a function in cell growth in the early developing leaf (Ferjani et al., 2008).

There are several candidates that could be the theoretical signal. RNAs, peptides, sugars, phytohormones, and redoxes have all been considered possible (Kim et al., 2005; Coupe et al., 2006). For example, plant hormonal pathways can be modulated by light in different ways and, indeed, a recent study on auxin flux carriers mutants suggested that light has an influence on SAM via affecting the distribution of auxin (Bainbridge et al., 2008). In addition, the control of organogenesis by light via activation of auxin and cytokinin signalling has been reported (Yoshida et al., 2011). Considering redox as a signal, in high light conditions, where the photosystem II (PSII) is under high excitation pressure, the plastoquinone (PQ) pool in chloroplast thylakoid membranes is reduced while it is oxidised under low light conditions, thus the light environment can be represented by the reduction/oxidation (redox) state of the photosynthetic electron transport component. The redox state of the PQ pool controls the transcription of photosynthetic genes such as the nuclear *Lhcb* gene family that encodes the chlorophyll a/ b binding proteins (*CAB*) of the light harvesting complex of the PSII (Escoubas et al., 1995; Fey et al., 2005). Sugar is the product of photosynthesis that can be transferred from the leaf to other parts of the plant and used in a variety of ways (Laine, 1994). Thus sugar is a signal candidate that can convey information wihin

plants. For example, the function of the enzyme hexokinase in glucose signalling system in *Arabidopsis* has been reported (Cho et al., 2006). Recently, there is strong evidence that trehalose-6-phosphate (T6P) plays an indispensible function as a sugar signal which links metabolism to development in plants (Paul et al., 2008). In addition, the regulation of gene expression by sugar is well documented (Koch, 2004). However, the exact function of these signal candidates still needs more verification. Furthermore, physiological and developmental analyses and, in particular, global gene expression profiling should be performed in order to confirm these speculations.

In *Arabidopsis*, several genes have been identified as high light intensity-activated genes, including the gene for chimeric chalcone synthase which is related to the signal transduction system activated by plant photoreceptors (Feinbaum et al., 1991; SchÄFer et al., 1997), a zinc finger transcription factor (Asako et al., 2000), ROS scavengers (Karpinski et al., 1997), the ELIP protein (early light induced protein) and stress-enhanced proteins which are homologous to *CAB* proteins (Heddad and Adamska, 2000). On the other hand, the study of Heddad and Adamska (2000) shows that the genes encoding for antenna components (LHCP), were down-regulated under high light condition. In rice, analysis of gene expression profile following transfer to a high light intensity also shows the down-regulation of genes encoding for the light harvesting protein, and up-regulation of stress-related genes and high expression of *ELIP2* (Murchie et al., 2005).

Taken all these together, the control of leaf thickness in response to different irradiance may be complicated, since the nature of the signal from the mature leaf is still unknown and many questions, including how plants control cell size and shape, remains to be ascertained. However, the results in Chapter 3 at least identify the developmental window during which leaf thickness can be set during rice development. Therefore, I decided to use microarray technology, which allows the monitoring of expression of thousands of genes at a time, to investigate the global gene expression profile in rice leaves undergoing alteration in thickness in response to different irradiance. I

hypothesised that change in gene expression underpins the control of leaf thickness and the results in this section identify a number of genes whose expression changes in P3-stage leaf 5 following a transfer from high light to low light.

5.2 Aim

1. To identify the genes potentially involved in the control of leaf thickness in response to altered light regime.

5.3 Brief methodology

5.3.1 RNA extraction

Leaf primordia (60 leaf primordia/ sample group) at P3 stage of leaf 5 were dissected and stored at -80 ºC before grinding in liquid nitrogen using a pre-cooled micro-pestle. The leaf primordia were then homogenized by grinding in 500 µl TRIzol® reagents before incubation for 2 minutes at 37ºC and then 5 minutes at room temperature. Chloroform (100 µl) was added and mixed with the homogenised tissues before further incubation at room temperature for 5 minutes. The homogenised tissues were centrifuged at 12,000xg at 4ºC for 10 minutes. The colourless upper aqueous phase was collected and then mixed with 300 µl of isopropyl alcohol before incubation at -20 ºC for overnight. Centrifugation at 12,000xg was then performed to collect the precipitated RNA before washing step using 80% ethanol. The RNA pellets were air dried and dissolved in 20 µl of nuclease-free water. RNA concentrations were measured at 260 nm by using a NanoDrop machine.

5.3.2 Microarray analysis

Rice plants were grown under high light condition (HL) until Leaf 5 (Lf5) developed to P3 stage and then were collected for micro-dissection and RNA extraction as 0 hr-HL sample. A number of rice plants were transferred from HL to LL and then RNA were extracted from the P3-stage Lf5 after 6 or 24 hours of transfer. Figure 5.1 shows a schematic of the leaf transfer experiment in relation to sample group classification used in this study. The microarray

analysis of 3 replicates per sample group was performed using the Affymetrix 57K Rice gene chip by NASC's Affymetrix service. Comparison of gene expression level between the sample groups was done using MAANOVA statistical analysis package in R programming (analysed by Ramil P. Mauleon, IRRI). John Storey's false discovery adjustment (jsFDR) method (Storey, 2002) was performed. The adjusted p-valuep-value threshold was 0.05. Probesets annotation were done using NetAffx™ Analysis center (http://www.affymetrix.com/analysis/ index.affx).

5.3.3 cDNA synthesis

One microgram of total RNA (DNA-free) was mixed with 1 μg of oligo-d(T)18 primer in a total volume of 20 μl, heated at 70ºC for 5 minutes and then incubated at 4ºC for 2 minutes before reverse transcription, in a total volume of 50 μl in the reaction mixture containing 5 μl of MMLV-RT buffer solution, 500 μM dNTP, 1 μl of 10,000 units MMLV-Reverse transcriptase, at 42ºC for 1 hour.

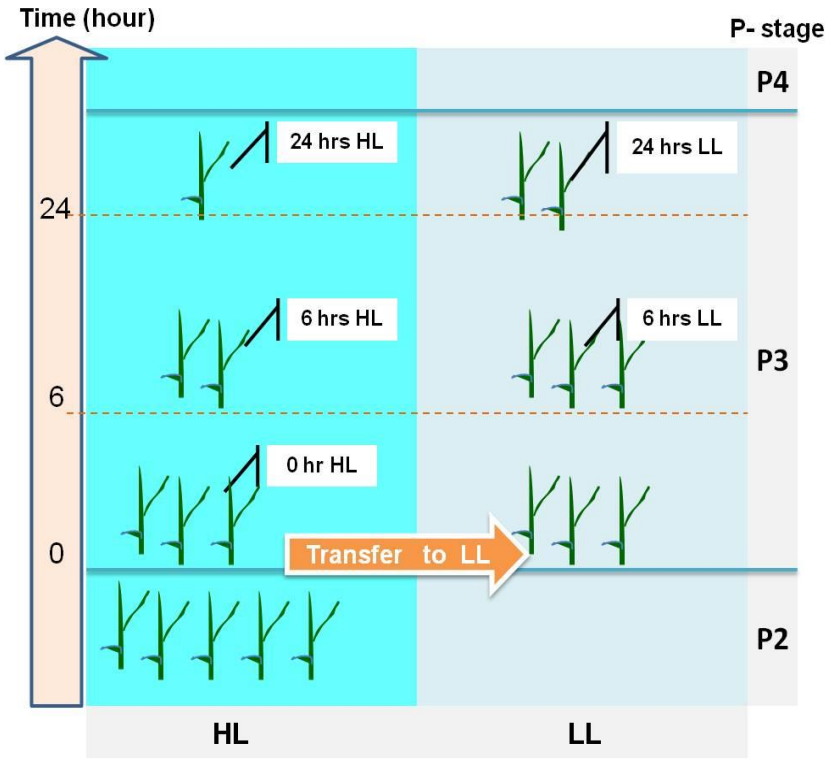

Figure 5.1 Schematic of transfer experiment from high light (HL) to low light (LL) performed when leaf 5 developed at P3-stage. A number of plants were transferred to LL and collected after 6 and 24 hours of transfer, thus stated as 6hrs LL and 24 hrs LL, respectively. Rice plants grown continually under HL in parallel to those transferred plants were also collected at 0 hr, 6 hrs and 24 hrs of transfer.

5.3.4 Quantitative polymerase chain reaction (qPCR)

The cDNAs using in this study were from the 6 hrs HL and 6hrs LL sample groups (Figure 5.1). qPCR reaction mixture in total volume of 20 μl contained 2 μl of cDNA (obtained from 1 μg RNA), 10 μl of 2x SYBR®Green PCR Mastermix, 1 μl of 10 μM forward primer and 1 μl of 10 μM reverse primer (primer sequences for all the genes of interest were listed in Chapter 2). The qPCR assays were done in triplicate for each gene of interest and run for 40 cycles using an ABI StepOnePlus™ PCR system. The elongation factor gene, EEF1A was used as an endogenous control in this study. A standard curve method was used for pre-screening the Ct values of the primers by using 4 different concentrations of cDNA obtained by 2 fold-serial dilutions.

5.3.5 *In Situ* hybridisation analysis

The RNA probes using in this study were designed using the Primer3 primer design program, primers sequences were listed in Chapter 2. The probes were synthesised through pBlueskript SK II (-) plasmid construction before in vitro transcription and labelling with digoxigenin-substituted nucleotide, DIG-UTP. Transverse sectioning of the young rice plants (at the position of the SAM) embedded in paraplasts was done and used for *in situ* hybridisation. The details of in situ hybridisation procedures were described in Chapter 2. The rice plants used in this study were the 6 hrs HL and 6hrs LL sample groups (Figure 5.1). The volume of the antisense and sense probe used for hybridisation was varied between 1, 5 and 10 µl.

5.4 Results

5.4.1 Change in gene expression following a transfer from HL to LL revealed by microarray analysis

The microarray analysis was performed using MAANOVA analysis package in Bioconductor/ R programming with the high stringent false discovery rate adjustment method of John Storey, jsFDR (Storey, 2002). For pairwise comparisons, the T-tests were performed within MAANOVA using a jsFDR adjusted *p*-value cut off at 0.05. The microarray analyses, using cut off value for FDR adjusted *p*-value at $p<0.05$, detected no differentially expressed genes) comparing the 6 hrs and 24 hrs transferred P3-stage Lf5 to those maintained under high light and collected for RNA extraction at the same time points (6 hrs HL and 24 hrs HL respectively). However, using a pre-adjusted P-value of $p<0.01$ as a cut-off, a number of genes showed a differential expression level ($p<0.01$) following a transfer from high light (HL) to low light (LL) for 6 and 24 hours (Table 5.1). Although these genes were not statistically different due to the high false discovery rate which occurred when using the un-adjusted P-value as a cut-off, I decided to further validate the microarray analysis results as these selected genes could be the biologically meaningful genes related to the control of leaf thickness.

Table 5.1 Selected genes show different expression levels according to pairwise comparisons between sample groups, t-tests (p<0.01)

Comparison	Count of significant (genes), p<0.01
0 hr HL & 6 hrs HL	34
0 hr HL & 6 hrs LL	35
6 hrs HL & 24 hrs HL	215
6 hrs HL & 6 hrs LL	85
6 hrs LL & 24 hrs LL	1229
24 hrs HL & 24 hrs LL	508

Table 5.1 shows the total number of genes that show different expression level following the transfer of the P3-stage leaf 5 (Lf5) from HL to LL and the rice plants were maintained under LL for 6 hours (6 hrs LL) or 24 hours (24 hrs LL). Various pairwise comparisons of gene expression level of the transferred groups to the other groups maintained under HL for 0, 6 or 24 hours were made. Comparing the 6 hrs HL and 6 hrs LL samples, there were 85 genes that were differentially expressed; 37 genes were down-regulated and 48 genes were up-regulated. Comparison between 24 hrs HL and 24 hrs LL samples showed that transferral of the P3-stage Lf5 from HL to LL for 24 hours led to down-regulation of 192 genes and up-regulation of 317 genes (508 genes in total). There were no overlapping gene identities within the genes list of the 6 hrs HL vs. 6 hrs LL results and the 24 hrs HL vs. 24 hrs LL results. Figure 5.2 illustrates these two comparison results using the volcano plots. For HL samples, the comparisons of 0 hrs HL to 6hrs HL and 6 hrs HL to 24 hrs HL given rise 34 and 215 genes that showed different expression level after maintaining the rice plants under HL for 6 and 24 hrs, respectively. 34 of these genes were also identified via the comparison of 6 hrs HL vs. 6 hrs LL and 24 hrs HL vs. 24 hrs LL. Similarly, among the 35 and 1229 genes selected by the comparison of 0 hr HL vs. 6 hrs LL and 6 hrs LL vs. 24 hrs LL respectively, there were 29 genes which were identified in both comparisons.

Table 5.2 shows number of overlapping genes within gene list result identified from each comparison. These differentially expressed genes can be categorised based on their biological functions into genes related to photosynthesis, plant development, phytohormone, stress, kinase, carbohydrate metabolism, membrane protein, protease, signal transduction, transcription factor and putative or unknown function protein.

Table 5.2 Number of overlapping genes within gene lists result of each comparison.

	0 hr HL vs. 6hrs HL	0 hr HL vs. 6hrs LL	6 hrs HL vs. 24hrs HL	6 hrs LL vs. 24hrs LL	6 hrs HL vs. 6 hrs LL	24 hrs HL vs. 24hrs LL
0 hr HL vs. 6hrs HL	34	3	0	0	5	0
0 hr HL vs. 6hrs LL	3	35	1	5	1	0
6 hrs HL vs. 24hrs HL	0	1	215	31	1	29
6 hrs LL vs. 24hrs LL	0	5	31	1229	1	28
6 hrs HL vs. 6 hrs LL	5	1	1	1	85	0
24 hrs HL vs. 24hrs HL	0	1	28	29	0	508

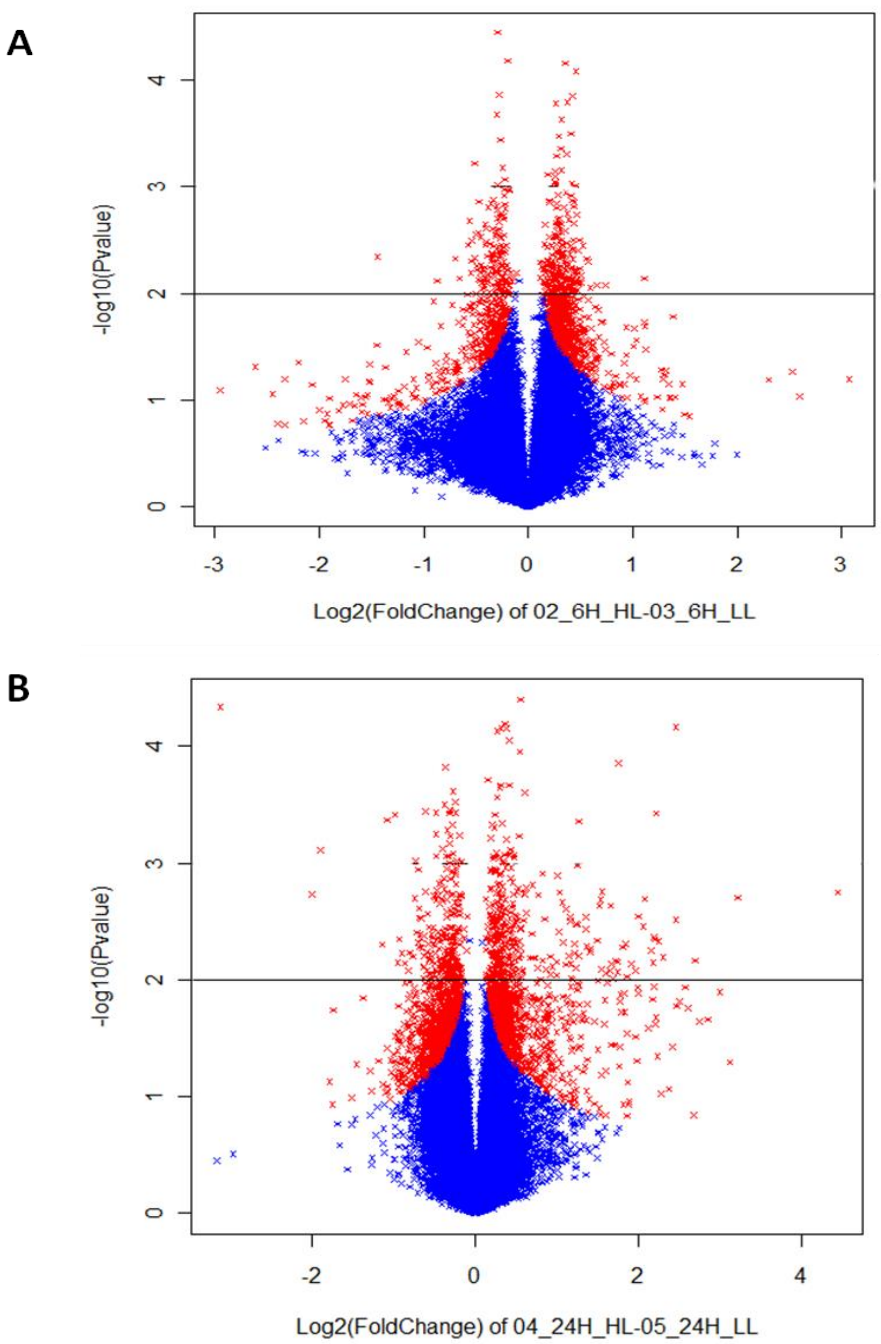

Figure 5.2 Volcano plots of $-\log_{10}$ P-value vs. $\log_2$ fold change from the comparison between **A)** 6hrsHL to 6hrsLL, **B**) 24hrsHL to 24hrsLL; $P<0.01$. The horizontal dimension is the fold change between the two and the vertical axis represents the *p*-value for a t-test of differences between samples. The horizontal black line represents a P-value of 0.01. Red crosses represent genes having a *p*-value less than 0.1 and/ or a fold change greater than 0.1. Blue crosses represent genes having a *p*-value more than 0.1 and/ or a fold change less than 0.1.

Table 5.3 and 5.4 show twenty of the genes selected by the cut-off (p < 0.01) that were differentially expressed in the comparison between 6hrs HL and 6 hrs LL samples. The genes listed in the tables are arranged by high to low value of fold change. The fold changes of these genes were mainly lower than 2 fold. This could be explained by the short period of 6 hrs transfer from HL to LL that may not be long enough to see a large difference in gene expression level. Table 5.5 and 5.6 also show twenty genes selected by the cut off and arranged by high to low value of fold change in gene expression level identified by the comparison of 24 hrs HL vs. 24 hrs LL. It should be noted that the comparison of 24 hrs HL vs. 24 hrs LL samples revealed that the genes related to light harvesting complex (LHC) and chlorophyll *a*/ *b* binding protein were up-regulated in the LL samples. This is consistent with a recent study indicating that chloroplast biogenesis and the photosynthetic machinery are activated early in the P4 stage of rice leaf development (Kusumi et al., 2010). In addition, low light acclimation by enhancing photon capture through increased light harvesting complex is frequently observed, as discussed previously. The full lists of differentially expressed genes following the transfer from HL to LL for 6 hours and 24 hours are shown in Appendix A-D.

Considering the control of leaf thickness, there were some genes in the top gene lists that have been reported to be related to leaf morphogenesis. Interestingly, the gene *OsDWARF* which is related to brassinosteroid biosynthesis showed down-regulation after 24hrs transfer to LL (Table 5.4). Mutation analysis in rice indicated defects in the organised arrangement and polar elongation of cells in the leaves and stem of *OsDWARF* mutants (Hong et al., 2002). These mutants, with a dwarf phenotype, developed severely malformed small leaves with tortuous and stiff blades. In addition, the *SCARECROW*-like (*Scl1*) and *SCARECROW* (*SCR*) genes, which regulate cell proliferation in *Arabidopsis* leaves (Dhondt et al., 2002), were also down-regulated in P3-stage Lf5 transferred to LL for either 6 or 24 hours. Interestingly, down-regulation of *SRF* 8, a member of *STRUBELLIG* (*SUB*) gene family, was observed following the transfer from HL to LL for 6 hours. This gene family encodes receptor-like kinases which are implicated in the control

of cell division (Eyuboglu et al., 2007). The potential role of these genes in the control of leaf thickness requires further investigation. Some of the differentially expressed genes are related to the candidate signal molecules previously described in the introduction, such as thioredoxin (gene Os07g0684100 encoding for thioredoxin-like 1) and trehalose-6-phosphate (gene Os07g0624600 encoding for trehalose-6 phosphate phosphatase), thus are interesting candidates for further investigation.

Table 5.3 Selection of genes down-regulated after transfer to low light for 6 hours, comparing between 6hrs HL vs. 6hrs LL.

Gene ID	Annotation	Fold change
Os.16037.1.S1_at	unknown	2.61
Os05g0433000	Serine/threonine-protein kinase SAPK4	0.91
Os07g0565400	Protein kinase domain containing protein, SRF8	0.87
Os03g0238800	Conserved hypothetical protein	0.70
Os02g0315600	Helix-loop-helix DNA-binding domain containing protein	0.66
Os01g0826000	Heavy metal transport/detoxification protein domain containing protein	0.57
Os04g0587100	Pectinesterase inhibitor domain containing protein	0.56
Os02g0751900	Type I inositol-1,4,5-trisphosphate 5-phosphatase CVP2	0.51
Os05g0351200	AP2; DNA-binding domain found in transcription regulators in plants such as APETALA2 and EREBP	0.50
Os03g0773600	Kinesin, motor region domain containing protein	0.48
Os10g0551200	Similar to Scl1 protein, GRAS family transcription factor	0.47
Os06g0321700	Conserved hypothetical protein	0.45
Os07g0158000	unknown	0.33
Os12g0283300	Hypothetical protein	0.30
Os03g0692500	Galectin, galactose-binding lectin family protein	0.30
Os01g0247900	AWPM-19-like family protein	0.28
Os12g0569000	Conserved hypothetical protein	0.26
Os12g0626200	Auxin responsive SAUR protein family protein	0.24
Os01g0145000	Protein of unknown function (DUF3681)	0.23
Os08g0169100	Hypothetical protein	0.20

Table 5.4 Selection of genes up-regulated after transfer to low light for 6 hours comparing between 6hrs HL and 6hrs LL.

Gene ID	Annotation	Fold change
Os11g0211800	Hypothetical protein	1.38
Os05g0163700	Acyl-coenzyme A oxidase 4, peroxisomal	1.11
Os01g0115700	Protein kinase-like domain containing protein	0.74
Os03g0246800	Sec7p-like protein	0.56
Os02g0194950	Similar to Transcription factor HBP-1b(C38)	0.52
Os08g0432600	Plant MuDR transposase domain containing protein, SWIM zinc finger	0.49
Os03g0702500	UDP-glucuronosyl/UDP-glucosyltransferase family protein	0.47
Os03g0277600	Domain of unknown function DUF26,Cysteine-rich Receptor-like Kinases (CRKs),	0.46
Os01g0353900 Os12g0630750	Hypothetical protein	0.45
Os07g0673801	Conserved hypothetical protein	0.44
Os11g0567800	Similar to HcrVf2 protein, Leucine rich repeat N-terminal domain	0.44
Os03g0163400	Protein of unknown function (DUF1668)	0.43
Os06g0137600	Ribosome-binding factor A family protein	0.43
Os10g0549850	Protein of unknown function (DUF3615)	0.41
Os12g0265500	HAT dimerisation domain containing protein	0.41
Os02g0188600	Conserved hypothetical protein	0.41
Os02g0585200	Heavy metal transport/detoxification protein domain containing protein	0.39
Os03g0439900	Peptidase aspartic, catalytic domain containing protein	0.38
Os02g0504000	Cytochrome P450	0.38

Table 5.5 Selection of genes down-regulated after transfer to low light for 24 hours, comparing between 24hrs HL vs. 24hrs LL.

Gene ID	Annotation	Fold change
Os03g0679700	Thiamine biosynthesis protein thiC	2.73
Os09g0480900	Anther-specific protein	2.11
Os10g0483500	Cytokinin dehydrogenase , FAD and cytokinin binding	2.02
Os01g0940000	Cytokinin dehydrogenase, FAD and cytokinin binding	1.96
Os05g0548900	Phosphoethanolamine methyltransferase	1.93
Os08g0529100	Proteasome subunit beta type 1	1.78
Os01g0659900	Cyclin-like F-box domain containing protein	1.64
Os09g0531600	putative zinc finger domain, LRP1 type	1.57
Os07g0524900	Protein of unknown function DUF6, transmembrane domain containing protein	1.56
Os04g0543600	Amino acid/polyamine transporter I family protein	1.54
Os07g0676600	Helix-loop-helix DNA-binding domain containing protein	1.50
Os12g0572800	RNA-binding region RNP-1 (RNA recognition motif)	1.47
Os11g0149400	Phytosulfokine precursor protein (PSK)	1.42
Os07g0624600	Trehalose-6-phosphate phosphatase	1.36
Os08g0220400	Pectinesterase	1.27
Os01g0940100	Hexokinase	1.26
Os10g0497700	COBRA-like protein (encoded by *OsBC1L4*)	1.23
Os01g0313300	AP2; DNA-binding domain found in transcription regulators in plants such as APETALA2 and EREBP	1.10
Os01g0727800	Protease-associated PA domain containing protein	1.07
Os11g0124300	SCARECROW	0.93
Os10g0521000	TRE1 (TREHALASE 1); alpha,alpha-trehalase/ trehalase	0.90
Os03g0602300	Cytochrome P450 85A1, Brassinosteriod biosynthesis enzyme, OsDWARF	0.71

Table 5.6 Selection of genes up-regulated after transfer to low light for 24 hours comparing between 24hrs HL vs. 24hrs LL.

Gene ID	Annotation	Fold change
Os04g0583200	Conserved hypothetical protein	5.56
Os02g0629000	Protein of unknown function, DUF584	3.75
Os09g0402100	PF1 protein; linker histone 1 and histone 5 domains	3.59
Os02g0818000	CBS domain containing protein	3.59
Os11g0671000	Auxin_repressed	3.53
Os05g0355400	Universal stress protein (Usp) family protein	3.38
Os07g0475700	Auxin responsive SAUR protein family protein	3.30
Os01g0102900	Light regulated Lir1 family protein	3.23
Os05g0525900	Zinc finger transcription factor PEI1	3.08
Os06g0142200	Early nodulin 93 ENOD93 protein	2.97
Os05g0344200	Conserved hypothetical protein	2.93
Os11g0242800	Chlorophyll a-b binding protein	2.90
Os04g0339400	Aldo/keto reductase family protein	2.73
Os02g0115700	Catalase isozyme A	2.71
Os06g0697000	Xyloglucan endotransglycosylase	2.68
Os10g0401000	Conserved hypothetical protein	2.67
Os11g0634200	Conserved hypothetical protein	2.65
Os04g0635400	DUF3774; Wound-induced protein	2.63
Os01g0667900	GRX_GRXh_1_2_like; Glutaredoxin (GRX) family	2.62
Os07g0684100	Thioredoxin-like 1	2.61

5.4.2 Validation of microarray analysis results by qPCR

To validate the results of microarray analysis, real-time quantitative PCR was performed. From the microarray results in 5.4.1, the selections, based on gene annotations and the predictions of gene function were made. Fourteen genes which might be related to the control of leaf thickness were selected for validation by qPCR. Table 5.7 shows the list and sequences of qPCR primer pairs designed for these genes. All the primers were screened for qPCR efficiency using the standard curve method. The slope of the standard curve was between -3.1 and -3.6 indicating a PCR reaction efficiency of between 90 and 110% (Figure 5.3). qPCR was done with 3

technical replicates and 3 biological replicates. The endogenous gene used in this study as a control was *eEFIa*. Gene expression levels were normalised using the Ct value of the endogenous control before calculation of relative quantification or fold change of the gene of interest compare to the calibrator. The 6 hrs HL samples were use as the calibrator for each individual gene, so the RQ value of this sample is equal 1. Table 5.7 shows RQ value with standard error of means for each gene of interest. The qPCR results confirmed the microarray results for 11 of the 14 genes tested, the exceptions being for the ACX4, UDPG, and cellulase genes which were not significantly differently expressed (ANOVA, $P<0.05$) in the qPCR analysis but were called as differentially expressed in the microarray analysis.

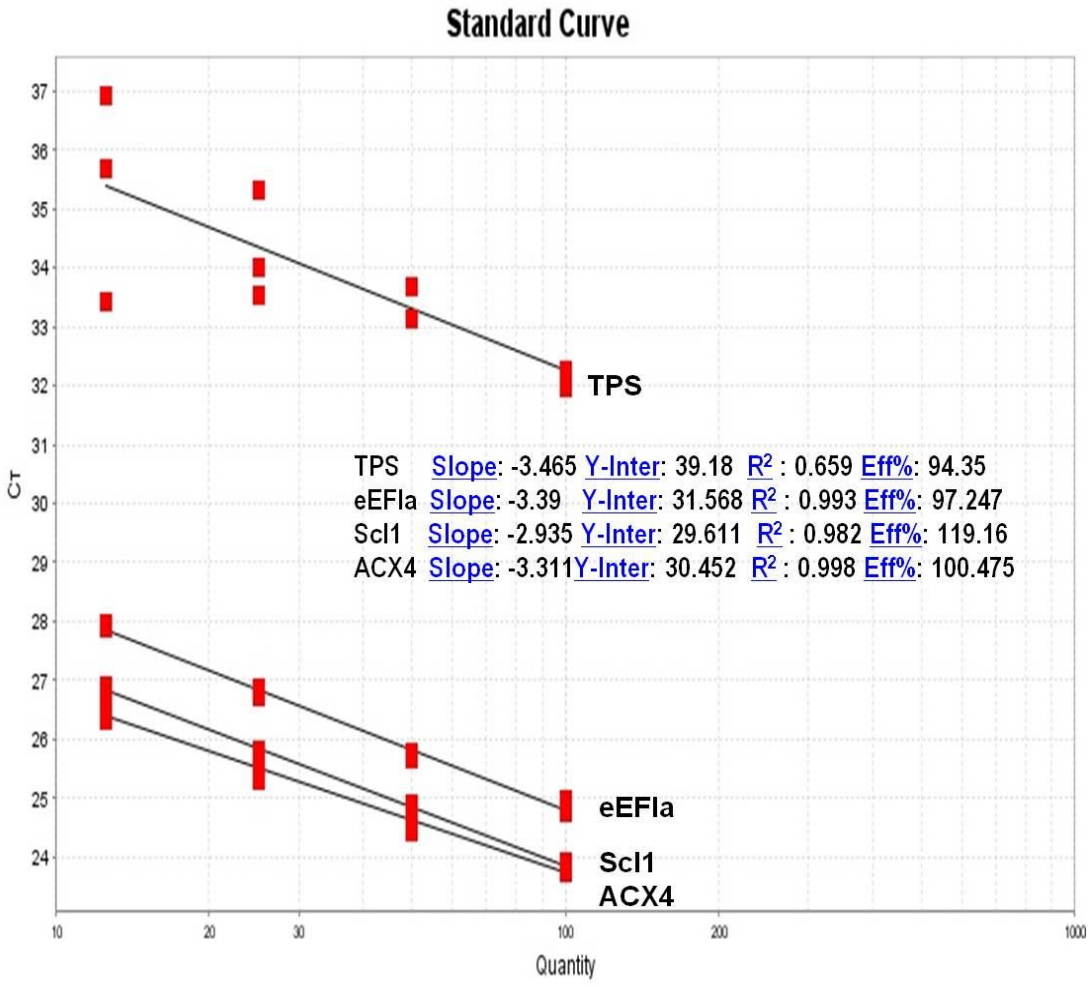

Figure 5.3 Selected standard curve of primer check. Primer name is indicated at the curve. Slope represents the slope of linear curve, Y-Inter is Y intercept, R^2 is the coeffiecient of determination and Eff% represent the efficiency of PCR reaction.

Table 5.7 Validation of microarray analysis by qPCR. The top genes selected from the 6 hours comparison were used.

Primer	Target Gene	Microarray result	qPCR result RQ	
ACX4	Acyl-coenzyme A oxidase 4, peroxisomal	up-regulated	0.994±	0.070
T6PP	Trehalose-6-phosphate phosphatase	down-regulated	0.313±	0.222 *
SAPK 4	SNF1-type serine-threonine protein kinase SAPK4	down-regulated	0.273±	0.089 *
SRF8	SRF8 (strubbelig receptor family 8); kinaseSRF3	down-regulated	0.324±	0.254 *
PecI	Pectinesterase inhibitor domain containing protein	down-regulated	0.709±	0.084 *
BST 1	BST1 (BRISTLED 1)	down-regulated	0.338±	0.100 *
Scl1	Scarecrow like -1 protein	down-regulated	0.461±	0.209 *
UDPG	UDP-glucuronosyl/UDP-glucosyltransferase family	up-regulated	1.057±	0.023
GAL4	Galectin, galactose-binding lectin family protein	down-regulated	0.557±	0.057 *
Cellulase	Cellulase	up-regulated	0.884±	0.260
AWPM	AWPM-19-like family protein (stress tolerance)	down-regulated	0.599±	0.126 *
AuxSAUR	Auxin responsive SAUR protein family protein	down-regulated	0.663±	0.098 *
16037	16037	down-regulated	0.484±	0.190 *
32313	32313	down-regulated	0.456±	0.260 *

RQ(relative quantitation), fold change calculated from $RQ=2^{-\Delta\Delta Ct}$. *Asterisks indicate significant difference (p<0.05).*

5.4.3 *In Situ* hybridisation analysis of lead genes

The microarray analysis identified two lead genes (*SRF8* and *Scl*-1) that previous data suggested are involved in the control of cell division and, thus, potentially might play a role in the control of leaf thickness. To further investigate the expression pattern of these genes, in situ hybridisations were performed to identify whether these genes showed any tissue specific expression pattern in the leaves responding to a change in irradiance level. The *in situ* hybridisation were done using 2 riboprobes specific to the *SRF8* and *Scl*-1 genes which showed down regulated expression in microarray analysis comparison between the 6hrs HL and 6hrs LL samples. Transverse sections of rice plants from both groups were used. The endogenous control gene for this study was *eEFIa*. Figure 5.4 shows a uniform *eEFIa* RNA expression pattern throughout the leaf sections. This positive control verified the functioning of the *in situ* hybridisation technique. A lower signal was observed in the 6hrs LL leaf samples compared to the 6hrs HL using the antisense probe for *SRF8*. A stronger signal was detected at the SAM and in the P1, P2, P3 and P4 stage of the 6hrs HL samples, especially at the edge of the P3-stage Lf5 compared to that of the 6hrs LL P3-stage Lf5 (Figure 5.5B and D). However, more replicates are needed to confirm these results. Hybridisation using the probe for the *Scl1* gene showed an inconclusive result (Figure 5.6) due to the quality of the hybridisation of LL samples that was not as good as HL samples. The data confirm that the Scl1 gene is expressed in the apex but an improved quality of in situ hybridisation is required in order to compare the signal between the two treatments.

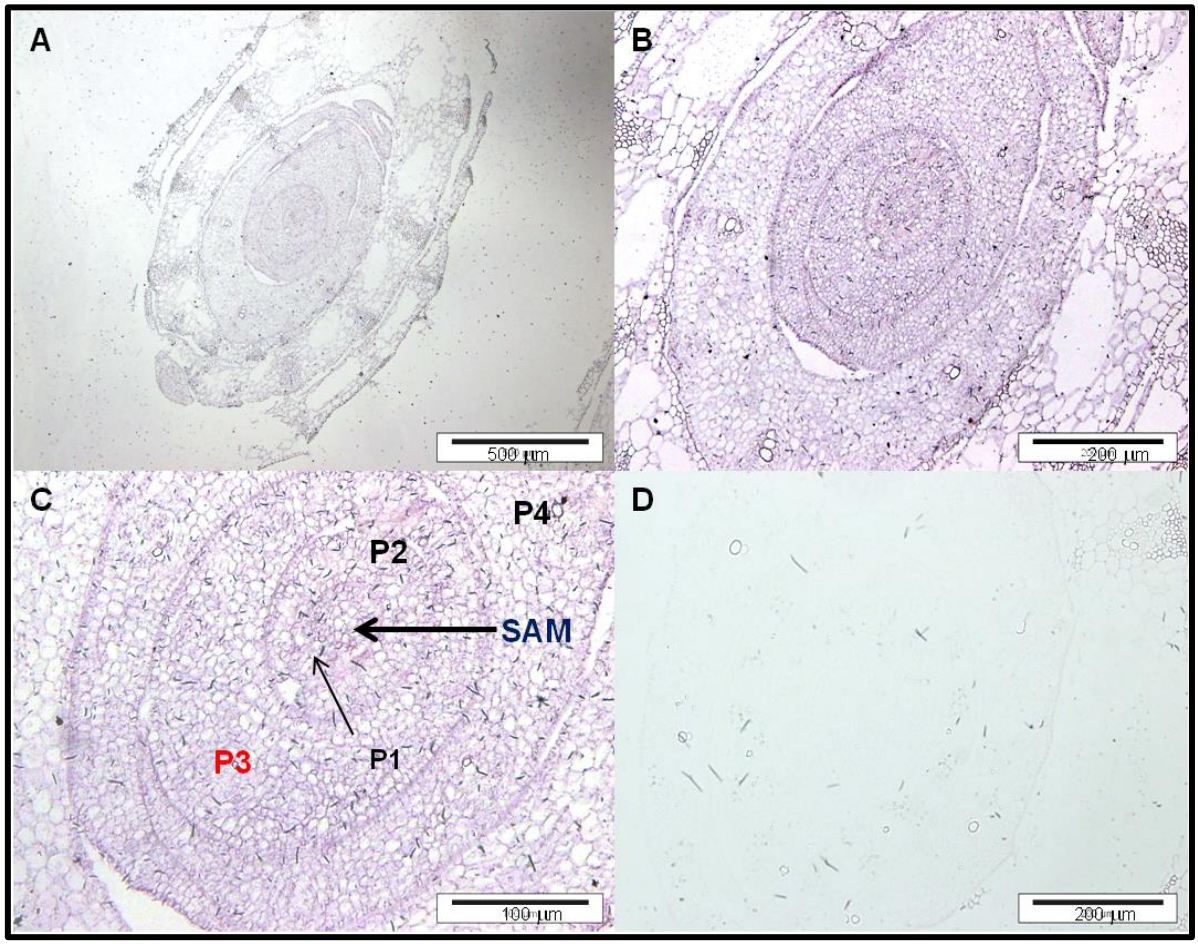

Figure 5.4 RNA expression pattern of the rice *eEFIa* gene in early leaf development under high light condition. **A)** Brightfield image of transverse sections hybridised with *eEFIa* probes. **B)**, **C**) Higher magnification images of the shoot apex showing a uniform signal (blue) reflecting the expression pattern of *eEFIa* in the SAM, P1, P2, P3 and P4 leaf. **D)** No signal was observed using an *eEFIa-sense* probe.

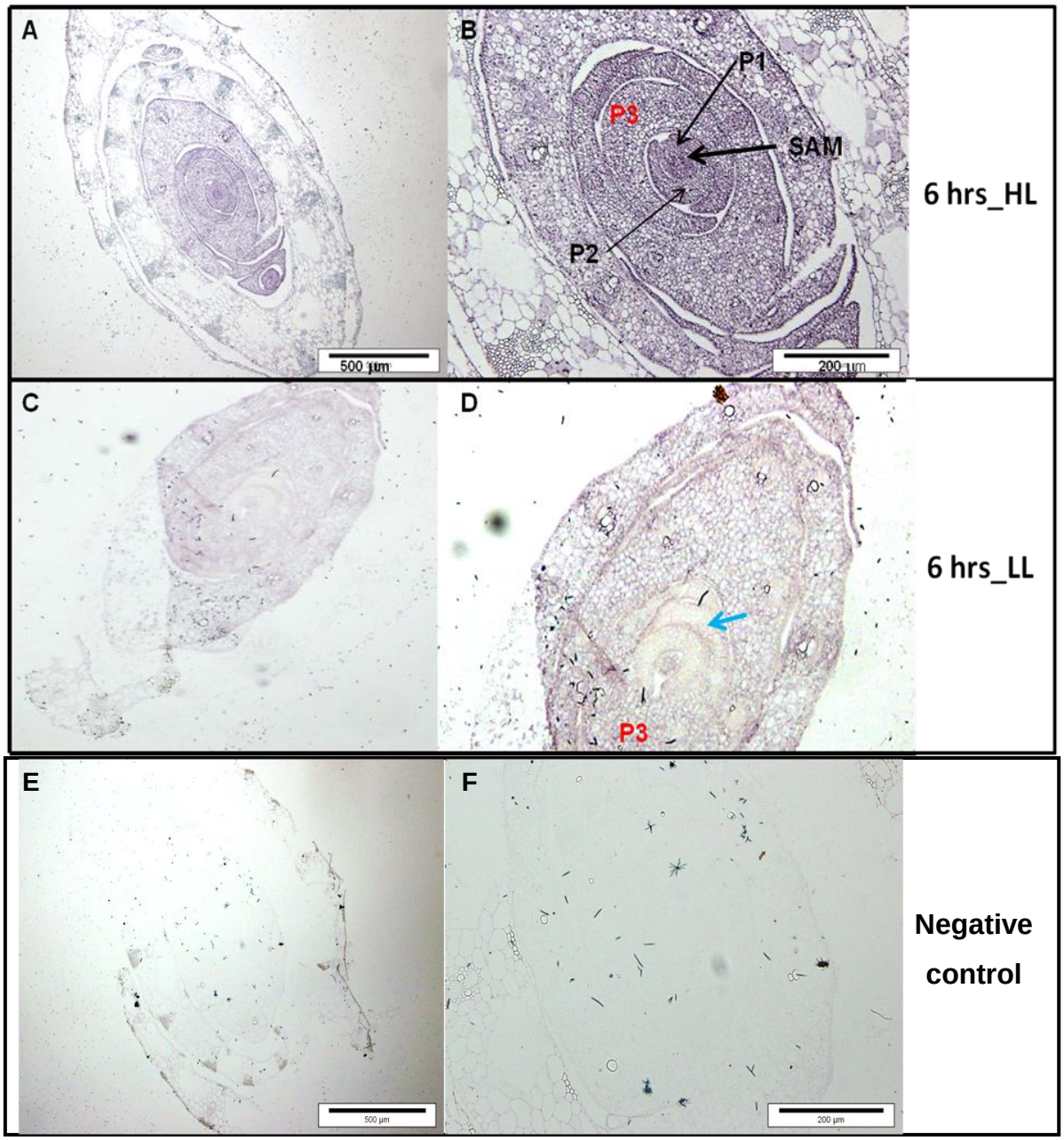

Figure 5.5 RNA expression pattern of the rice *SRF8* gene in early leaf development of rice. **A)** Brightfield image of a transverse section of 6hrs HL leaves hybridised with *SRF8* probes. Signal (blue) is observed throughout the section. **B)** Higher magnification of **A)** showing higher expression in shoot apical meristem (SAM). **C)** Brightfield image of a transverse section of 6hrs LL leaves hybridised with *SRF8* probes. **D)** Higher magnification of **C)** showing lower signal in the P3-stage leaf5 (blue arrow). **E)**, **F)** No signal was observed using a *Scl1-sense* probe hybridised with transverse sections through the apex.

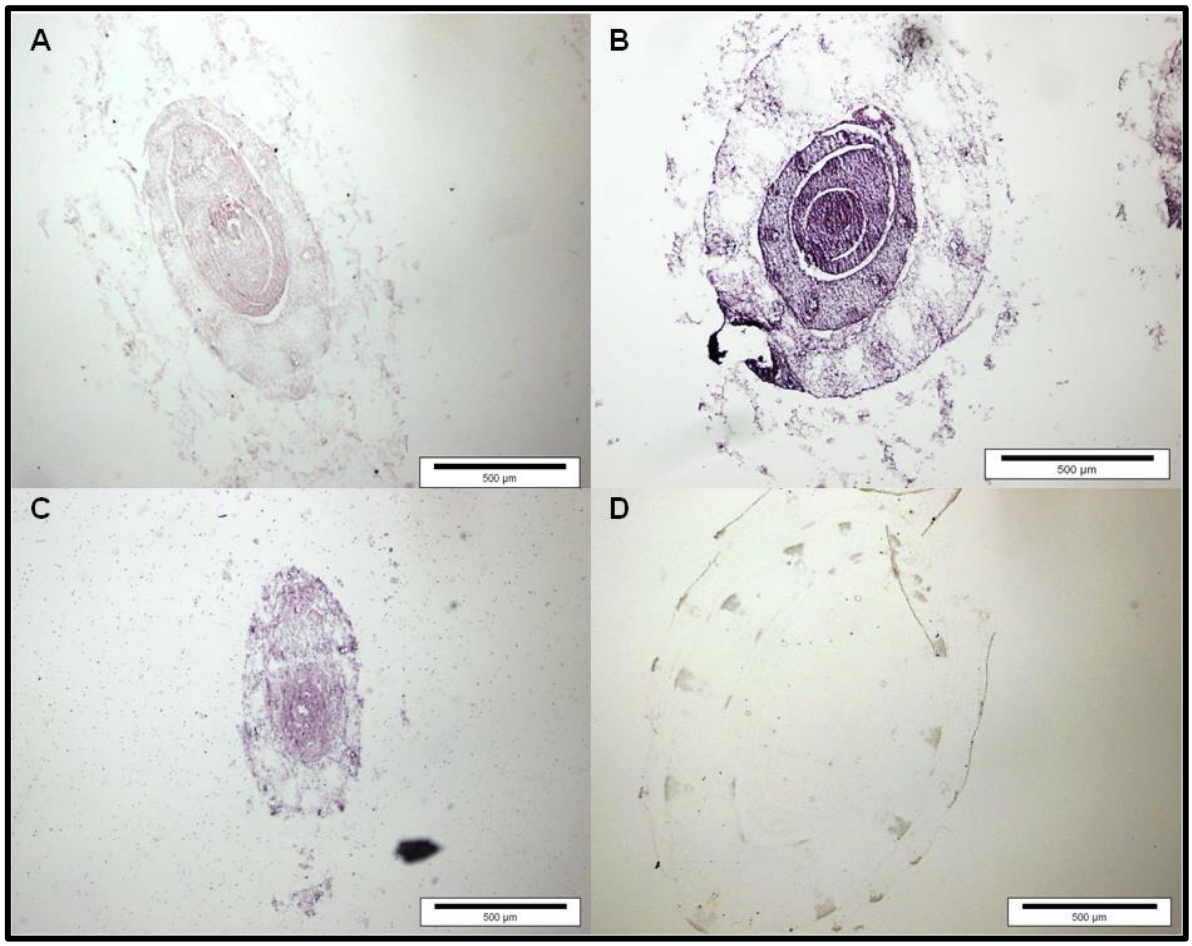

Figure 5.6 RNA expression pattern of the rice *Scl1* gene in early leaf development. **A)** and **B)** Brightfield images of a transverse section of a 6hrs HL leaf hybridised with *Scl1* antisense probe. **C)** Brightfield image of a transverse section of a 6hrs LL leaves hybridised with antisense *Scl1* probe. **D)** No signal is observed in section hybridised with a *Scl1-sense* probe.

5.5 Discussion

To identify genes potentially involved in the control of leaf thickness, a microarray analysis was performed. Initially the high stringent false discovery adjustment method of John Storey (jsFDR) in R/ MAANOVA was used and this indicated that no genes were differentially expressed following the transfer of the P3-stage rice leaves from HL to LL for 6 hours or 24 hours (jsFDR corrected, p-value <0.05). However, when the selection stringency was weakened by analysing the un-adjusted *p*- value, 85 genes showed a differential expression ($p<0.01$) comparing the 6hrs HL and 6hrs LL samples, and 508 genes comparing the 24hrs HL and 24hrs LL samples. qPCR analysis indicated that 11 of 14 selected lead genes based on this analysis showed an altered transcript level, suggesting that the lower stringency microarray analysis did identify genes showing a differential expression pattern. Two of these genes were then taken forward for analysis by in situ hybridisation and the preliminary data indicated that one of these genes (*SRF8*) showed an altered expression pattern that was consistent by all three methods of analysis (microarray, qPCR and in situ hybridisation).

Large scale gene analysis methods are very powerful approaches for identifying lead genes involved in biological processes. However, the statistical analysis of these data is not trivial and requires a judgement of when altered gene expression is "significant". A stringent filter can lead to potentially interesting gene expression changes being missed, whereas a less stringent filter has the risk of increasing the number of false positives. Any microarray result needs to be validated by independent methods and we used two approaches (qPCR and in situ hybridisation). Our results indicate that, at least for this investigation, a relatively non-stringent microarray analysis led to the identification of lead genes which could mostly be validated by qPCR. Since qPCR can be performed in a relatively rapid and medium-throughput manner, this combination of methods was effective. In situ hybridisation is much more technically demanding and time consuming and can only be implemented for a small number of lead genes. In our case, we used the microarray/ qPCR approach to identify a reasonable number of leads, then used a literature

search to identify which of these were worth investing time and effort for further investigation. Of the two genes investigated by in situ hybridisation, one of them (SRF8) looks promising as a gene which might be functionally involved in the control of leaf thickness in response to altered irradiance.

SRF8 is a member of the *LLR-V/STRUBELLIG RECEPTOR FAMILY* (*SRF*) gene family encoding putative leucine-rich repeat receptor like kinases (LLR-RLKs). The gene family represented by *STRUBELLIG* (*SUB*), is involved in cellular morphogenesis in a number of different plant organs (Chevalier et al., 2005) and is implicated in the control of the orientation of cell division plane and the regulation of cell size, cell number and cell shape. These RLKs play an important role in transmission of signals across membranes and SRF4 is reported as a direct positive regulator of leaf size (Eyuboglu et al., 2007). In this study, down-regulation of *SRF8* was observed following the transfer from HL to LL for 6 hours. Strikingly, a recent study indicates that the key function of *ANGUSTIFOLIA* (*AN*) in plant tissue morphogenesis is mediated by a *SUB*-signalling mechanism (Bai et al., 2013). This is intriguing since, in *Arabidopsis*, the *AN* mutants have a defect in cell elongation in leaf width, and an enhanced cell elongation in the leaf thickness direction, resulting in larger cell size, and thicker and narrower leaves than in wild type (Tsuge et al., 1996)

In addition to SRF8, some of the other differentially expressed genes identified here could be involved in the control of leaf thickness, although these genes require further characterisation at the expression level before taking them further for functional analysis For example, down-regulation of the genes *SCARECROW-like* (*Scl1*) and *SCARECROW* (*SCR*) in the P3-stage Lf5 transferred to LL for either 6 or 24 hours is interesting. *SCR* is a member of the GRAS family of the transcription factors (Lee et al., 2008) that plays an important role in the control of cell division in the developing Arabidopsis leaf (Dhondt et al., 2002). Mutation analysis in *Arabidopsis* demonstrated an inhibition of leaf growth in *scr* mutants caused by a prolonged S-phase duration mediated by up-regulation of the genes encoding for cell cycle inhibitors (Dhondt et al., 2002). The *scr* mutants, which have a strong defect in cell division, showed a retardation of leaf growth and severe reduction in

final leaf area compared to wild type. This can be compared to the results in Chapter 3 showing that LL- leaves had a lower growth rate and smaller mesophyll cell size than HL-leaves. In addition, a number of genes related to plant transcriptional regulation also showed different gene expression levels following a transfer from HL to LL. It remains to be seen if these transcription regulators and protein kinases affect cell proliferation or cell size or both and thus influence leaf thickness.

It is noteworthy that the *THIAMINE C SYNTHASE* (*THIC*) gene was the top down-regulated gene after the transfer from HL to LL for 24 hrs, since *THIC*, the circadian clock-driven thiamine biosynthetic gene participates in the regulation of plant central carbohydrate metabolism and in the light/ dark metabolic transition. Thiamine biosynthesis is regulated by the circadian clock through the promoter region of THIC gene which contains a region for riboswitch gene expression control. Plants altered in the riboswitch activity showed reduced photosynthesis rate, growth retardation and chlorosis (Bocobza et al., 2013). It would be interesting to see whether altered THIC expression plays a roel in the decreased growth of LL-transferred P3 leaves.

The microarray data presented here also identified changes in gene expression of genes related to the candidate signals involved in relaying irradiance information from the mature leaves to the developing leaves For example, thioredoxin-like 1 and trehalose-6 phosphate phosphatase, potentially influence redox state and sugar signalling, respectively. At some point an irradiance-related signal from the mature leaves much reach the target developing leaves and there must be a mechanism by which this signal(s) is transduced. Enzymes involved in the turnover/metabolism of such signals might play an important role in the response system. Functional analysis and further expression analysis of these putative signal-response genes would be an interesting line of study.

Chapter 6 | GENERAL DISCUSSION

6.1 Response of rice leaf morphology to irradiance

It has been long known that two different types of leaf, sun-type and shade-type, develop when plants are exposed to high or low irradiance, respectively. The sun-type leaves tend to be thicker and are capable of higher maximal photosynthetic rates than shade leaves (Björkman, 1981). As a consequence, leaf thickness was incorporated into the profile of ideotype rice (Cassman, 1994; Peng, 2008) by IRRI. However, how and when the control of rice leaf thickness occurs in response to altered light regime is unclear. In Chapter 3, the response of rice leaves to changes in light environment was assayed by switching them from high light (HL) to low light (LL) conditions or vice versa at P1, P2, P3, P4 and P5-stage of rice leaf development. The fact that a young rice leaf develops from the shoot apical meristem encased by the preceding leaf sheaths was the major challenge in this study. The advantage of classification of rice leaf developmental stages by means of plastochron age (P-stage) and using the emergent length of another leaf as a proxy for prediction of leaf developmental stage were first exploited, thus data on the relationship between leaf 3 (Lf3) emergent lengths and leaf 5 (Lf5) P-stage were collected. Subsequently, the collected data were used as a reference for transferring rice plants at each developmental stage from HL to LL or LL to HL. The results presented in the chapter from both transfer experiments reveal that the stage from P2 to P4 is a developmental window during which IR64 rice leaves show a response to altered light regimes via a change in leaf thickness. This finding is consistent with the report that rice leaf thickness was set prior the emergence of the leaf blade, though the exact stage when the setting occurred was not defined (Murchie et al., 2005). Strikingly, it was also shown in Chapter 3 that leaves transferred at the P1 stage did not respond to altered irradiance by adjustment of their final thickness. Similarly, the P5 transferred leaves did not respond to altered irradiance. A plausible explanation for these might be the cessation of cell division occurring at the P4 stage, with subsequent cell growth occurring without accompanying division (Itoh et al., 2005; Murchie et al., 2005). Since changes in light environment at the P5 stage of Lf 5 could not induce a change in leaf thickness, these data suggest

that cell division processes are linked with the ability of the leaf to respond to altered irradiance by change of growth in the adaxial/abaxial axis. Thus the specific state of competence of the responding cells, rather than specific properties of light or photoreceptor system involved in perceiving the light signal, seems to be a key to the response (Hart, 1988).

The results shown in chapter 3 support the hypothesis that the differentiation of a new leaf primordia into sun or shade type leaf can be remotely regulated by other exposed parts of the plants, i.e. mature leaves which already experience the actual light environment (Lake et al., 2001; Yano and Terashima, 2001; Lake et al., 2002; Thomas et al., 2004; Coupe et al., 2006; Ferjani et al., 2008). Yano and Terashima (2004) studied the development of sun and shade leaves in *C. album* and reported that the leaf thickness, cell layer number and cross sectional area of palisade tissue increased when the mature leaves were exposed to HL, but decreased when the mature leaves were exposed to LL. On the other hand, the acclimation in the ultrastructure of chloroplasts was independent of the signal. Therefore, these studies suggest the long distance signalling regulates the orientation of cell division and, thus, the differentiation of sun and shade leaves at the shoot apex. Although, the results presented here do not provide any direct information on the nature of the putative signal, it is worthwhile to note that a histological analysis indicates that a differentiated vascular system does not appear in the developing rice leaf until approximately the P2 stage of rice leaf development (Itoh et al., 2005). Our data are thus consistent with the existence of a vascular-borne signal which can alter leaf thickness between P2 to P4-stage which is the stage at which cell division in the rice leaf blade begins to terminate. According to this interpretation, the lack of response of the P1-stage leaf primordia to LL transfer could reflect the lack of a functional vascular system at this early stage of leaf development. The reason why the P1-transferred leaves do not respond later in development to a low irradiance signal, which presumably is still being generated by the LL-exposed older leaves, is open to speculation, but it is possible that the irradiance-control of leaf thickness involves the responding leaf perceiving a change in irradiance-

related signal rather than measuring the absolute level of signal. In this scenario, if the signal change occurs during the P1 developmental stage then in our experimental set up there would be no change in signal later in development and, consequently, no-response would be observed. Assuming that, low irradiance leads to a signal in the exposed leaves which is then transported to the young developing leaves, this signal will be continually generated. Consequently, the lack of change in leaf thickness in P2, P3 and P4 leaves after transfer at P1 stage from HL to LL would be explained by a system in which the responding leaf perceives a change in level of the signal, which only occurs shortly after the change in irradiance level. Although, the vascular-borne signal inducing a systemic long distance signalling in plant defence is well documented (Heil and Ton, 2008), the putative signal regulating leaf thickness translocated through vascular system proposed in here is open to conjecture as there are other signalling systems in plant that do not require the vascular system i.e. auxin signalling. An experiment investigating the change in leaf thickness following a transfer of P1-stage leaf primordia from HL to LL and then transfer back to HL when the leaf primordia develops to P2- or P3-stage, where the differentiation of vascular system occurs, should proof this speculation.

The results in Chapter 3 indicated that the high light-acclimated rice leaves were thicker than the low light-acclimated leaves due to a larger mesophyll cell size and no change in cell layer number, which is different from some other plants in which sun leaves were thicker than shade leaves by having a greater number of mesophyll cell layers (Lambers et al., 1998; Yano and Terashima, 2004). Mutation analysis in rice shows that phytochrome B influences leaf area and stomatal density (Liu et al., 2012), with mature leaves of *phy*B mutant rice having larger epidermal cells and lower stomatal density than wild type leaves. It has been suggested that the mutation of *phy*B is correlated with high expression level of genes involved in plant growth, e.g., *ERECTA* and *EXPANSIN* genes, resulting in the larger epidermal cells. It is noteworthy that phytochrome is one of the candidate molecules implicated in the long distance signalling system (Ferjani et al., 2008). Therefore, there is a

possibility that phytochrome B affects the control of leaf thickness in rice. Consequently, the larger mesophyll cell size of HL-leaves observed here might be related to the function of phytochrome B; a chromoprotein that regulates the expression of a large number of light-responsive genes in plants (Franklin et al., 2003; Franklin and Quail, 2010). Taken together, it can be summarised that the control of leaf thickness in rice is related to a sensing of the alteration in light intensity by an unknown receptor in mature leaves that leads to the transfer of a signal from the mature to developing leaves, where the orientation of cell division and growth are then determined accordingly. The developmental window where changes in cell division and growth leading to altered leaf thickness in rice occur is during the P2 to P4 stage, as shown by the results in Chapter 3 (3.5).

Smaller stomata in rice leaves growing under LL and ambient CO_2 condition were observed in this present study, which is consistent with the recent investigation indicating that stomata of LL grown rice plants were significantly smaller under ambient CO_2 (Hubbart et al., 2013). There was no significant difference in stomatal density between either HL leaves and LL leaves or P1-transferred leaves and the LL leaves. However, a significant difference in stomatal density was observed when rice plants were transferred from HL to LL at P3 and P5-stage of Lf5, with the stomatal density of these transferred leaves being lower than in LL leaves. This correlates with the finding that epidermal differentiation, including stomata differentiation, in developing rice leaves begins in the P3 stage and is completed by the P5 stage (Itoh et al., 2005). In addition to the process of individual stomata differentiation, epidermal cell files in the rice leaf can be distinguished as either stomata-containing or non-stomata containing cell files. The results in chapter 3 indicated an irradiance-dependent alteration in file width which the stomata-containing cell files were wider than the non-stomata ones. Due to an arrangement of the structure of the grass leaf into cell files, file width will influence stomatal size. This is consistent with the recent study reporting that differences in stomatal density are largely influenced by differences in epidermal cell size (Savvides et al., 2012). The results in Chapter 3 showed no

significant differences in epidermal cell size between treatments using ambient CO_2, so that there were no significant differences in stomatal density between the different treatments. This is consistent with the study of Hubbart (2013) which showed that a lower stomatal density in rice leaves grown under low light required elevated CO_2. However, the rather low stomatal density observed in the P3- and P5- transferred leaves is intriguing and needs further study.

An interesting and surprising observation from my work is that leaf thickness can be set at an extremely early stage of leaf development. The accepted paradigm is that photosynthetic activity responds relatively rapidly to environmental parameters, including irradiance, so how could a leaf become unresponsive to these triggers? At initiation a leaf primordium consists of a few hundred of cells and it is thought that the photosynthetic machinery does not become fully formed until much later after a number of cell divisions. Recently there has been significant interest and advance in our understanding of how environmental factors might trigger epigenetic setting of gene expression (Coustham et al., 2012). Variation of flowering and alignment of vernalisation which involves the epigenetic silencing of the floral repressor *FLC* through the Polycomb mechanism and chromatin remodelling, is crucial for the adaptation of *A. thaliana* in response to winter length. The study of Coustham et al. (2012) reveals that *cis* polymorphisms within the *FLC* induce the quantitative modulation of the Polycomb silencing mechanism that influence developmental timing, thus variation for response to the winter length occurs. This suggests that an epigenetic mechanism, e.g., quantitative modulation of chromatin silencing mechanisms through *cis* polymorphisms, might be a mechanism playing an important role in the acclimation of plants to changing environment. In addition, DNA methylation is one of the mechanisms playing a fundamental role in epigenetic regulation in plant developmental processes and stress responses (Suzuki and Bird, 2008; Chinnusamy and Zhu, 2009). A recent study in brown cotton (Li et al., 2011) revealed variation in DNA methylation patterns and levels in response to different light quality that is also accompanied by changes in gene expression level. These observations suggest an epigenetic regulation of light responses is possible. Whether such epigenetic

regulation of gene expression is involved in the control of leaf thickness is an area for future research.

6.2 Does alteration in leaf form effect leaf performance?

In chapter 4, physiological characteristics and changes in leaf thickness in response to light regime were concomitantly analysed following the transfer of P1-, P3-, and P5- stage leaf 5 from HL to LL. The results revealed that all of the transferred leaves acclimated to LL condition and thus displayed physiological characteristics that were similar to LL-grown leaves, even though the P1- and P5-transferred leaves were unresponsive to the trigger of lower irradiance in terms of leaf form (they had relatively thick leaves, similar to HL-grown leaves). The level of Rubisco protein in the mature Lf5 of P1-, P3- and P5- transferred leaves correlated with leaf thickness but could not be statistically distinguished from LL leaves. The CO_2 assimilation rate of all the transferred leaves was comparable to LL –leaves that is lower than the HL-leaves. This is consistent with the lower V_{cmax} of the transferred leaves and LL-leaves than HL-leaves. The results correlate with the study of Makino et.al, (1985) in rice leaves, showing that RubisCO activity is linearly correlated with the rate of CO_2 assimilation at each level of irradiance. It indicates that the rate of CO_2 assimilation in rice leaves, under ambient CO_2 level, is limited during their entire lifespan by RubisCO capacity. Lower Chl a:b ratio observed in the transferred leaves suggested an increase in chlorophyll *b* and light harvesting complex (LHC), which is common for shade-acclimated leaves since light gathering is emphasised under light limited conditions (Thornber et al., 1993). These observations indicate adaptations to low light intensity occurred at the chloroplast level, that these adaptations are more plastic than the modification at the leaf architecture, and that they can occur later in development, at a stage where change in leaf structure is not feasible. It has been reported that transfer of rice plants from LL to HL after full leaf extension causes a decrease in chlorophyll *b level*, thus Chl a:b ratio increases (Murchie et al., 2005). The decrease in chlorophyll *b* level is believed to help avoidance of photo-oxidation and over-excitation of chlorophyll protein complexes that

can be regulated by degradation of the LHC. This indicates a chloroplast-level acclimation of rice leaves that occurs independently of leaf age (Murchie et al., 2005). The results reported here support these observations as all the transferred leaves, including the P1- and P5-transferred leaves which displayed HL-type leaf thickness, were acclimated to low light conditions. The charateristics of leaves acclimated to low irradiance is well documented. An increase in the relative amount of chlorophyll *b* incorporated with the reduction in Chl a:b ratio is one such charateristics. The increase in chlorophyll *b* is associated with an increase in LHC-II content; so that the plants acclimated to low irradiance have a larger antenae for PS-II which enhances their photon capture efficiency. In rice leaves, after full expansion, low irradiance also strongly retards the decline in chlorophyll content (Hidema et. al, 1991) and LHCII protein content (Hidema et. al. 1992).

Considering the stomatal conductance (g_s) of the transferred leaves, although the thickness of P1- and P5-transferred leaves was relatively similar to HL leaves and their g_s were slightly higher than LL leaves, they were not significantly different from LL-leaves. This is consistent with the stomatal density results that were either not significantly different or lower between the transferred leaves and LL leaves, since g_s is determined by stomatal pore size and stomatal density (Franks and Beerling, 2009). The results presented here suggest the coordinate function of stomatal conductance and leaf internal surface area determine CO_2 supply and transpiration. It can be said that a leaf that increases internal surface area via a thicker mesophyll layer (as in the P1- and P5- transferred leaves) without increasing $g_{s,}$ as well as other aspects of the photosynthetic machinery, cannot achieve a high photosynthetic rate.

6.3 How is leaf thickness controlled by changing irradiance?

Light itself does not carry any information specific to particular morphogenic steps including the control of leaf thickness, but light initiates many different types of response through the different states of competence of the responding cells (Hart, 1988). However, the specificity of the responses leading to the regulation of leaf thickness is puzzling. In chapter 5, the genes

potentially involved in the control of leaf thickness were identified using microarray analysis. Three replicates of RNA samples obtained from P 3- stage leaf primordia of Lf5 maintained under HL for 6 and 24 hours and that were transferred from HL to grow under LL for 6 and 24 hours were used for the analysis. The combined microarray data from all 3 replicates were analysed using the high stringent false discovery adjustment method of John Storey (jsFDR) in R/ MAANOVA. There were no differentially expressed genes following the transfer of the P3-stage rice leaves from HL to LL for 6 hours or 24 hours (jsFDR corrected, *p*-value <0.05). However, selection of differentially expressed genes from the un-adjusted *p*- values resulted in 85 and 508 genes that showed differences in gene expression levels after transfer from HL to LL for 6 hours and 24 hours respectively ($p<0.01$). Some of the selected genes were further analysed by qPCR and *in situ* hybridisation analysis which confirmed the microarray analysis.

The interpretation of microarrays depends on the statistical approach taken, with a variety of stringencies possible. Low stringency approaches run the risk of identifying many false positives which make further investigation /identification of important genes difficult. Alternatively, too stringent approaches can lead to potentially interesting changes in gene expression being missed. Our approach was to start with a very stringent filter on the data, then to look at the results as this stringency was decreased. This allowed us to identify a number of lead genes which is tractable for future investigation. As with any statistical approach, the size and number of biological replicates is the key. We used three biological replicates in our analysis using dissected P3-stage primordial. Increasing the number of P3- leaf primordia used for RNA extraction for each sample group, and increasing the number of samples could increase the statistical power of the analysis.

There were some genes in the gene lists that have been reported to be related to leaf morphogenesis and can be related to the control of leaf thickness. It is interesting that the gene *OsDWARF*, which is related to brassinosteroid biosynthesis, showed down-regulation after 24hrs transfer to LL. It is known that mutation of OsDwarf in rice leads to defects in the

organised arrangement and polar elongation of cells in the leaves and stem (Hong et al., 2002). Moreover, *SCARECROW-like* (*Scl1*) and *SCARECROW* (*SCR*) genes, which are reported as regulators of cell proliferation in *Arabidopsis* leaves (Dhondt et al., 2002), were also down-regulated in P3-stage Lf5 transferred to LL for either 6 or 24 hours. There were some genes in the differentially expressed gene lists that encode for proteins related to the signalling, such as thioredoxin and trehalose-6-phosphate. There is strong evidence that trehalose-6-phosphate (T6P) plays an indispensible role as a sugar signal which links metabolism to development in plants (Paul et al., 2008). Considering redox as a signal responding to changes in irradiance, the redox state of the PQ pool controls the transcription of photosynthetic genes such as the nuclear *Lhcb* gene family that encodes the chlorophyll a/ b binding proteins (CAB) of the light harvesting complex of the PSII (Escoubas et al., 1995; Fey et al., 2005). In high light conditions, photosystem II (PSII) is under high excitation pressure and the plastoquinone (PQ) pool in chloroplast thylakoid membranes is reduced, while it is oxidised under low light conditions. Thus the light environment can be reflected by the reduction/oxidation (redox) state of the photosynthetic electron transport chain. In addition, photosynthates, i.e. sugar, may also act as light signal in plants (Ono et. al., 2001). As the photosensory signal(s) should be transfer from mature leaves to a developing leaf, photosynthates are one of the most likely signal candidates. However, the exact relationship between the hypothetical signalling system and these candidate signal molecules is a future challenge which requires further research, as is the connection to the control of leaf thickness.

The results also indicate changes in expression level after transfer to LL for 6 hours of genes encoding proteins categorised as kinase proteins, such as the down regulation of a *STRUBELLIG RECEPTOR FAMILY* (*SRF*) gene represented by *STRUBELLIG* (*SUB*), which is a class of receptor-like kinases (RLKs). RLKs play an important role in transmission of signals across membranes and SRF4 has been reported as a direct positive regulator of leaf size (Eyuboglu et al., 2007). Strikingly, a recent study indicates that the key function of *ANGUSTIFOLIA* (*AN*) in plant tissue morphogenesis is mediated by a

SUB-signalling mechanism (Bai et al., 2013). This is intriguing since, in *Arabidopsis*, the *AN* mutants have a defect in cell growth in the lateral plane, and an enhanced growth in the leaf thickness direction, resulting in a larger cell size, and thicker and narrower leaves than in wild type (Tsuge et al., 1996). In addition, a number of genes related to plant transcriptional regulation also showed different gene expression levels following a transfer from HL to LL. It remains to be seen if these transcription regulators and protein kinases affect cell proliferation or cell size or both and, thus, influence leaf thickness. It is noteworthy that the *THIAMINE C SYNTHASE* (*THIC*) gene was the most significantly down-regulated gene after the transfer from HL to LL for 24 hrs, since *THIC* (a circadian clock-driven thiamine biosynthetic gene) participates in the regulation of plant central carbohydrate metabolism and in the light/ dark metabolic transition. Thiamine biosynthesis is regulated by the circadian clock through the promoter region of THIC gene which contains a region for riboswitch gene expression control. Plants altered in riboswitch activity showed reduced photosynthesis rate, growth retardation and chlorosis (Bocobza et al., 2013). The down-regulation of the genes *SCARECROW-like* (*Scl1*) and *SCARECROW* (*SCR*) in the P3-stage Lf5 transferred to LL for either 6 or 24 hours is interesting, since SCR is a member of the GRAS family of the transcription factors (Lee et al., 2008) that plays an important role in the control of cell division in the developing Arabidopsis leaf (Dhondt et al., 2002). Mutational analysis in *Arabidopsis* demonstrated an inhibition of leaf growth in *scr* mutants caused by a prolonged S-phase duration, mediated by up-regulation of genes encoding cell cycle inhibitors (Dhondt et al., 2002). The *SCR* mutants, which have a defect in cell division, showed a retardation of leaf growth and severe reduction in final leaf area compared to wild type. This can be compared to the results in Chapter 3 where LL- leaves showed a lower growth rate and smaller mesophyll cell size than HL-leaves. However, the relationship between these differentially expressed genes and the control of rice leaf thickness remains to be tested.

According to the microarray analysis results presented here a molecular mechanism of leaf thickness control in rice in response to irradiance can be

proposed as shown in Figure 6.1. In this model the putative light sensor (phytochrome b (Phy B) and plastoquinone (PQ)) sense the light intensity in association with the different photosynthetic rate in mature leaves resulting in a high sugar concentration under high light condition and low sugar concentration under low light condition. Sugar is the putative signal sent through the vascular system to a developing leaf inside the leaf sheath. The differences in sugar concentration may play a role in the regulation in expression of some genes involved in either carbohydrate metabolism (e.g, the *THIC* gene), or leaf morphogenesis (e.g., *OsDWARF*, *ANGUSTIFOLIA* via *SUB*).

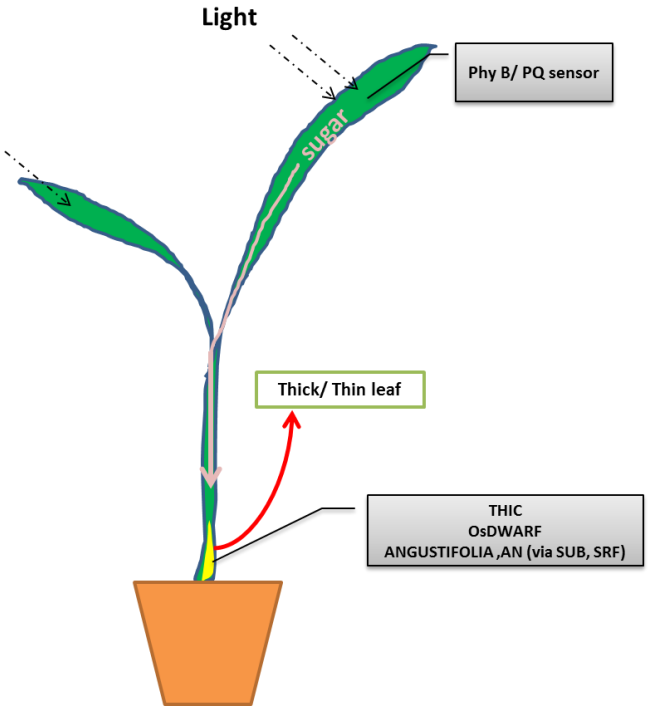

Figure 6.1 a model of rice leaf thickness control proposed from the microarray results. In mature leaf (green), light intensity is sensed via phytochrome B (Phy B) or plastoquinone pool (PQ) incorporating with the different photosynthetic rate influenced by high or low light intensity resulting in high or low sugar signal, respectively. Then, the signal is sended through vascular system to the developing leaf (yellow) and regulates some genes that might be related to the control leaf thickness in rice that a high light or low light intensity induces thick leaf or thin leaf, respectively.

6.4 Concluding remarks and future perspectives

Differences in light intensity induce sun- and shade-type rice leaves with differences in leaf thickness and physiological performance .It is believed that a thicker leaf is required to support the greater CO_2 demand necessary to support the high CO_2 assimilation of HL-acclimated plants, as thicker leaves leads to have a higher ratio of mesophyll cell surface area to leaf surface area, causing a lower resistance to CO_2 internal diffusion in HL leaves compared to LL leaves (Lichtenhaler, 1985; Terashima et al., 2001; Oguchi et al., 2003). While high light (HL) induced the development of thicker rice leaves with a visibly larger mesophyll cell size, transferring the leaves to low light (LL) conditions caused a LL-acclimated photosynthetic response. This suggests that leaf anatomical adjustment and leaf photosynthetic acclimation occur independently. Thus, as shown here, P1- and P5- transferred leaves with HL-type leaf thickness were capable of acclimation to low light conditions by having LL-type physiological characteristics. It can be said that it is not leaf thickness but light that is the major factor influencing other photosynthetic components, thus leaf photosynthesis. It might be useful to study this using an inverse system of the transfer experiments so that rice plants are transferred from LL to HL at the different developmental stages, so that the HL-acclimation of the thin leaves induced by LL condition can be investigated.

Although, the developmental window where rice leaf thickness is set in response to the different light regimes was discovered in this study, the exact mechanism for the systemic signalling, recognition, and the target of the regulation of leaf thickness remain unclear. As previously mentioned, studies of sun- and shade-leaves development have revealed the phenomena that the differentiation of new leaf primordia into sun- or shade-leaf is controlled by more mature leaves (Lake et al., 2001; Yano and Terashima, 2001; Lake et al., 2002; Coupe et al., 2006; Jiang et al., 2011). An altered balance between periclinal and anticlinal divisions of the palisade cells accounted for the differences between the architecture of the palisade layers in sun and shade leaves of *C. album* (Yano and Terashima, 2004). The results reported here

revealed that the mesophyll cells of the thicker HL-rice leaves were larger than those of LL-leaves, suggesting that cell expansion is the strategy used to increasing leaf mesophyll surface area (S_{mes}) (Terashima et al., 2011). As cell proliferation and cell expansion are involved in the control of leaf size, the signals involved in the control of these cell activities in the mesophyll cell layers is an interesting topic for future studies on the regulation of leaf thickness in rice leaves.

Cell proliferation and post-mitotic cell expansion occur simultaneously but separately in the different regions of the same developing leaf (Donnelly et al., 1999; White, 2006). A precise programmed exit from the mitotic cell cycle and the cessation of post-mitotic cell expansion together determine leaf size (White, 2006). Therefore, in addition to the long distance signalling system controlled by mature leaves, leaf shape and size are also regulated locally in each primordium by a short-distance signalling system. Characterisation of this short distance signalling system and how it interacts with the long distance signalling system controlling leaf thickness is a challenge for the future. A variety of mutants in Arabidopsis with altered cell size and number provides one approach to tackle this problem (Horiguchi et al., 2006) and the identification of a similar array of mutants in rice would be very useful. In addition, advance in the use of artificial microRNA expression systems (Schwab et al., 2006) and development of tissue-specific inducible gene expression systems (Brand et al., 2006) in rice would provide the tools to tackle this problem. This could open up a challenging field of research on the organ-wide regulation of cell proliferation and expansion that will help us unravel the puzzle of the regulation of leaf thickness.

Further analysis of some of the genes identified by the microarray analysis reported here could prove very useful in understanding the control of leaf thickness in rice. One gene that might be a good candidate for analysis is the STRUBELLIG (SUB) gene which is linked to the function of a regulator of polarised cell expansion; ANGUSTIFOLIA (AN). *AN* influences the expansion of leaf cells in Arabidopsis in the lateral plane (Tsukaya, 2005) and loss of function of ANGUSTIFOLIA3 (AN3), which encodes a transcriptional co-

activator, results in a production of a narrow leaf shape with fewer but larger cells (again in Arabidopsis) (Tsukaya, 2003; Horiguchi et al., 2005). Since the present study showed that HL rice leaves were thicker than LL leaves with a larger mesophyll cell size and also narrower than the LL-leaves, it is possible that a similar genetic system controls leaf form in rice. These lead genes provide a resource for future work in this area.

References

Anderson, J., W. Chow, et al. (1995). "The grand design of photosynthesis: Acclimation of the photosynthetic apparatus to environmental cues." Photosynthesis Research **46**(1-2): 129-139.
Araya, T., K. O. Noguchi, et al. (2008). "Manipulation of light and CO2 environments of the primary leaves of bean (Phaseolus vulgaris L.) affects photosynthesis in both the primary and the first trifoliate leaves: involvement of systemic regulation." Plant, Cell & Environment **31**(1): 50-61.
Bai, Y., P. Vaddepalli, et al. (2013). "ANGUSTIFOLIA is a central component of tissue morphogenesis mediated by the atypical receptor-like kinase STRUBBELIG." BMC Plant Biology **13**(1): 16.
Bailey, S., R. Walters, et al. (2001). "Acclimation of Arabidopsis thaliana to the light environment: the existence of separate low light and high light responses." Planta **213**(5): 794-801.
Ballantine, J. E. M. and B. J. Forde (1970). "The Effect of Light Intensity and Temperature on Plant Growth and Chloroplast Ultrastructure in Soybean." American Journal of Botany **57**(10): 1150-1159.
Barton, M. K. and R. S. Poethig (1993). "Formation of the shoot apical meristem in Arabidopsis thaliana: an analysis of development in the wild type and in the shoot meristemless mutant." Development **119**(3): 823-831.
Bassham, J. A., A. A. Benson, et al. (1950). "The path of car bon in photosynthesis: VIII. the role of malic acid." Journal of Biological Chemistry **185**(2): 781-787.
Björkman, O. (1968). "Carboxydismutase Activity in Shade-adapted and Sun-adapted Species of Higher Plants." Physiologia Plantarum **21**(1): 1-10.
Björkman, O. (1981). Responses to different quantum flux densities. Encyclopedia of plant physiology vol. 12A: Physiological plant ecology I. Response to the physiological environment. O. L. Lange, P. S. Nobel and H. Z. Osmond. Berlin, Springer-Verlag**:** 57-107.
Boardman, N. K. (1977). "Comparative Photosynthesis of Sun and Shade Plants." Annual Review of Plant Physiology **28**(1): 355-377.
Bocobza, S. E., S. Malitsky, et al. (2013). "Orchestration of Thiamin Biosynthesis and Central Metabolism by Combined Action of the Thiamin Pyrophosphate Riboswitch and the Circadian Clock in Arabidopsis." The Plant Cell Online **25**(1): 288-307.
Bolhar-Nordenkampf, H. R. and G. Draxler (1993). Functional Leaf Anatomy. Photosynthesis and Production in a Changing Environment : A Field and Laboratory Manual. D. O. Hall, J. M. O. Scurlock, H. R. Bolhar-Nordenkampf, R. C. Leegood and S. P. Long. London, Chapman&Hall**:** 91-112.
Bolstad, B. M., R. A. Irizarry, et al. (2003). "A comparison of normalization methods for high density oligonucleotide array data based on variance and bias." Bioinformatics **19**(2): 185-193.
Bradford, M. M. (1976). "A rapid and sensitive method for the quantitation of microgram quantities of protein utilizing the principle of protein-dye binding." Analytical Biochemistry **72**(1-2): 248-254.

Brand, L., M. Hörler, et al. (2006). "A Versatile and Reliable Two-Component System for Tissue-Specific Gene Induction in Arabidopsis." Plant Physiology **141**(4): 1194-1204.
Caemmerer, S. and G. D. Farquhar (1981). "Some relationships between the biochemistry of photosynthesis and the gas exchange of leaves." Planta **153**(4): 376-387.
Cassman, K. G., Ed. (1994). Breaking the yield barrier: Proceedings of a workshop on rice yield potential in favorable environments, IRRI, International Rice Research Institute, P.O. Box 933, Manila 1099, Philippines.
Chinnusamy, V. and J.-K. Zhu (2009). "Epigenetic regulation of stress responses in plants." Current Opinion in Plant Biology **12**(2): 133-139.
Corbett, W. R. (2011). Dichanthelium dichotomum (Native) 2.
Coupe, S. A., B. G. Palmer, et al. (2006). "Systemic signalling of environmental cues in Arabidopsis leaves." Journal of Experimental Botany **57**(2): 329-341.
Coustham, V., P. Li, et al. (2012). "Quantitative Modulation of Polycomb Silencing Underlies Natural Variation in Vernalization." Science **337**(6094): 584-587.
Dashek, V. D. and M. Harrison, Eds. (2006). Plant cell biology. Mitosis in plant cell. Enfield, New Hamshire, USA, Science Publishers.
Devlin, P. F., P. R. H. Robson, et al. (1999). "Phytochrome D Acts in the Shade-Avoidance Syndrome in Arabidopsis by Controlling Elongation Growth and Flowering Time." Plant Physiology **119**(3): 909-916.
Dhondt, S., F. Coppens, et al. (2002). "SHORT-ROOT and SCARECROW Regulate Leaf Growth in Arabidopsis by Stimulating S-Phase Progression of the Cell Cycle." Plant Physiology **154**(3): 1183-1195.
Doerner, P. W. (1994). "Cell Cycle Regulation in Plants." Plant Physiol. **106**(3): 823-827.
Donnelly, P. M., D. Bonetta, et al. (1999). "Cell Cycling and Cell Enlargement in Developing Leaves of Arabidopsis." Developmental Biology **215**(2): 407-419.
Esau, K., Ed. (1977). Anatomy of Seed Plants. New York, John Wiley & Sons.
Escoubas, J. M., M. Lomas, et al. (1995). "Light intensity regulation of cab gene transcription is signalled by the redox state of the plastoquinone pool." Proceedings of the National Academy of Sciences **92**(22): 10237-10241.
Eshed, Y., A. Izhaki, et al. (2004). "Asymmetric leaf development and blade expansion in Arabidopsis are mediated by KANADI and YABBY activities." Development **131**(12): 2997-3006.
Eyuboglu, B., K. Pfister, et al. (2007). "Molecular characterisation of the STRUBBELIG-RECEPTOR FAMILY of genes encoding putative leucine-rich repeat receptor-like kinases in Arabidopsis thaliana." BMC Plant Biology **7**(1): 16.
Ezhova, T. (2007). "Genetic control of early stages of leaf development." Russian Journal of Developmental Biology **38**(6): 363-373.
FAO (2009). How to feed the world 2050. How to feed the world 2050. F. a. A. O. o. t. U. Nations. Rome.

FAOSTAT. (2011). "Food and Agriculture Organisation of the United Nations 2011."
Farquhar, G. D., S. Caemmerer, et al. (1980). "A biochemical model of photosynthetic CO2 assimilation in leaves of C3 species." Planta **149**(1): 78-90.
Farquhar, G. D. and T. D. Sharkey (1982). "Stomatal Conductance and Photosynthesis." Annual Review of Plant Physiology **33**(1): 317-345.
Ferjani, A., S. Yano, et al. (2008). Control of Leaf Morphogenesis by Long- and Short-Distance Signaling: Differentiation of Leaves Into Sun or Shade Types and Compensated Cell Enlargement. Plant Growth Signaling, Springer Berlin Heidelberg. **10:** 47-62.
Fey, V., R. Wagner, et al. (2005). "Photosynthetic redox control of nuclear gene expression." Journal of Experimental Botany **56**(416): 1491-1498.
Fleming, A. (2006). "The integration of cell proliferation and growth in leaf morphogenesis." Journal of Plant Research **119**(1): 31-36.
Fleming, A. J., S. McQueen-Mason, et al. (1997). "Induction of Leaf Primordia by the Cell Wall Protein Expansin." Science **276**(5317): 1415-1418.
Flexas, J., M. Ribas-CarbÓ, et al. (2008). "Mesophyll conductance to CO2: current knowledge and future prospects." Plant, Cell & Environment **31**(5): 602-621.
Franklin, K. A., S. J. Davis, et al. (2003). "Mutant Analyses Define Multiple Roles for Phytochrome C in Arabidopsis Photomorphogenesis." The Plant Cell **15**(9): 1981-1989.
Franklin, K. A. and P. H. Quail (2010). "Phytochrome functions in Arabidopsis development." Journal of Experimental Botany **61**(1): 11-24.
Franks, P. J. and D. J. Beerling (2009). "Maximum leaf conductance driven by CO2 effects on stomatal size and density over geologic time." Proceedings of the National Academy of Scienes of the United States of America **106**(25): 10343-10347.
Friml, J. (2003). "Auxin transport - shaping the plant." Curr Opin Plant Biol **6**(1): 7-12.
Friml, J., A. Vieten, et al. (2003). "Efflux-dependent auxin gradients establish the apical-basal axis of Arabidopsis." Nature **426**(6963): 147-153.
Garnier, E., J. L. Salager, et al. (1999). "Relationships between Photosynthesis, Nitrogen and Leaf Structure in 14 Grass Species and Their Dependence on the Basis of Expression." New Phytologist **143**(1): 119-129.
Givnish, T. J. (1988). "Adaptation to Sun and Shade: a Whole-Plant Perspective." Australian Journal of Plant Physiology **15**(2): 63-92.
Hall, D. O., J. M. O. Scurlock, et al. (1993). Photosynthesis in the changing environment. london, Chapman & Hall.
Hanba, Y., H. Kogami, et al. (2004). "The effect of growth irradiance on leaf anatomy and photosynthesis in maple species." Science Access **3**(1): -.
Hanba, Y. T., H. Kogami, et al. (2002). "The effect of growth irradiance on leaf anatomy and photosynthesis in *Acer* species differing in light demand." Plant, Cell & Environment **25**(8): 1021-1030.
Hanson, H. C. (1917). "Leaf-Structure as Related to Environment." American Journal of Botany **4**(9): 533-560.
Hart, J. W. (1988). Light and plant growth. London, Unwin Hyman Ltd.

Heil, M. and J. Ton (2008). "Long-distance signalling in plant defence." Trends in Plant Science 13(6): 264-272.
Hidema, J., A. Makino, et al. (1992). "Changes in the Levels of Chlorophyll and Light-Harvesting Chlorophyll a/b Protein of PS II in Rice Leaves Aged under Different Irradiances from Full Expansion through Senescence." Plant and Cell Physiology 33(8): 1209-1214.
Hidema, J., A. Makino, et al. (1991). "Photosynthetic Characteristics of Rice Leaves Aged under Different Irradiances from Full Expansion through Senescence." Plant Physiology 97(4): 1287-1293.
Hikosaka, K. and I. Terashima (1995). "A model of the acclimation of photosynthesis in the leaves of C3 plants to sun and shade with respect to nitrogen use." Plant, Cell & Environment **18**(6): 605-618.
Hong, Z., M. Ueguchi-Tanaka, et al. (2002). "Loss-of-function of a rice brassinosteroid biosynthetic enzyme, C-6 oxidase, prevents the organized arrangement and polar elongation of cells in the leaves and stem." The Plant Journal **32**(4): 495-508.
Horiguchi, G., U. Fujikura, et al. (2006). "Large-scale histological analysis of leaf mutants using two simple leaf observation methods: identification of novel genetic pathways governing the size and shape of leaves." The Plant Journal **48**(4): 638-644.
Horiguchi, G., G.-T. Kim, et al. (2005). "The transcription factor AtGRF5 and the transcription coactivator AN3 regulate cell proliferation in leaf primordia of Arabidopsis thaliana." The Plant Journal **43**(1): 68-78.
Hu, Y., Q. Xie, et al. (2003). "The Arabidopsis Auxin-Inducible Gene ARGOS Controls Lateral Organ Size." Plant Cell **15**(9): 1951-1961.
Hubbart, S., S. Bird, et al. (2013). "Does growth under elevated CO_2 moderate photoacclimation in rice?" Physiologia Plantarum **148**(2): 297-306.
Hubbart, S., S. Peng, et al. (2007). "Trends in leaf photosynthesis in historical rice varieties developed in the Philippines since 1966." Journal of Experimental Botany **58**(12): 3429-3438.
Hunt, R. (1982). Plant growth curves: the functional approach to plant growth analysis. London, Edward Arnold.
Imai, K., Y. Suzuki, et al. (2008). "Changes in the synthesis of rubisco in rice leaves in relation to senescence and N influx." Annals of Botany **101**(1): 135-144.
Itoh, J.-I., H. Kitano, et al. (2000). "SHOOT ORGANIZATION genes regulate shoot apical meristem organization and the pattern of leaf primordium initiation in rice." Plant Cell **12**(11): 2161-2174.
Itoh, J.-I., K.-I. Nonomura, et al. (2005). "Rice plant development: from zygote to spikelet." Plant and Cell Physiology **46**(1): 23-47.
Jiang, C.-D., X. Wang, et al. (2011). "Systemic regulation of leaf anatomical structure, photosynthetic performance, and high-light tolerance in Sorghum." Plant Physiology **155**(3): 1416-1424.
Jurik, T. W. (1986). "Temporal and spatial patterns of specific leaf weight in successional northern Hardwood tree species." American Journal of Botany **73**(8): 1083-1092.
Kamiya, N., J. Itoh, et al. (2003). "The SCARECROW gene's role in asymmetric cell divisions in rice plants." Plant J **36**(1): 45-54.

Kang, J. and N. Dengler (2002). "Cell cycling frequency and expression of the homeobox gene ATHB-8 during leaf vein development in Arabidopsis." Planta **216**(2): 212-219.
Karpinski, S., H. Reynolds, et al. (1999). Systemic signaling and acclimation in response to excess excitation energy in Arabidopsis. **284:** 654-657.
Kim, G.-T., S. Yano, et al. (2005). "Photomorphogenesis of leaves: shade-avoidance and differentiation of sun and shade leaves." Photochemical & Photobiological Sciences **4**(9): 770-774.
Kim, J. H. and H. Kende (2004). "A transcriptional coactivator, AtGIF1, is involved in regulating leaf growth and morphology in Arabidopsis." Proceedings of the National Academy of Scienes of the United States of America **101**(36): 13374-13379.
Krause, G. H., E. Grube, et al. (2004). Do mature shade leaves of tropical tree seedlings acclimate to high sunlight and UV radiation? **31:** 743-756.
Kusumi, K., Y. Chono, et al. (2010). "Chloroplast biogenesis during the early stage of leaf development in rice." Plant Biotechnology **27**(1): 85-90.
Kusumi, K., S. Hirotsuka, et al. (2012). "Increased leaf photosynthesis caused by elevated stomatal conductance in a rice mutant deficient in SLAC1, a guard cell anion channel protein." Journal of Experimental Botany **63**(15): 5635-5644.
Laemmli, U. K. (1970). "Cleavage of Structural Proteins during the Assembly of the Head of Bacteriophage T4." Nature **227**(5259): 680-685.
Lake, J. A., W. P. Quick, et al. (2001). "Plant development: Signals from mature to new leaves." Nature **411**(6834): 154-154.
Lake, J. A., F. I. Woodward, et al. (2002). "Long □distance CO_2 signalling in plants." Journal of Experimental Botany **53**(367): 183-193.
Lambers, H., F. S. Chapin III, et al. (1998). Plant physiological ecology. USA, Springer.
Lawler, D. W. (1993). Photosynthesis: molecular, physiological and environmental processes. Essex, Longman Scientific & Technical.
Lee, B. H., J.-H. Ko, et al. (2009). "The Arabidopsis GRF-INTERACTING FACTOR gene family performs an overlapping function in determining organ size as well as multiple developmental properties." Plant Physiology **151**(2): 655-668.
Lee, M.-H., B. Kim, et al. (2008). "Large-scale analysis of the GRAS gene family in Arabidopsis thaliana." Plant Molecular Biology **67**(6): 659-670.
Li, T., H. Fan, et al. (2011). "Effect of different light quality on DNA methylation variation for brown cotton (Gossypium hirstum)." African Journal of Biotechnology **10**(33): 6220-6226.
Lichtenhaler, H. and A. Wellburn (1983). "Determinantions of total carotenoids and chlorophylls a and b of leaf extracts in different solvents." Biochemical Society Transactions **11**: 591-592.
Lichtenhaler, H. K. (1985). Differences in morphology and chemical composition of leaves grown at differnt light intensities and qualities. Control of leaf growth. N. R. Baker, W. J. Davies and C. K. Ong. Cambridge, Cambridge University Press**:** 201-221.
Lincoln, C., J. Long, et al. (1994). "A knotted1-like Homeobox gene in Arabidopsis is expressed in the vegetative meristem and dramatically

alters leaf morphology when overexpressed in transgenic plants." Plant Cell **6**(12): 1859-1876.
Liu, J., F. Zhang, et al. (2012). "Phytochrome B control of total leaf area and stomatal density affects drought tolerance in rice." Plant Molecular Biology **78**(3): 289-300.
Long, J. A., E. I. Moan, et al. (1996). "A member of the KNOTTED class of homeodomain proteins encoded by the STM gene of Arabidopsis." Nature **379**(6560): 66-69.
Lopez-Juez, E., J. Bowyer, et al. (2007). "Distinct leaf developmental and gene expression responses to light quantity depend on blue-photoreceptor or plastid-derived signals, and can occur in the absence of phototropins." Planta **227**(1): 113-123.
Makino, A., T. Mae, et al. (1985). "Photosynthesis and ribulose-1,5-bisphosphate carboxylase/oxygenase in rice leaves from emergence through senescence. Quantitative analysis by carboxylation/oxygenation and regeneration of ribulose 1,5-bisphosphate." Planta 166(3): 414-420
Marshall, W., K. Young, et al. (2012). "What determines cell size?" BMC Biology **10**(1): 101.
McClendon, J. H. (1962). "the relationship between the thickness of deciduous leaves and their maximum photosynthetic rate." American Journal of Botany **49**(4): 320-322.
McHale, N. A. and R. E. Koning (2004). "PHANTASTICA regulates development of the adaxial mesophyll in Nicotiana leaves." Plant Cell **16**(5): 1251-1262.
Mercade, J., A. Espinosa, et al. (2009). "Orymold: ontology based gene expression data integration and analysis tool applied to rice." BMC Bioinformatics **10**(1): 158.
Mitchell, P. L., J. E. Shehy, et al. (1998). Potential Yields and efficiency of radiation use in rice. IRRI discussion paper series No. 32. I. R. R. Institue. Manila (Philippines).
Miyoshi, K., B.-O. Ahn, et al. (2004). "PLASTOCHRON1, a timekeeper of leaf initiation in rice, encodes cytochrome P450." Proceedings of the National Academy of Sciences of the United States of America **101**(3): 875-880.
Murchie, E. H. and P. Horton (1997). "Acclimation of photosynthesis to irradiance and spectral quality in British plant species: chlorophyll content, photosynthetic capacity and habitat preference." Plant, Cell & Environment **20**(4): 438-448.
Murchie, E. H. and P. Horton (1997). "Acclimation of photosynthesis to irradiance and spectral quality in British plant species: chlorophyll content, photosynthetic capacity and habitat preference." Plant, Cell and Environment **20**(4): 438-448.
Murchie, E. H., S. Hubbart, et al. (2005). "Acclimation of photosynthesis to high irradiance in rice: gene expression and interactions with leaf development." Journal of Experimental Botany **56**(411): 449-460.
Murchie, E. H., S. Hubbart, et al. (2005). Acclimation of photosynthesis to high irradiance in rice: gene expression and interactions with leaf development. **56:** 449-460.

Nath, U., B. C. W. Crawford, et al. (2003). "Genetic Control of Surface Curvature." Science **299**(5611): 1404-1407.
Nishimura, A., M. Ito, et al. (2002). "OsPNH1 regulates leaf development and maintenance of the shoot apical meristem in rice." Plant J **30**(2): 189-201.
Nobel, P. S. (2009). Physicochemical and Environmental Plant Physiology, Elsevier Science.
Nobel, P. S., I. N. Forseth, et al. (1993). Canopy structure and light interception. Photosynthesis and Production in a Changing Environment : A Field and Laboratory Manual. D. O. Hall, J. M. O. Scurlock, H. R. Bolhar-Nordenkampf, R. C. Leegood and S. P. Long. London, Chapman&Hall**:** 79-90.
Nobel, P. S., L. J. Zaragoza, et al. (1975). "Relation between Mesophyll Surface Area, Photosynthetic Rate, and Illumination Level during Development for Leaves of Plectranthus parviflorus Henckel." Plant Physiology **55**(6): 1067-1070.
Oguchi, R., K. Hikosaka, et al. (2003). "Does the photosynthetic light-acclimation need change in leaf anatomy?" Plant, Cell & Environment **26**: 505-512.
Ohno, C. K., G. V. Reddy, et al. (2004). "The Arabidopsis JAGGED gene encodes a zinc finger protein that promotes leaf tissue development." Development **131**(5): 1111-1122.
Paul, M. J., L. F. Primavesi, et al. (2008). "Trehalose Metabolism and Signaling." Annual Review of Plant Biology **59**(1): 417-441.
Paulilo, M. T. S., R. T. Besford, et al. (1994). "Rubisco and PEP carboxylase responses to changing irradiance in a Brazilian Cerrado tree species, Qualea grandiflora Mart. (Vochysiaceae)." Tree Physiology **14**(2): 165-177.
Peng, S., Khusha, S.G.,Virka, P., Tangb, Q. and Zoub, Y. (2008). "Progress in ideotype breeding to increase rice yield potential " Field Crops Research **108**(1): 32-38.
Poethig, R. S., Ed. (1984). Cellular parameters of leaf morphogenesis in maize and tobacco. In Contemporary Problems in Plant Anatomy. Orlando, Academic Press.
Powell, Anahid E. and M. Lenhard (2012). "Control of organ size in plants." Current biology : CB **22**(9): R360-R367.
Pritchard, S. G., H. H. Rogers, et al. (1999). "Elevated CO_2 and plant structure: a review." Global Change Biology **5**: 807-837.
Quail, P. H. (2002). "Photosensory perception and signalling in plant cells: new paradigms?" Current Opinion in Cell Biology **14**(2): 180-188.
Reich, P. B., M. B. Walters, et al. (1998). "Photosynthesis and respiration rates depend on leaf and root morphology and nitrogen concentration in nine boreal tree species differing in relative growth rate." Functional Ecology **12**(3): 395-405.
Reinhardt, D., E. R. Pesce, et al. (2003). "Regulation of phyllotaxis by polar auxin transport." Nature **426**(6964): 255-260.
Sage, T. L. and R. F. Sage (2009). "The functional anatomy of rice leaves: implications for refixation of photorespiratory CO_2 and efforts to

engineer C4 photosynthesis into rice." Plant Cell Physiol. **50**(4): 756-772.
Salisbury, F. B. and C. W. Ross (1992). Plant Physiology. California, Wadworth Publishing.
Satina, S., A. F. Blakeslee, et al. (1940). "Demonstration of the three germ layers in the shoot apex of datura by means of induced polyploidy in periclinal chimeras." American Journal of Botany **Vol. 27**: 895-905.
Savvides, A., D. Fanourakis, et al. (2012). "Co-ordination of hydraulic and stomatal conductances across light qualities in cucumber leaves." Journal of Experimental Botany **63**(3): 1135-1143.
Schneider, C. A., W. S. Rasband, et al. (2012). "NIH Image to ImageJ: 25 years of image analysis." Nat Meth **9**(7): 671-675.
Schwab, R., S. Ossowski, et al. (2006). "Highly specific gene silencing by artificial micrornas in Arabidopsis." The Plant Cell Online **18**(5): 1121-1133.
Sharkey, T. D., C. J. Bernacchi, et al. (2007). "Fitting photosynthetic carbon dioxide response curves for C3 leaves." Plant, Cell & Environment **30**(9): 1035-1040.
Sharman, B. C. (1942). "Onset of reproductive phase in grasses and cereals." Nature **150**: 208-208.
Sheehy, J. E., A. B. Ferrer, et al. (2008). Harnessing photosynthesis in tomorrow's world: Humans, Crop Production and Poverty Alleviation. Photosynthesis. Energy from the Sun**:** 1237-1242.
Shen, W.-H. (2002). "The plant E2F-Rb pathway and epigenetic control." Trends in Plant Science **7**(11): 505-511.
Sinha, N. (1999). "Leaf Development in Angiosperms." Annu Rev Plant Physiol Plant Mol Biol **50**: 419-446.
Smillie, I. R. A., K. A. Pyke, et al. (2012). "Variation in vein density and mesophyll cell architecture in a rice deletion mutant population." Journal of Experimental Botany.
Smith, K. W., C. Vogelman, et al. (1997). "Leaf form and photosynthesis; Do leaf structure and oreintation interact to regulate internal light and carbon dioxide?" Bioscience **47**(11): 9.
Smith, L. G. and S. Hake (1992). "The Initiation and Determination of Leaves." Plant Cell **4**(9): 1017-1027.
Smith, L. G., S. Hake, et al. (1996). "The tangled-1 mutation alters cell division orientations throughout maize leaf development without altering leaf shape." Development **122**(2): 481-489.
Snow, M. and R. Snow (1932). "Experiments on Phyllotaxis. I. The effect of isolating a primordium." Philosophical Transactions of the Royal Society of London **221**: 1-43.
Snow, M. and R. Snow (1959). "Regulation of sizes of leaf primordia by older leaves" Proceedings of the Royal Society of London **151**(942): 39-47.

Storey, J. D. (2002). "A direct approach to false discovery rates." Journal of the Royal Statistical Society: Series B (Statistical Methodology) **64**(3): 479-498.

Sussex, I. M. (1955). "Morphogenesis in Solanum tuberosum L. Apical structure and developmental pattern of the juvenile shoot." Phytomorphology **5**: 253-273.
Sussex, I. M. (1989). "Developmental programming of the shoot meristem." Cell **56**(2): 225-229.
Suzuki, M. M. and A. Bird (2008). "DNA methylation landscapes: provocative insights from epigenomics." Nat Rev Genet **9**(6): 465-476.
Suzuki, Y., A. Makino, et al. (2001). "Changes in the turnover of Rubisco and levels of mRNAs of rbcL and rbcS in rice leaves from emergence to senescence." Plant, Cell & Environment **24**(12): 1353-1360.
Sylvester, A. W., L. Smith, et al. (1996). "Acquisition of identity in the developing leaf." Annual Review of Cell and Developmental Biology **12**(1): 257-304.
Syvertsen, J. P., J. Lloyd, et al. (1995). "On the relationship between leaf anatomy and CO_2 diffusion through the mesophyll of hypostomatous leaves." Plant, Cell and Environment **18**(2): 149-157.
Taiz, L. and E. Zeiger (2010). Plant Physiology, Sinauer Associates.
Terashima, I., Y. T. Hanba, et al. (2006). "Irradiance and phenotype: comparative eco-development of sun and shade leaves in relation to photosynthetic CO2 diffusion." Journal of Experimental Botany **57**(2): 343-354.
Terashima, I., Y. T. Hanba, et al. (2011). "Leaf functional anatomy in relation to photosynthesis." Plant Physiology **155**(1): 108-116.
Terashima, I., S.-I. Miyazawa, et al. (2001). "Why are sun leaves thicker than shade leaves? — Consideration based on analyses of CO_2 diffusion in the leaf." Journal of Plant Research **114**(1): 93-105.
Thomas, P. W., F. I. Woodward, et al. (2004). "Systemic irradiance signalling in tobacco." New Phytologist **161**(1): 193-198.
Thornber, J. P., G. F. Peter, et al. (1993). "Light harvesting in photosystems I and II." Biochemical Society transactions **21**(1): 15-18.
Tsiantis, M., R. Schneeberger, et al. (1999). "The maize rough sheath2 gene and leaf development programs in monocot and dicot plants." Science **284**(5411): 154-156.
Tsuge, T., H. Tsukaya, et al. (1996). "Two independent and polarized processes of cell elongation regulate leaf blade expansion in Arabidopsis thaliana (L.) Heynh." Development **122**(5): 1589-1600.
Tsukaya, H. (2003). "Organ shape and size: a lesson from studies of leaf morphogenesis." Current Opinion in Plant Biology **6**(1): 57-62.
Tsukaya, H. (2005). "Leaf shape: genetic controls and environmental factors." The International journal of developmental biology **49**(5-6): 547-555.
Tsukaya, H. (2006). "Mechanism of leaf-shape determination." Annual Review of Plant Biology **57**(1): 477-496.
Turnbull, G. N. C., Ed. (2005). Plant architecture and its manipulation; Annual plant reviews , volume 17. Cellular architecture: Regulation of cell size, cell shape and organ initiation, Blackwell Publishing.
Vile, D., E. Garnier, et al. (2005). "Specific leaf area and dry matter content estimate thickness in laminar leaves." Ann Bot **96**(6): 1129-1136.

Waites, R. and A. Hudson (1995). "phantastica: a gene required for dorsoventrality of leaves in Antirrhinum majus." Development **121**(7): 2143-2154.
Waites, R., H. R.N., et al. (1998). "The PHANTASTICA gene encodes a MYB transcription factor involved in growth and dorsoventrality of lateral organs in Antirrhinum " Cell **93**(5): 779-789.
Walbot, V. (1985). "On the life strategies of plants and animals." Trends in Genetics **1**: 165-169.
Werger, M. J. A. and T. Hirose (1991). "Leaf nitrogen distribution and whole canopy photosynthetic carbon gain in herbaceous stands." Vegetatio **97**(1): 11-20.
Weston, E., K. Thorogood, et al. (2000). "Light quantity controls leaf-cell and chloroplast development in Arabidopsis thaliana wild type and blue-light-perception mutants." Planta **211**(6): 807-815.
White, D. W. R. (2006). "PEAPOD regulates lamina size and curvature in Arabidopsis." Proceedings of the National Academy of Sciences **103**(35): 13238-13243.
Wilson, D. and J. P. Cooper (1969). "Effect of light intensity during growth on leaf anatomy and subsequent light-saturated photosynthesis among contrasting lolium genotypes." New Phytologist **68**(4): 1125-1135.
Wong, S. C., I. R. Cowan, et al. (1979). "Stomatal conductance correlates with photosynthetic capacity." Nature **282**(5737): 424-426.
Yamaguchi, T., N. Nagasawa, et al. (2004). "The YABBY Gene DROOPING LEAF Regulates Carpel Specification and Midrib Development in Oryza sativa." Plant Cell **16**(2): 500-509.
Yano, S. and I. Terashima (2001). "Separate localization of light signal perception for sun or shade type chloroplast and palisade tissue differentiation in *Chenopodium album*." Plant and Cell Physiology **42**(12): 1303-1310.
Yano, S. and I. Terashima (2004). "Developmental process of sun and shade leaves in *Chenopodium album* L." Plant, Cell & Environment **27**(6): 781-793.
Zhu, X.-G., S. P. Long, et al. (2010). "Improving Photosynthetic Efficiency for Greater Yield." Annual Review of Plant Biology **61**(1): 235-261.

Appendix

Appendix A List of the genes that were down-regulated after transfer to low light for 6 hours, comparing between 6hrs HL vs. 6hrs LL. The *p*-value < 0.01 were used as the cut-off for the gene selection.

ProbeID	Annotation	Fold change
Os.16037.1.S1_at	unknown	2.61
OsAffx.32313.1.A1_at	unknown	1.44
OsAffx.27184.1.S1_at	Serine/threonine-protein kinase SAPK4	0.91
Os.44473.1.S1_at	Protein kinase domain containing protein	0.87
Os.57427.1.S1_x_at	Conserved hypothetical protein	0.70
Os.49098.1.S1_x_at	Helix-loop-helix DNA-binding domain containing protein	0.66
Os.6864.1.S1_at	Heavy metal transport/detoxification protein domain containing protein	0.57
OsAffx.26542.1.S1_at	Pectinesterase inhibitor domain containing protein	0.56
OsAffx.5022.1.S1_at	unknown	0.54
OsAffx.25727.1.A1_at	unknown	0.54
OsAffx.5551.1.A1_at	unknown	0.52
Os.53144.1.S1_at	Type I inositol-1,4,5-trisphosphate 5-phosphatase CVP2	0.51
Os.25316.1.S1_at	Kinesin, motor region domain containing protein	0.48
Os.46878.1.S1_at	Similar to Scl1 protein, GRAS family transcription factor	0.47
Os.56310.1.A1_s_at	Conserved hypothetical protein	0.45
OsAffx.11013.1.S1_at	unknown	0.41
OsAffx.15396.1.S1_at	unknown	0.41
Os.55203.1.S1_at	unknown	0.41
OsAffx.26292.1.S1_at	unknown	0.40
OsAffx.2020.1.S1_at	unknown	0.38
OsAffx.3507.1.S1_at	unknown	0.36
OsAffx.18940.1.S1_at	unknown	0.34
Os.55405.1.S1_at	unknown	0.33
OsAffx.7632.1.S1_at	Hypothetical protein	0.30
OsAffx.13411.1.S1_at	Galectin, galactose-binding lectin family protein	0.30
OsAffx.3311.1.S1_at	unknown	0.29
OsAffx.20873.1.S1_at	unknown	0.29
OsAffx.9154.1.S1_at	unknown	0.29
OsAffx.14077.1.S1_x_at	unknown	0.29
Os.30173.2.S1_at	AWPM-19-like family protein	0.28
Os.10192.1.S1_at	Conserved hypothetical protein	0.26
Os.55333.1.S1_at	Auxin responsive SAUR protein family protein	0.24
OsAffx.31898.1.S1_at	unknown	0.23
OsAffx.22785.1.S1_x_at	Protein of unknown function (DUF3681)	0.23
OsAffx.17616.1.S1_at	unknown	0.22
Os.13704.1.S1_x_at	Hypothetical protein	0.20

Appendix B List of the genes that were up-regulated after transfer to low light for 6 hours comparing between 6hrs HL and 6hrs LL. The *p*-value < 0.01 were used as the cut-off for the gene selection.

ProbeID	Gene Title	Fold change
Os.9836.1.S1_at	Hypothetical protein	1.38
Os.12993.1.S1_at	Acyl-coenzyme A oxidase 4, peroxisomal	1.11
Os.45531.1.S1_at	Protein kinase-like domain containing protein	0.74
Os.56716.1.S1_at	unknown	0.57
Os.10527.1.S2_a_at	Sec7p-like protein	0.56
OsAffx.2562.1.S1_at	Similar to Transcription factor HBP-1b(C38)	0.52
OsAffx.17314.2.S1_at	Plant MuDR transposase domain containing protein, SWIM zinc finger	0.49
OsAffx.11505.1.S1_at	unknown	0.48
Os.51915.2.S1_at	UDP-glucuronosyl/UDP-glucosyltransferase family protein	0.47
Os.17918.1.S1_at	Domain of unknown function DUF26,Cysteine-rich Receptor-like Kinases (CRKs),	0.46
Os.27370.1.S2_at	Hypothetical protein	0.45
OsAffx.28946.1.S1_at	Conserved hypothetical protein	0.44
Os.52228.1.S1_at	Similar to HcrVf2 protein, Leucine rich repeat N-terminal domain	0.44
OsAffx.5856.1.S1_at	unknown	0.43
OsAffx.24996.1.S1_at	Protein of unknown function (DUF1668)	0.43
Os.5449.1.S2_at	Ribosome-binding factor A family protein	0.43
OsAffx.13835.1.S1_at	unknown	0.43
OsAffx.4878.1.S1_at	unknown	0.42
OsAffx.7922.1.S1_at	Protein of unknown function (DUF3615)	0.41
OsAffx.30515.1.S1_at	HAT dimerisation domain containing protein	0.41
OsAffx.17068.1.S1_at	unknown	0.41
Os.9952.1.S1_at	Conserved hypothetical protein	0.41
OsAffx.27689.1.S1_at	unknown	0.39
OsAffx.2891.1.S1_s_at	Heavy metal transport/detoxification protein domain containing protein	0.39
Os.31497.2.S1_x_at	Peptidase aspartic, catalytic domain containing protein	0.38
Os.23296.1.S1_x_at	Cytochrome P450	0.38
OsAffx.29985.1.S1_at	unknown	0.37
OsAffx.30795.1.S1_x_at	unknown	0.36
OsAffx.19128.1.A1_at	unknown	0.35
Os.12036.2.S1_at	Endonuclease/exonuclease/phosphatase domain containing protein	0.35
Os.53458.1.S1_at	O-methyltransferase ZRP4	0.34

Appendix B (continued)

ProbeID	Gene Title	Fold change
Os.49950.1.S1_at	leucine-rich repeat receptor-like protein kinase	0.32
Os.32667.1.S1_at	Similar to Cellulase	0.32
Os.50443.1.S1_at	Hypothetical protein	0.32
OsAffx.13420.1.S1_at	unknown	0.31
OsAffx.19478.2.S1_s_at	Major facilitator superfamily MFS_1 protein	0.30
Os.46556.2.A1_at	P-loop NTPase; P-loop containing Nucleoside Triphosphate Hydrolases	0.29
OsAffx.15388.1.S1_at	unknown	0.29
Os.50754.1.A1_x_at	Similar to Aldehyde oxidase 3	0.28
OsAffx.20217.1.S1_at	unknown	0.27
Os.23578.1.S1_at	Hypothetical protein	0.27
OsAffx.32109.1.S1_x_at	Conserved hypothetical protein	0.27
Os.2325.1.S1_at	Aldehyde dehydrogenase NAD(P)-dependent family protein	0.26
Os.4907.1.S1_at	unknown	0.26
OsAffx.29871.2.S1_x_at	Similar to PDR-like ABC transporter	0.26
OsAffx.27319.1.S1_at	unknown	0.26
OsAffx.11400.1.S1_s_at	unknown	0.25
OsAffx.14274.1.A1_at	Conserved hypothetical protein	0.19

Appendix C List of the genes that were down-regulated after transfer to low light for 24 hours, comparing between 24hrs HL vs. 24hrs LL. The *p*-value < 0.01 were used as the cut-off for the gene selection.

Gene ID	Annotaion	Fold change
Os.18490.3.S1_at	Thiamine biosynthesis protein thiC	2.73
Os.5682.1.S1_at	Anther-specific protein	2.11
Os.46895.1.S1_at	Cytokinin dehydrogenase , FAD and cytokinin binding	2.02
Os.50470.1.S1_at	Cytokinin dehydrogenase, FAD and cytokinin binding	1.96
Os.17921.1.S1_at	Phosphoethanolamine methyltransferase	1.93
Os.53150.1.S1_at	Proteasome subunit beta type 1	1.78
Os.41468.1.S1_at	Cyclin-like F-box domain containing protein	1.64
OsAffx.23744.1.S1_s_at	Conserved hypothetical protein	1.59
Os.32212.1.A1_at	RNA dependent RNA polymerase family protein	1.59
Os.49536.1.S1_at	Stearoyl-acyl carrier protein desaturase	1.57
Os.17403.1.S1_a_at	Cyclin-like domain containing protein	1.57
OsAffx.30149.1.S1_s_at	putative zinc finger domain, LRP1 type	1.57
OsAffx.26451.1.S1_at	Protein of unknown function DUF6, transmembrane domain containing protein	1.56
Os.49457.1.A1_at	Amino acid/polyamine transporter I family protein	1.54
OsAffx.28948.1.S1_at	Helix-loop-helix DNA-binding domain containing protein	1.50
Os.7929.1.S1_a_at	Conserved hypothetical protein	1.48
Os.4125.1.S1_at	RNA-binding region RNP-1 (RNA recognition motif)	1.47
Os.25215.1.A1_at	Cyclin-like F-box domain containing protein; Antagonist of mitotic exit network protein 1	1.46
Os.55658.1.S1_at	EF-hand, calcium binding motif; Parvalbumin family protein	1.46
Os.55696.1.S1_at	Conserved hypothetical protein	1.44
Os.1307.1.S1_a_at	Phytosulfokine precursor protein (PSK)	1.42
Os.20045.1.S1_at	Splicing factor PWI domain containing protein	1.38
Os.55557.1.S1_at	TGF-beta receptor, type I/II extracellular region family protein	1.37
Os.56349.1.S1_at	Trehalose-6-phosphate phosphatase	1.36
Os.54940.1.S1_at	Isopenicillin N synthase family protein; flavanone-3-hydroxylase	1.32
Os.7929.2.S1_a_at	Conserved hypothetical protein	1.31
Os.50596.1.S1_at	Ubiquitin domain containing protein	1.30
Os.7593.1.S1_at	Pectinesterase	1.27
Os.52037.1.S1_at	Hexokinase	1.26
Os.2436.1.S1_at	Receptor-like protein kinase	1.25
OsAffx.2249.1.S1_at	unknown	1.25
OsAffx.29961.1.S1_at	Zinc finger, BED-type predicted domain containing protein	1.24
Os.57022.1.S1_at	KH, type 1 domain containing protein	1.24
Os.15633.1.S2_at	COBRA-like protein (encoded by OsBC1L4)	1.23
Os.22374.1.S2_a_at	4-coumarate-CoA ligase-like protein (Adenosine monophosphate binding protein 3 AMPBP3)	1.17

Appendix C (continued)

Gene ID	Annotaion	Fold change
Os.53539.1.S1_at	Hypothetical protein	1.15
Os.42069.1.S1_x_at	Dynein light chain 1, cytoplasmic	1.14
Os.12000.1.S1_at	EF-Hand type domain containing protein	1.13
Os.4680.2.S1_x_at	Dimethylaniline monooxygenase-like protein (Flavin-containing monooxygenase YUCCA)	1.12
Os.9355.1.S1_at	Protein of unknown function DUF702 family protein	1.12
Os.55538.1.S1_at	Conserved hypothetical protein	1.12
Os.47761.1.S1_at	Glutamate decarboxylase isozyme 3	1.10
Os.20278.1.S1_at	Protein kinase-like domain containing protein	1.10
Os.8031.1.S1_at	AP2; DNA-binding domain found in transcription regulators in plants such as APETALA2 and EREBP (ethylene responsive element binding protein).	1.10
Os.32943.1.S1_at	AAA ATPase domain containing protein	1.09
OsAffx.25032.1.S1_s_at	Chloroplast serine acetyltransferase	1.07
Os.20579.1.S1_at	Protease-associated PA domain containing protein	1.07
Os.10251.1.S1_at	Very-long-chain 3-ketoacyl-CoA synthase family protein	1.05
Os.20233.1.S1_at	unknown	1.01
Os.48994.1.A1_at	unknown	1.01
Os.6248.1.S1_s_at	Phosphoenolpyruvate carboxylase	0.99
Os.57028.1.S1_at	Phospholipase/Carboxylesterase family protein	0.99
Os.7054.1.S1_a_at	Ribosomal L28e protein family protein	0.98
Os.34631.1.S1_at	P-loop containing Nucleoside Triphosphate Hydrolases	0.98
Os.3388.2.S1_a_at	Similar to Y19 protein; SANT; 'SWI3, ADA2, N-CoR and TFIIIB' DNA-binding domains	0.98
Os.52184.1.S1_at	Conserved hypothetical protein	0.97
Os.53619.1.S1_at	SNC1; Synaptobrevin/VAMP-like protein [Intracellular trafficking and secretion]	0.96
OsAffx.27621.1.S1_s_at	Avr9/Cf-9 rapidly elicited protein 231;Glycosyltransferase family A (GT-A)	0.96
Os.50505.2.S1_at	DUF247; Plant protein of unknown function	0.95
Os.24753.1.S1_at	Esterase/lipase/thioesterase domain containing protein	0.94
OsAffx.10786.1.S1_at	unknown	0.94
Os.18262.1.S1_at	unknown	0.93
Os.23932.1.A1_at	No apical meristem (NAM) protein domain containing protein	0.93
Os.47623.1.A1_at	SCARECROW	0.93
Os.50954.1.S1_at	unknown	0.92
Os.46844.1.S1_at	Lipolytic enzyme, G-D-S-L family protein	0.92
Os.28968.1.S1_at	Conserved hypothetical protein	0.91
Os.54742.1.S1_at	Dihydrouridine synthase, DuS family protein	0.91
Os.38110.1.S1_at	TRE1 (TREHALASE 1); alpha,alpha-trehalase/ trehalase	0.90
Os.23236.1.S1_at	translation elongation factor EF-2 subunit	0.90

Appendix C (continued)

Gene ID	Annotaion	Fold change
Os.50155.1.S1_at	Conserved hypothetical protein	0.89
Os.55608.1.S1_at	Two-component response regulator ARR1. Splice isoform 2	0.87
OsAffx.20084.1.S1_at	unknown	0.87
Os.11456.1.S1_at	Pectin methylesterase isoform alpha	0.86
Os.10454.1.S1_a_at	Phosphoenolpyruvate carboxylase	0.85
Os.52804.1.S1_at	UspA domain containing protein	0.84
Os.51800.1.S1_at	Chaperonin Cpn60/TCP-1 family protein	0.83
Os.56345.1.S1_at	Conserved hypothetical protein	0.83
Os.6237.1.S1_at	unknown function DUF674 family protein	0.82
Os.51697.1.S1_at	Origin recognition complex 5	0.81
Os.11730.1.S1_at	Conserved hypothetical protein	0.81
Os.46465.1.S1_a_at	KH domain containing protein	0.81
Os.7144.2.S1_a_at	pyruvate phosphate dikinase	0.80
Os.28399.1.S3_at	Hypothetical protein	0.79
Os.3895.1.S1_at	ATPase, P-type, K/Mg/Cd/Cu/Zn/Na/Ca/Na/H-transporter family protein	0.78
Os.49120.1.S1_at	Membrane bound O-acyl transferase, MBOAT family protein	0.78
Os.31518.1.S1_at	Type B-like cyclin (Fragment)	0.78
OsAffx.6057.1.S1_s_at	Mitochondrial uncoupling protein, Mitochondrial carrier protein	0.78
Os.49165.1.S2_at	RNA-binding region RNP-1 (RNA recognition motif) domain containing protein	0.77
Os.47824.1.S1_at	Eukaryotic protein of unknown function (DUF914)	0.76
Os.11812.1.S1_at	SAM dependent carboxyl methyltransferase family protein	0.75
Os.51485.1.S1_at	Phosphate starvation regulator protein (Regulatory protein of P- starvation acclimation response Psr1)	0.75
Os.1715.1.S1_at	Rhomboid-like protein family protein	0.74
Os.12719.2.S1_at	IDI2; Predicted translation initiation factor 2B subunit, eIF-2B alpha/beta/delta family	0.74
Os.50613.1.S1_at	Conserved hypothetical protein	0.74
Os.11313.1.S1_at	Pathogen-related protein (JIOsPR10)	0.74
OsAffx.17402.1.S1_at	C2 calcium/lipid-binding region, CaLB domain containing protein	0.74
Os.37148.1.S1_at	Conserved hypothetical protein	0.73
Os.34249.1.S1_at	Auxin response factor, Plant-specific B3-DNA binding domain	0.73
Os.4810.1.S1_s_at	Conserved hypothetical protein	0.73
Os.48351.1.S1_at	Basic blue protein (Cusacyanin) (Plantacyanin) (CBP)	0.72
Os.20190.1.S1_at	Pleckstrin homology-type domain containing protein, RhoGAP; RhoGAP: GTPase-activator protein (GAP) for Rho-like GTPases	0.72
OsAffx.2912.1.S1_at	unknown	0.71
Os.51699.1.S1_at	Conserved hypothetical protein	0.71
Os.7370.1.S1_at	Cytochrome P450 85A1, OsDWARF	0.71

Appendix C (continued)

Gene ID	Annotaion	Fold change
Os.9325.1.S1_at	Protein of unknown function UPF0220 family protein	0.70
OsAffx.2191.1.S1_at	Zinc finger, CCCH-type domain containing protein	0.70
Os.49634.1.S1_x_at	Dynein light chain 1, cytoplasmic	0.69
Os.11272.1.S1_at	Conserved hypothetical protein	0.69
Os.21231.1.S1_at	HLH; Helix-loop-helix domain	0.68
Os.52834.1.S1_at	Conserved hypothetical protein	0.68
Os.19374.1.S1_at	unknown	0.67
Os.5591.1.S1_at	Conserved hypothetical protein	0.67
OsAffx.32073.1.S1_at	Leucine-rich repeat, plastid	0.67
Os.52353.1.S2_at	PKc_like; Protein Kinases, catalytic domain	0.66
OsAffx.3382.1.S1_at	unknown	0.66
Os.55711.1.S1_at	unknown	0.64
Os.8401.1.S1_at	Eukaryotic translation initiation factor 5 (eIF-5)	0.64
Os.50445.1.S1_at	serine-type endopeptidase inhibitor activity	0.63
Os.57121.1.S1_at	unknown	0.62
Os.49692.1.S1_at	Transferase family protein	0.62
Os.15397.1.S1_at	Ferredoxin-dependent bilin reductase	0.61
Os.23036.1.A1_at	RNA polymerase, RBP11-like domain containing protein	0.61
Os.46892.2.S1_at	Conserved hypothetical protein	0.61
OsAffx.24532.1.A1_at	unknown	0.60
Os.10838.3.S1_at	Molybdenum cofactor biosynthesis domain containing protein	0.60
Os.46868.1.S1_x_at	TRAF-like domain containing protein	0.60
OsAffx.13918.1.S1_at	unknown	0.60
Os.34249.2.S1_at	Auxin_resp; Auxin response factor; Plant-specific B3-DNA binding domain	0.59
Os.20298.1.S1_at	Conserved hypothetical protein	0.59
Os.7930.1.S1_x_at	Mito_carr; Mitochondrial carrier protein	0.59
Os.47739.1.S1_at	Homeodomain-like containing protein	0.58
Os.9238.2.S1_at	HSP20-like chaperone domain containing protein	0.57
Os.32978.1.S1_at	Homeobox domain containing protein	0.57
Os.54906.1.S1_at	STKc_AGC; Catalytic domain of AGC family Protein Serine/Threonine Kinases	0.57
Os.22910.1.S1_at	Beta-glucosidase/6-phospho-beta-glucosidase/beta-galactosidase [Carbohydrate transport and metabolism]	0.56
Os.30696.1.S1_at	Conserved hypothetical protein	0.56
Os.19005.1.S1_at	ATP binding protein, putative, expressed	0.56
Os.56382.1.S1_at	PKc; Catalytic domain of Protein Kinases	0.55
OsAffx.10002.1.S1_at	unknown	0.55
Os.53355.1.S1_s_at	Amino acid-binding ACT domain containing protein	0.54
Os.10746.1.S1_a_at	Serine/threonine-protein kinase SAPK7	0.54
OsAffx.30547.1.S1_at	Complex 1 LYR protein family protein	0.54
OsAffx.10902.1.S1_at	Branch; Core-2/I-Branching enzyme	0.53
Os.54992.1.S1_at	unknown	0.53
Os.8450.2.S1_at	Amino acid carrier (Fragment)	0.52

Appendix C (continued)

Gene ID	Annotaion	Fold change
Os.46873.1.S1_a_at	Cyclin-like F-box domain containing protein	0.52
Os.18552.1.S1_at	Peptidase S10, serine carboxypeptidase family protein	0.52
Os.50.3.S1_x_at	Peptidase, trypsin-like serine and cysteine domain containing protein	0.51
Os.52305.2.S1_x_at	En/Spm-like transposon proteins family protein	0.50
OsAffx.22827.1.S1_x_at	unknown	0.50
Os.23924.2.S1_at	Hypothetical protein	0.49
Os.45991.1.S1_x_at	Glycosyl transferase, family 14 protein	0.49
Os.8034.1.S1_at	Conserved hypothetical protein	0.48
Os.6435.1.S1_at	Predicted hydrolase (HAD superfamily), Pyrimidine 5-nucleotidase family protein	0.48
OsAffx.4714.1.S1_at	unknown	0.48
Os.34865.2.S1_x_at	P-loop containing Nucleoside Triphosphate Hydrolases	0.48
OsAffx.17736.1.S1_at	unknown	0.47
Os.8592.1.S1_at	Ovarian tumour, otubain domain containing protein	0.47
Os.26816.1.A1_s_at	Protein kinase domain containing protein	0.45
OsAffx.21485.1.S1_at	Myb_DNA-bind_3; Myb/SANT-like DNA-binding domain	0.45
OsAffx.18825.1.S1_at	NB-ARC domain containing protein	0.44
Os.28828.1.S2_at	WRKY3 (WRKY14) (WRKY transcription factor 16) (WRKY16)	0.44
Os.50542.1.S1_at	Biotin/lipoate A/B protein ligase family	0.43
Os.49442.2.S1_x_at	Conserved hypothetical protein	0.43
OsAffx.12704.1.S1_at	unknown	0.43
Os.24469.1.A1_at	unknown	0.43
Os.4733.1.S1_at	Protein of unknown function DUF89 family protein	0.43
Os.26430.1.A1_at	Homeodomain-like containing protein	0.43
Os.10847.1.A1_at	Conserved hypothetical protein	0.42
Os.7913.1.S1_a_at	MAP kinase homolog	0.42
OsAffx.2764.1.S1_at	unknown	0.42
Os.50344.1.S1_at	Reverse transcriptase, RNA-dependent DNA polymerase family protein	0.41
OsAffx.10943.1.S1_at	unknown	0.41
Os.5670.1.S1_at	Glycosyl hydrolases family 28	0.40
Os.22730.1.S1_at	Low molecular mass heat shock protein Oshsp17.7	0.40
Os.50056.1.S1_at	Tau95; RNA polymerase III transcription factor (TF)IIIC subunit	0.40
Os.53852.1.S1_at	Glutathione-conjugate transporter AtMRP4	0.40
Os.5096.1.S1_at	Succinate dehydrogenase, cytochrome b subunit family protein	0.39
Os.11745.1.S1_at	Conserved hypothetical protein	0.37
OsAffx.11040.1.S1_at	unknown	0.37
Os.48912.1.S1_at	Hypothetical protein	0.36
Os.10472.1.S1_at	Conserved hypothetical protein	0.36
OsAffx.16043.1.S1_at	unknown	0.35

Appendix C (continued)

Gene ID	Annotaion	Fold change
OsAffx.16653.2.S1_at	unknown	0.34
OsAffx.23947.1.S1_at	Leucine rich repeat, N-terminal domain containing protein	0.34
Os.9272.1.S1_at	unknown function UPF0061 family protein	0.34
Os.4883.1.S1_at	Med11; Mediator complex protein	0.33
OsAffx.4124.1.S1_at	unknown	0.32
OsAffx.27060.1.S1_at	ZnF_PMZ; plant mutator transposase zinc finger	0.29
Os.10438.1.S1_at	PLN02720; complex II	0.25
Os.29095.1.S1_at	unknown	0.17

Appendix D List of the genes that were up-regulated after transfer to low light for 24 hours comparing between 24hrs HL vs. 24hrs LL. The *p*-value < 0.01 were used as the cut-off for the gene selection.

Gene ID	Annotaion	Fold change
Os.26511.1.S1_at	Conserved hypothetical protein	5.56
Os.20206.1.S1_at	Protein of unknown function, DUF584	3.75
OsAffx.29994.1.S1_s_at	PF1 protein; linker histone 1 and histone 5 domains	3.59
Os.12129.1.S1_a_at	CBS domain containing protein	3.59
Os.12735.1.S1_at	Auxin_repressed; Dormancy/auxin associated protein	3.53
Os.22312.3.A1_a_at	Universal stress protein (Usp) family protein	3.38
Os.37213.1.S1_at	Auxin responsive SAUR protein family protein	3.30
Os.38378.1.S1_a_at	Light regulated Lir1 family protein	3.23
Os.6318.1.S1_at	Zing finger transcription factor PEI1	3.08
Os.10497.1.S1_s_at	Conserved hypothetical protein	3.03
Os.37834.1.S1_a_at	Ripening-associated protein; Gn_AT_II; Glutamine amidotransferases class-II (GATase)	2.99
Os.15896.1.S1_at	Conserved hypothetical protein	2.97
Os.8850.1.S1_x_at	Conserved hypothetical protein	2.97
Os.38638.1.S1_at	Early nodulin 93 ENOD93 protein	2.97
Os.37909.1.S1_at	Conserved hypothetical protein	2.93
Os.12181.1.S1_s_at	Chlorophyll A-B binding protein ; ASCAB9-A (ASCAB9-B) (Fragment)	2.90
Os.49582.1.S1_at	Conserved hypothetical protein	2.84
OsAffx.14074.1.S1_at	Conserved hypothetical protein	2.83
Os.11266.1.S1_at	Aldo/keto reductase family protein	2.73
Os.9172.2.S1_x_at	Catalase isozyme A	2.71
Os.22839.1.S1_at	Xyloglucan endotransglycosylase	2.68
Os.50366.1.S1_x_at	Conserved hypothetical protein	2.67
Os.11907.1.S1_at	Conserved hypothetical protein	2.65
Os.6764.2.S1_at	DUF3774; Wound-induced protein	2.63
Os.11657.1.S1_at	GRX_GRXh_1_2_like; Glutaredoxin (GRX) family	2.62
Os.11997.1.S1_at	Thioredoxin-like 1	2.61
Os.12391.1.S1_a_at	Glycosyl transferase, family 20 domain containing protein	2.58
Os.20548.1.S1_at	Conserved hypothetical protein	2.55
OsAffx.12078.1.A1_at	Dynein_light; Dynein light chain type 1	2.53
Os.17294.1.S1_a_at	Conserved hypothetical protein	2.51
OsAffx.27459.2.S1_s_at	Early nodulin 93 ENOD93 protein	2.50
Os.7612.1.S1_at	Similar to Bowman-Birk type trypsin inhibitor (WTI)	2.49
Os.50234.1.S1_at	Conserved hypothetical protein	2.49
Os.12735.1.S1_s_at	Auxin_repressed; Dormancy/auxin associated protein	2.49
Os.46941.1.S1_s_at	Conserved hypothetical protein	2.48

Appendix D (continued)

Gene ID	Annotaion	Fold change
Os.8188.1.S1_s_at	Universal stress protein (Usp) family protein	2.48
Os.9172.1.S1_x_at	catalase_clade_1; Clade 1 of the heme-binding enzyme catalase	2.45
OsAffx.30538.1.S1_x_at	SANT; N-CoR and TFIIIB' DNA-binding domains	2.41
Os.6662.1.S1_at	Conserved hypothetical protein	2.41
Os.12363.1.S1_at	light-dependent protochlorophyllide reductase (LPOR)-like	2.35
Os.10333.1.S1_at	Twin-arginine translocation pathway signal domain containing protein	2.27
Os.26517.1.S1_at	Protein of unknown function (DUF295),F-box	2.23
Os.27683.2.S1_s_at	Amino acid-binding ACT domain containing protein	2.23
Os.20482.1.S1_at	Cyclin-like F-box domain containing protein	2.22
OsAffx.19515.1.S1_s_at	Conserved hypothetical protein	2.21
Os.52993.1.S1_at	Conserved hypothetical protein	2.20
Os.49074.1.A1_at	unknown	2.19
OsAffx.22588.1.S1_at	Conserved hypothetical protein	2.17
Os.19114.1.S1_at	Similar to T24D18.17 protein (Tubby-like protein TULP8)	2.17
Os.10736.1.S1_at	Conserved hypothetical protein	2.16
Os.5147.1.S1_at	Sugar-starvation induced protein	2.15
Os.7705.1.S1_at	DUF3774; Wound-induced protein	2.12
Os.6205.1.S1_a_at	Zinc finger, RING-type domain containing protein, E3 ubiquitin-protein ligase RMA2	2.10
Os.7988.1.S1_s_at	Fructose-bisphosphate aldolase, chloroplast precursor	2.03
Os.10620.1.S1_at	Glyoxalase/bleomycin resistance protein/dioxygenase domain containing protein	2.00
Os.10742.1.S1_at	Conserved hypothetical protein	2.00
OsAffx.26803.1.S1_at	IQ calmodulin-binding region domain containing protein	1.98
Os.55270.1.S1_s_at	Conserved hypothetical protein	1.97
Os.10423.1.S1_at	Ethylene insensitive 3 family protein	1.95
Os.12793.1.S1_x_at	unknown	1.95
Os.14564.1.S1_at	Peptide N-acetyl-beta-D-glucosaminyl asparaginase amidase A	1.95
Os.35013.1.S1_at	Protein phosphatase type 2C	1.94
Os.22197.1.S1_at	Esterase/lipase/thioesterase domain containing protein	1.92
Os.34624.1.S1_at	Formiminotransferase, N-terminal domain containing protein	1.92
Os.26537.1.S1_a_at	Glycoside hydrolase, family 1 protein;Beta-glucosidase/6-phospho-beta-glucosidase/beta-galactosidase [Carbohydrate transport and metabolism]	1.91
Os.8570.4.S1_at	Conserved hypothetical protein	1.90
Os.26698.1.S1_a_at	USP_Like; Usp: Universal stress protein family	1.90
Os.12400.4.S1_at	Protein of unknown function DUF81 family protein; TauE; Sulfite exporter TauE/SafE	1.89
Os.4671.2.S1_a_at	Leucine-rich repeat, cysteine-containing subtype containing protein; Antagonist of mitotic exit network protein 1	1.88
Os.55283.1.S1_at	SIK1 protein (Nucleolar protein NOP56)	1.87

Appendix D (continued)

Gene ID	Annotaion	Fold change
Os.18335.3.S1_x_at	Fructose-bisphosphate aldolase, chloroplast precursor	1.86
OsAffx.24726.1.S1_s_at	Conserved hypothetical protein	1.85
Os.34624.2.S1_s_at	Formiminotransferase, N-terminal domain containing protein	1.85
Os.37955.1.S1_at	Conserved hypothetical protein	1.85
Os.7890.2.S1_x_at	Similar to LHC I type IV chlorophyll binding protein	1.84
Os.1475.1.S1_at	Acid phosphatase; Haloacid dehalogenase-like hydrolases	1.84
OsAffx.6372.1.S1_s_at	Protein of unknown function DUF125, transmembrane family protein	1.84
OsAffx.31409.1.S1_s_at	Universal stress protein (Usp) family protein	1.84
Os.55236.1.S1_at	Protein of unknown function DUF581 family protein	1.83
OsAffx.4296.1.S1_at	Glutaredoxin-like, plant II family protein	1.83
Os.46842.1.S1_at	Conserved hypothetical protein	1.82
Os.4999.1.S1_at	Similar to Chaperone protein dnaJ	1.82
Os.27139.1.A1_at	BTB/POZ domain	1.81
Os.26695.1.S1_at	OsNAC6 protein	1.81
Os.17487.1.S1_at	CONSTANS-like protein, B-Box-type zinc finger	1.79
Os.25589.1.S1_at	Octicosapeptide/Phox/Bem1p domain containing protein	1.79
Os.48456.1.S1_at	PRONE (Plant-specific Rop nucleotide exchanger)	1.79
Os.40424.1.S1_at	Protein of unknown function DUF506	1.78
OsAffx.12774.1.S1_s_at	Mitochondrial substrate carrier family protein	1.77
OsAffx.26803.1.S1_x_at	IQ calmodulin-binding region domain containing protein	1.77
Os.52381.1.S1_at	unclassifiable transcripts	1.77
OsAffx.12379.1.S1_at	Photosystem II oxygen evolving complex protein PsbQ family protein	1.76
Os.8700.1.S1_at	Dynein light chain type 1	1.76
Os.12388.1.S1_at	Anth (Pollen-specific desiccation-associated LLA23 protein)	1.75
OsAffx.12645.1.S1_s_at	Helix-loop-helix DNA-binding domain containing protein	1.74
Os.27837.1.S1_at	GATA transcription factor 3 (AtGATA-3)	1.73
Os.52647.1.S1_at	Aldose 1-epimerase family protein	1.73
Os.7622.1.S1_at	GRAM domain containing protein	1.72
Os.12199.1.S1_at	No apical meristem (NAM) protein domain containing protein	1.72
Os.26710.1.S1_at	NPH3;Photoreceptor-interacting protein-like	1.70
Os.55256.1.S1_at	Conserved hypothetical protein	1.70
Os.26537.2.S1_x_at	Glycoside hydrolase, family 1 protein	1.70
Os.53275.1.S1_at	Conserved hypothetical protein	1.69
Os.11194.1.S1_at	Auxin_repressed; Dormancy/auxin associated protein	1.69
Os.26436.1.S1_at	unknown	1.68

Appendix D (continued)

Gene ID	Annotaion	Fold change
Os.7890.1.S1_a_at	LHC I type IV chlorophyll binding protein	1.67
Os.12713.1.S1_at	Light-harvesting complex I (Fragment);Chlorophyll A-B binding protein	1.65
Os.12400.2.S1_x_at	Protein of unknown function DUF81 family protein; TauE; Sulfite exporter TauE/SafE	1.63
OsAffx.2477.1.S1_x_at	DNA-binding protein DF1;MADF_DNA_bdg; Alcohol dehydrogenase transcription factor Myb/SANT-like	1.63
Os.31975.1.S1_x_at	Zinc finger, CCCH-type domain containing protein	1.62
Os.38638.3.S1_x_at	Early nodulin 93 ENOD93 protein	1.61
Os.25589.3.S1_x_at	Conserved hypothetical protein	1.61
Os.25589.3.S1_at	Conserved hypothetical protein	1.60
Os.37818.1.A1_at	unknown	1.59
Os.9660.1.S1_at	Protein of unknown function DUF125	1.59
Os.26698.4.S1_s_at	USP_Like; Usp: Universal stress protein family	1.59
Os.55583.1.S1_at	Zinc finger, RING-type domain containing protein	1.58
OsAffx.23005.1.S1_x_at	Conserved hypothetical protein	1.57
Os.11387.1.S1_a_at	Beta-fructofuranosidase ;H32_B_Fructosidase; Glycosyl hydrolase family 32	1.57
Os.11795.1.S1_s_at	Plastid-specific 30S ribosomal protein 1, chloroplast precursor	1.55
Os.14318.1.S1_at	TA1 protein; HLH; Helix-loop-helix domain, found in specific DNA- binding proteins that act as transcription factors	1.52
Os.27517.1.A1_s_at	Cyclin-like F-box domain containing protein,kelch-like protein	1.52
Os.14686.1.S1_at	Protein of unknown function DUF597 family protein; PLATZ	1.52
Os.11795.1.S1_a_at	Plastid-specific 30S ribosomal protein 1, chloroplast precursor	1.51
Os.25952.1.S1_at	Conserved hypothetical protein	1.51
Os.4458.1.S1_at	Zinc finger, RING-type domain containing protein	1.51
Os.9481.1.S1_at	Nodulin-like domain containing protein	1.50
Os.26537.1.S1_at	Glycoside hydrolase, family 1 protein	1.50
Os.47358.1.A1_at	Conserved hypothetical protein; PsbP	1.49
Os.51291.1.S1_at	Conserved hypothetical protein	1.48
Os.5318.1.S1_a_at	Tetratricopeptide region domain containing protein	1.48
OsAffx.32309.1.A1_at	unknown	1.47
Os.4679.1.S1_at	Conserved hypothetical protein	1.47
Os.17405.1.S1_a_at	Allantoin permease	1.46
Os.6618.1.S1_at	Late embryogenesis abundant (LEA) group 1 family protein	1.45
Os.11913.2.S1_a_at	Auxin_repressed; Dormancy/auxin associated protein	1.43
OsAffx.23005.1.S1_at	Conserved hypothetical protein	1.42
OsAffx.29241.1.S1_s_at	EGF-like region domain containing protein	1.41
Os.32455.1.S1_at	Domain of unknown function (DUF814)	1.39
Os.4757.1.S2_at	unknown	1.39
Os.49042.1.A1_s_at	Zinc finger transcription factor	1.38
Os.7890.1.S1_x_at	Os08g0435900	1.38
Os.8901.1.S1_at	C2 domain containing protein	1.37
Os.51391.1.S1_at	Protein of unknown function (DUF3464)	1.36
OsAffx.27508.82.S1_x_at	Conserved hypothetical protein	1.36
Os.7751.1.S1_at	Basic helix-loop-helix dimerisation region bHLH domain containing protein	1.34

Appendix D (continued)

Gene ID	Annotaion	Fold change
Os.46304.1.S1_a_at	Hypothetical protein	1.34
Os.17446.2.S1_at	Cyclin-like F-box domain containing protein	1.32
Os.38580.1.S1_at	Protein kinase-like domain containing protein	1.32
OsAffx.30647.1.S1_x_at	Conserved hypothetical protein	1.31
Os.38638.4.S1_s_at	Early nodulin 93 ENOD93 protein	1.31
Os.26761.2.S1_x_at	Photosystem II reaction center J protein	1.31
Os.37955.1.S1_a_at	Conserved hypothetical protein	1.30
Os.27254.1.S1_s_at	Protein of unknown function (DUF506)	1.30
Os.6375.2.S1_x_at	Os01g0859200	1.30
Os.12889.1.S1_x_at	Hypothetical protein	1.29
Os.7931.1.S1_a_at	Phytoene synthase 1	1.29
Os.9093.1.S1_at	unknown	1.28
OsAffx.14413.1.S1_at	unknown	1.27
OsAffx.30533.1.S1_s_at	Mitochondrial carrier protein family protein	1.27
Os.55583.1.S1_x_at	Zinc finger, RING-type domain containing protein~contains InterPro domain	1.26
Os.54859.1.S1_at	Conserved hypothetical protein	1.26
Os.8622.1.S1_at	AUX/IAA protein family protein	1.26
Os.38278.2.S1_at	Plant-specific B3-DNA binding domain	1.25
Os.11166.1.S1_s_at	Glutaredoxin-like, plant II family protein	1.24
Os.27494.1.S1_at	Conserved hypothetical protein	1.24
Os.35815.1.S1_at	Peptidyl-prolyl cis-trans isomerase, cyclophilin type domain containing protein	1.22
Os.24901.1.A1_at	Lycopene epsilon-cyclase (Fragment)	1.22
Os.52498.1.S1_at	Asp/Glu racemase family protein	1.22
Os.21349.1.S1_at	Expansin-like protein A	1.21
Os.34466.1.S1_s_at	Kv1.4 voltage-gated K+ channel family protein	1.21
Os.6767.1.S1_at	Conserved hypothetical protein	1.20
OsAffx.4277.1.S1_s_at	UDP-glucuronosyl/UDP-glucosyltransferase family protein	1.20
Os.50349.2.S1_at	Conserved hypothetical protein	1.19
Os.12342.1.S1_at	unknown	1.18
Os.11953.1.S1_at	Conserved hypothetical protein	1.18
Os.17111.2.S1_x_at	Cytochrome P450, PLN03195; fatty acid omega-hydroxylase	1.16
OsAffx.30689.1.S1_at	COX2; Cytochrome C oxidase subunit II	1.16
Os.1465.1.S1_at	Taurine catabolism dioxygenase TauD/TfdA family protein	1.14
Os.3246.1.S1_at	Cyclin-like F-box domain containing protein	1.14
Os.26761.1.S1_s_at	Photosystem II reaction center J protein	1.13
Os.11064.1.S1_a_at	Centrin(Centrins are required for duplication of centrioles), EF-hand, calcium binding motif	1.12
Os.55599.1.S1_at	unknown	1.11
Os.53627.1.S1_at	unknown	1.10

Appendix D (continued)

Gene ID	Annotaion	Fold change
OsAffx.28833.1.S1_x_at	GRAS family transcription factor	0.83
OsAffx.12634.1.S1_at	Conserved hypothetical protein	0.83
Os.8015.1.S1_at	unknown	0.82
Os.5577.1.S1_at	Aldehyde dehydrogenase	0.81
Os.38399.1.S1_at	unknown	0.81
OsAffx.20681.1.S1_s_at	conserved hypothetical protein	0.81
Os.27394.1.A1_at	PKc_like; Protein Kinases, catalytic domain	0.81
OsAffx.4966.1.S1_at	unknown	0.80
Os.20239.1.S1_at	ACR4~contains InterPro domain(s)	0.78
Os.12804.1.S1_at	Protein kinase-like domain containing protein	0.77
OsAffx.17830.2.S1_x_at	unknown	0.77
Os.52467.1.S1_x_at	Conserved hypothetical protein	0.76
OsAffx.13558.1.S1_x_at	Actin-binding WH2 domain containing protein	0.76
Os.11038.1.S1_at	Rubber elongation factor protein (REF)	0.75
Os.5850.1.S1_at	Ethylene response factor 2; AP2; DNA-binding domain found in transcription regulators in plants such as APETALA2 and EREBP	0.75
OsAffx.30257.1.S1_at	Protein kinase-like domain containing protein	0.74
Os.52467.1.S1_at	Conserved hypothetical protein	0.74
Os.25324.2.S1_at	CemA family protein	0.74
Os.50601.1.S1_x_at	GH3 auxin-responsive promoter	0.74
Os.26698.4.S1_x_at	Universal stress protein (Usp) family protein	0.74
Os.10401.1.S1_s_at	PQ loop repeat	0.71
Os.51635.1.A1_at	non-protein coding transcript	0.70
Os.27727.1.S1_s_at	plastid	0.69
Os.20677.1.S1_at	Raffinose synthase protein	0.69
Os.46522.1.S1_a_at	conserved hypothetical protein	0.69
OsAffx.29998.1.S1_at	Protein kinase-like domain containing protein	0.69
Os.9206.1.S1_at	CBS domain containing protein	0.68
Os.49611.1.S1_at	Fatty acid elongase 3-ketoacyl-CoA synthase 1	0.68
Os.10830.1.S1_at	HLH; Helix-loop-helix domain, found in specific DNA-binding proteins that act as transcription factors; 60-100 amino acids long.	0.68
Os.8979.1.S1_at	kelch-like protein,Cyclin-like F-box domain containing protein	0.68
Os.6182.1.S1_at	Conserved hypothetical protein	0.66
Os.39997.2.S1_x_at	unknown	0.66
Os.54952.1.S1_at	SGNH_plant_lipase_like	0.66
Os.49432.1.S1_at	Zinc finger, RING-type domain containing protein	0.66
OsAffx.30075.1.S1_at	unknown	0.66
OsAffx.23996.1.S1_at	TAXI-I inhibits degradation of xylan in the cell wall.	0.65
Os.7244.1.S1_at	Acyl-CoA dehydrogenase	0.65
Os.11179.1.S1_at	Conserved hypothetical protein	0.64

Appendix D (continued)

Gene ID	Annotaion	Fold change
Os.14813.1.S1_at	Na+/H+ antiporter, b_cpa1	0.64
Os.31380.1.A1_x_at	Transposase_24; Plant transposase (Ptta/En/Spm family)	0.63
Os.4724.1.S1_at	Conserved hypothetical protein	0.62
OsAffx.13678.1.S1_at	unknown	0.62
Os.12475.1.S1_s_at	AUX1-like protein	0.61
Os.52897.1.S1_at	Basic helix-loop-helix dimerisation region bHLH domain containing protein; V-type ATP synthase subunit I	0.60
Os.55303.1.S1_at	Zinc finger, RING-type domain containing protein	0.59
OsAffx.20077.1.S1_at	Protein of unknown function DUF26 domain containing protein	0.58
Os.23434.1.S1_s_at	ABC transporter-like protein	0.58
OsAffx.6493.1.S1_at	unknown	0.55
OsAffx.27569.1.S1_at	unknown	0.55
OsAffx.17948.1.S1_x_at	Calcium-binding EF-hand domain containing protein	0.54
Os.8116.1.S1_at	Protein kinase domain containing protein	0.53
Os.8831.1.S1_at	acetylglucosaminyltransferase family protein	0.53
OsAffx.16099.1.S1_at	unknown	0.52
Os.623.1.S1_x_at	Similar to I-box binding factor (Fragment); SANT; N-CoR and TFIIIB" DNA-binding domains	0.52
OsAffx.28615.1.A1_at	unknown	0.52
Os.51191.1.S1_x_at	Conserved hypothetical protein	0.51
Os.51797.1.S1_x_at	unknown	0.51
OsAffx.31130.1.S1_at	Helix-loop-helix DNA-binding domain containing protein	0.51
OsAffx.30356.2.S1_x_at	EGF-like, type 3 domain containing protein	0.51
Os.23107.1.S1_at	bZIP transcription factor	0.50
OsAffx.13071.1.S1_at	unknown	0.49
OsAffx.29049.1.S1_at	unknown	0.49
Os.52127.1.S1_at	TGF-beta receptor, type I/II extracellular region family protein; MFS; The Major Facilitator Superfamily (MFS)	0.49
OsAffx.16693.1.S1_x_at	UV radiation resistance protein and autophagy-related subunit 14	0.49
OsAffx.27399.1.S1_at	pentatricopeptide (PPR) repeat-containing protein	0.48
OsAffx.15495.1.S1_at	Conserved hypothetical protein	0.48
OsAffx.7664.1.S1_x_at	GCN5-like 1 family protein	0.48
OsAffx.4326.1.A1_at	unknown	0.46
OsAffx.24548.1.S1_at	unknown	0.46
OsAffx.14801.1.S1_at	unknown	0.45
OsAffx.16166.1.S1_at	Conserved hypothetical protein	0.45
OsAffx.9637.1.S1_at	unknown	0.44
OsAffx.15157.1.S1_at	unknown	0.44
Os.411.2.S1_x_at	bZIP transcription factor	0.44
OsAffx.17466.1.S1_at	unknown	0.43
Os.46490.2.S1_at	unknown	0.42

Appendix D (continued)

Gene ID	Annotaion	Fold change
OsAffx.19070.1.S1_at	unknown	0.42
Os.2599.1.S1_at	Cyclin-like F-box domain containing protein	0.42
OsAffx.28064.1.S1_at	unknown	0.41
Os.10707.2.S1_at	DNA polymerase, beta-like region domain containing protein	0.41
OsAffx.16800.1.S1_at	unknown	0.41
Os.57123.1.S1_at	Cellulose synthase-like A4	0.40
OsAffx.4455.1.S1_at	unknown	0.40
OsAffx.13224.1.S1_at	unknown	0.39
OsAffx.25594.1.S1_at	Growth-regulating factor 3	0.37
Os.7464.1.S1_at	Conserved hypothetical protein	0.37
Os.55838.1.S1_at	TGF-beta receptor, type I/II extracellular region family protein	0.37
Os.28576.1.S1_at	LEA_2; Late embryogenesis abundant protein	0.36
OsAffx.2958.1.S1_at	Cellular retinaldehyde-binding/triple function; SEC14; Sec14p-like lipid-binding domain	0.35
OsAffx.14274.1.A1_at	Conserved hypothetical protein	0.34
Os.11816.1.S1_at	Aldo_ket_red; Aldo-keto reductases (AKRs) are a superfamily of soluble NAD(P)(H) oxidoreductases	0.28
OsAffx.30685.1.S1_x_at	unknown	0.27
Os.54937.1.S1_at	AB-hydrolase associated lipase region domain containing protein	0.26
OsAffx.26559.1.S1_at	Protein of unknown function (DUF3735)	0.26
Os.29095.1.S1_at	unknown	0.17